Facies and Stratigraphic Architecture of Two Early Miocene Fault-Block Carbonate Platforms in North Sardinia (Italy, Western Mediterranean Sea)

Dissertation

zur Erlangung des Doktorgrades der Naturwissenschaften

im Department Geowissenschaften der Universität Hamburg

vorgelegt von
Merle-Friederike Benisek

aus Amberg

Hamburg 2008

Als Dissertation angenommen vom Department für Geowissenschaften der Universität Hamburg

Auf Grund der Gutachten von Prof. Dr. C. Betzler
und Prof. Dr. M. Mutti

Hamburg, den 11.07.2008

Prof. Dr. Kay-Christian Emeis
Leiter des Departments Geowissenschaften

Table of Content

Summary

The aim of this work is to characterize Early Miocene carbonate platforms, which have been formed at the transition between tropical and subtropical climatic conditions (transitional carbonates). The two working areas are situated in the North of Sardinia, the second largest island in the Mediterranean Sea. Stratigraphical relations, cyclicity, depositional geometries, as well as facies arrangement were surveyed using geological mapping, large-scale field panoramas, and sedimentological sections. Field observations were backed up by thin section analysis.

Studies in the first working area in the Perfugas Basin (Sedini Limestone Unit, Sedini carbonate platform), yielded a depositional model which, with respect to platform geometries, differs from conventional models for tropical or temperate carbonates. The Sedini Limestone Unit consists of two depositional sequences. Sequence 1 is a carbonate ramp and includes two higher-frequency sequences (a and b). The ramp contains rhodalgal to bryoalgal and foramol-deposits with subordinate chlorozoan elements. Six high-frequency sequences (a-f) constitute the Sequence 2, which contains rhodalgal to molechfor and minor chlorozoan elements in its lower part and evolves into a transitional carbonate factory with rhodalgal and chlorozoan components throughout the succession. The lower Sequence 2 (2a-2d) consists of large-scale cross-bedded packstones and grainstones, locally interbedded with coralline-algal bindstones. They are interpreted as submarine dunes, which are sporadically stabilized by early cementation and coralline-algal encrustation. Bioturbated wackestones and packstones represent basinal deposits. In sequence 2d, small coral bioherms occur. Sequence 2e contains coral reefs, coralline-algal bindstones, and up to 27° steep, rhodolithic clinoforms. Sequence 2f contains bioclastic packstones and floatstones with minor corals and coralline algae. The limited outcrop control disallows interpretation.
In summary, Sequence 2 records the evolution of the carbonate depositional system from a carbonate ramp (Sequence 1) to a steep-flanked platform, with submarine dunes representing the incipient margin in the sequences 2a-2d. In its late stage (2e), a coral-reef flat with a basinward transition to coralline-algal bindstones and a steep rhodolithic platform-slope established. A palaeobathymetric reconstruction based on the distribution of coralline-algal genera and subfamilies from the platform margin to the toe-of-slope yielded water depths of approximately 40-60m. Geometrical reconstruction shows that the inner platform coral-reef flat formed in

water depths of approximately 20m. This unusual, "deep" setup might be characteristic for transitional carbonates. The platform top and margin do not necessarily build up to sea level. The development of the carbonate factories is not thought to be a result of a climatic change. It is rather considered as an establishing carbonate factory adapting to sea-level fluctuations under the influence of a constant subtropical to tropical climate.

In the second working area, the Porto Torres Basin, a mixed carbonate-siliciclastic succession was studied. The succession is fragmented by a series of approximately North-South trending, east and west-dipping normal faults, resulting in a complex horst-and-graben arrangement. Geological mapping and facies analysis yielded a tectonostratigraphic and depositional model. The carbonate succession contains four tectonostratigraphic units, which are separated by angular and erosional unconformities. Unit 1 is a carbonate ramp containing a rhodalgal lithofacies with minor chlorozoan elements. In Unit 2, a system of submarine dunes with a foramol to molechfor lithofacies developed, in which subordinate rhodalgal elements occur. Unit 3 is a carbonate ramp consisting of rhodalgal-type sediment. Unit 4 contains chlorozoan deposits. Syndepositional tectonic activity, resulting in repeated reorganization of the depositional system, was the main influence on formation of depositional geometries.

These findings emphasize the considerable impact of the basinal and tectonic setting on the stratigraphic architecture of carbonate platforms. The differences between the Sedini Limestone Unit and the Porto Torres Basin also show that transitional carbonates can develop different platform geometries in a similar structural and climatic setting.

Zusammenfassung

Ziel dieser Arbeit ist die Charakterisierung von Karbonatplattformen, die sich während des frühen Miozäns im klimatischen Übergangsbereich zwischen tropisch und subtropisch bildeten (*transitional carbonates*, Übergangskarbonate). Die zwei Arbeitsgebiete befinden sich im Norden der Mittelmeerinsel Sardinien. Mithilfe geologischer Kartierungen, großformatiger Aufschlusspanoramen und Dünnschliffanalysen wurden stratigraphische Modelle entwickelt, auf deren Grundlage die Zyklizität der Ablagerungen, die Entwicklung der Plattformgeometrien, sowie die Faziesverteilung innerhalb der Plattformen rekonstruiert wurden.

Die Untersuchungen im ersten Arbeitsgebiet im Perfugas Becken (Sedini Karbonatplattform, *Sedini Limestone Unit*) ergaben ein Ablagerungsmodell, das hinsichtlich der Plattformgeometrien von herkömmlichen Modellen tropischer oder nicht tropischer Karbonate abweicht. Die Sedini Karbonatplattform besteht aus zwei Ablagerungssequenzen. Sequenz 1 beeinhaltet zwei höherfrequente Sequenzen (a und b) und bildet eine Rampengeometrie aus. Die Ablagerungen sind umgelagerte Sedimente einer warm-temperierten bis subtropischen Karbonatproduktion der *Rhodalgal*- und *Bryoalgal*-Lithofazies mit untergeordneten *Chloralgal*-Elementen. Sequenz 2 setzt sich aus sechs hochfrequenten Sequenzen (a-f) zusammen. In ihrem unteren Teil (2a-2d) enthält die Sequenz 2 vornehmlich Elemente der *Rhodalgal*-und *Molechfor*-Lithofazies, weiterhin treten vereinzelt fragmentierte Komponenten der *Chlorozoan*-Lithofazies auf. In ihrem oberen Abschnitt (2e) entwickelt sich die Karbonatproduktionstätte zu einem Hybrid zwischen einer *Rhodalgal*-Lithofazies und einer *Chlorozoan*-Lithofazies. Die Ablagerungen der Sequenz 2 überliefern die Entwicklung von der flachen Rampengeometrie zu einer Plattform mit einem bis zu 27° steilen, von Rotalgen dominierten Hang und einem flachen inneren Bereich, in dem Korallenriffe auftreten. Die Versteilung des Reliefs ist an einen Gürtel submariner Dünen gebunden, welcher temporär durch frühe Zemente und Rotalgeninkrustationen stabilisiert wird und den initialen Plattformrand bildet.
Die Zusammensetzung der Rotalgenvergesellschaftungen am Plattformhang zeigen, dass dieser in Wassertiefen zwischen 40 und 60m lag. Geometrische Rekonstruktion und Korallenwuchsformen ergeben eine Wassertiefe von 20m für den inneren Plattformbereich. Dieser ungewöhnlich „tiefe“ Aufbau könnte ein Charakteristikum von Übergangskarbonaten sein. Der innere Plattformbereich und der Plattformrand erreichen nicht notwendigerweise den Meeresspiegel.

Die Veränderung in der Zusammensetzung der Karbonat produzierenden Organismen ist nicht an einen Klimawechsel gebunden. Vielmehr passt sich das Ablagerungssystem, unter konstant tropisch bis subtropischen Klimabedingungen, an Schwankungen des relativen Meerespiegels an.

Das zweite Arbeitsgebiet (Porto-Torres Becken) enthält eine gemischt karbonatisch-siliziklastische Abfolge, die durch eine Reihe von Nord-Süd streichenden Abschiebungen zergliedert ist. Durch geologische Kartierungen konnte ein tektonostratigraphisches Modell erstellt werden. Die Abfolge besteht aus vier tektonostratigraphischen Einheiten, die durch Winkel- und Erosionsdiskordanzen voneinander getrennt sind. Einheit 1 ist eine Karbonatrampe, die eine *Rhodalgal*-Lithofazies mit untergeordneten Elementen der *Chlorozoan*-Lithofazies enthält. Während der Ablagerung der Einheit 2 entstand ein weitläufiges System submariner Dünen mit bioklastischen Sedimenten der *Foramol*-, *Molechfor*- und untergeordnet der *Rhodalgal*-Lithofazies. Einheit 3 ist eine Karbonatrampe, die aus *Rhodalgal*-Ablagerungen aufgebaut ist. Einheit 4 besteht ausschließlich aus Elementen der *Chlorozoan*-Lithofazies.
Wiederholte Zergliederung und Restrukturierung des Ablagerungsraumes durch synsedimentäre tektonische Aktivität beeinflusste die Ausbildung der Ablagerungsgeometrien maßgeblich. Diese Ergebnisse unterstreichen den maßgeblichen Einfluss des tektonischen Milieus und der beckenspezifischen Vorraussetzungen auf den stratigraphischen Aufbau von Karbonatplattformen (Bosence, 2005). Die Unterschiede zwischen der Sedini Karbonatplattform und der Karbonatabfolge des Porto-Torres Beckens zeigen außerdem, dass Übergangskarbonate unter ähnlichen strukturellen und klimatischen Vorraussetzungen unterschiedliche Plattformgeometrien ausbilden können.

Acknowledgements

My sincere thanks go to Professor Maria Mutti and Professor Christian Betzler for initiating this project and offering me the opportunity to participate.

Christian Betzler guided me through this work with endless support and patience. He spent countless hours revising text and figures and discussing the subject. Thank you dearly for your consideration and for pushing things forward whenever necessary.

Discussions with Maria Mutti were always inspiring and informative. Thank you also for organizing so many things for us in Sardinia.

Gabriela Marcano did most of the field work with me. Thank you very much for the good times in Sardinia, the discussions in the field, office or our homes, and for thoroughly revising the manuscript. Mirto and Seadas!

Lucia Simone, Gabriele Carannante, and Marco Murru kindly introduced us to the Miocene of Sardinia. Professor Giacomo Oggiano and Professor Vincenzo Pascucci from the University of Sassari provided support in the early stages of this work.

Many, many thanks go out to the people of Sardinia. With their hospitality, friendliness and helpfulness they made field work an enjoyable and often adventurous event.

I want to thank Carla Müller for determination of the calcareous Nannoplankton. Juan Carlos Braga is thanked for discussing on coralline-algal identification. Reviews by Professor Werner Piller, Professor Giacomo Oggiano, and Doctor Marco Brandano helped to improve the chapter II.1.a.

This work was funded by the Deutsche Forschungsgemeinschaft. The financial support allowed me to participate in international meetings and to travel to the study areas several times

A lot of people in our institute contributed to this work, each of them in their very own way:

Annemarie Gerhard was always helpful in solving administrative tasks. Martina Pabst, Eva Koziarski and Kirsten Schuett helped whenever hard-to-get literature had to be obtained.

Dr. Sebastian Lindhorst, thank you for solving any imaginable problem with a genuine, pragmatic approach and good humour. Thank you also for helping in so many ways, with the printing, the computers, and many more.

Niels Buurman helped whenever necessary, regardless of being busy himself. Katja Buurman revised the manuscript and found countless little and big things. Thank you both for being friends. Katja, thanks for good times climbing THE ROCK, and nice afternoons with Pelle and Armin. I wish you and Pelle and Niels all the best, wherever you may be in the future.

Elmar Moser revised the Geological Framework chapter and expanded my understanding of Sardinia´s structural geology; as well as my hitherto existing definition of how much Rum goes into a Cuba Libre.

Helge Finckenstein is the Master of the References. Thank you endlessly for double-checking the citations so thoroughly.

Jan-Christian Albertsen, Niko Baristeas, Sebastian Cäsar, Hanns-Pidder Gienapp, David Jaramillo, Janna Just, Pamela Kardas, Christina Mayr, Birgit Nagel, Henrieta Röben, Miriam Römer, and Susan Wiggershaus were indispensable contributors to this work. Thank you all for the good times in Sardinia!
Special thanks go to Sebastian Cäsar for sacrificing countless hours of his time, helping to generate the compiled geological map and the unit map.

My friends Marie Janssen, Sassa Freuer, Maren, Joshua and Stephan Rauer-Gömann never let me down, regardless of what happened. You guys rock.

Anette von der Handt, ingenious inventoress of the theory of everything. I don´t know what I would have done without your constructive remarks on some of the chapters via the Hamburg-Honolulu hotline. Thank you sincerely for our conversations and for being my friend for almost ten years now (wow!).

Sönke Horn answered numerous emergency phone-calls, helping me with phrasing and prepositions. Thank you for revising parts of the text and for putting on your dancing shoes each time the Golden Pudel called.

Daniela Dangeleit, Mechthild Kummetz, Dr. Anika Parbs and Dr. Caroly Wegner, you are my geology girls. The time we spend together is rare, but worthwhile!

Meredith Davies read the majority of this thesis and helped to improve my English, which took her hours and days. Thank you a thousand times for that, and also for coming over almost once a week with Ulrich to support my social activities.

My world-champion parents Regine and Michael Hagen supply endless support in every way. Thank you a thousand times for that, especially for being such dedicated and adjuvant grandparents for Armin.

My brother Eike and my sister-in-law Marina, thank you for being there, for emergency baby-sitting and nice balcony parties.

Artur Benisek is gratefully acknowledged for his support.

Armin, my son and moon, you are the most beautiful and precious gift I have ever received.

I. INTRODUCTION

I.1. Outline of the Thesis

This dissertation is subdivided into four major chapters. Chapter I is the Introduction. It consists of the geological evolution of Sardinia (I.2.), and a brief description concerning the issues and aims of this work (I.3). Chapter II reports the results of the research. Two study areas in North Sardinia have been examined, the first is the Perfugas Basin (II.1.), and the second is the Porto Torres Basin (II.2.).

Chapter II.1. opens with a description of the stratigraphy, sedimentary environments and depositional geometries of the Sedini carbonate platform (II.1.a.). This section is based on a manuscript accepted for publication in the IAS Special Publication of the ESF LESC Exploratory workshop in Potsdam 2005. Chapter II.1.b. addresses the coralline-algal dominated margin and slope of the Sedini carbonate platform. This section is supposed to be submitted to FACIES directly after thesis submission. Chapter II.1. closes with a detailed description of the lithofacies distinguished in the Sedini carbonate platform.
Chapter II.2. begins with a summary of previous knowledge concerning the Porto Torres Basin (II.2.a.). The next section concentrates on tectonostratigraphy, facies relations and depositional controls in the marine carbonates studied in the Porto Torres Basin (II.2.b.). It is followed by a depositional model (II.2.c.). Chapter II.2. closes with an outlook section (II.2.d.).

Chapter III is the General Discussion. Two issues are debated: The relation between the carbonate factory and depositional geometries (III.1.), and the role of coralline algae in the carbonate successions of northern Sardinia (III.2.).

The Thesis closes with a Synthesis (Chapter IV). The Appendix provides basic data.

I.2. Geological Framework

This chapter focuses on the Cenozoic (divided in pre-rift, syn-rift and post-rift stages) development of Sardinia. Palaeozoic and Mesozoic episodes are briefly described.

Sardinia, after Sicily, is the second largest mediterranean island (Fig. I.2.1). It is situated in the western Mediterranean Sea and forms the western margin of the Tyrrhenian Sea, which is bordered to the east by the Apennine Peninsula. To the west, the island is bound by the Western Mediterranean Basin.

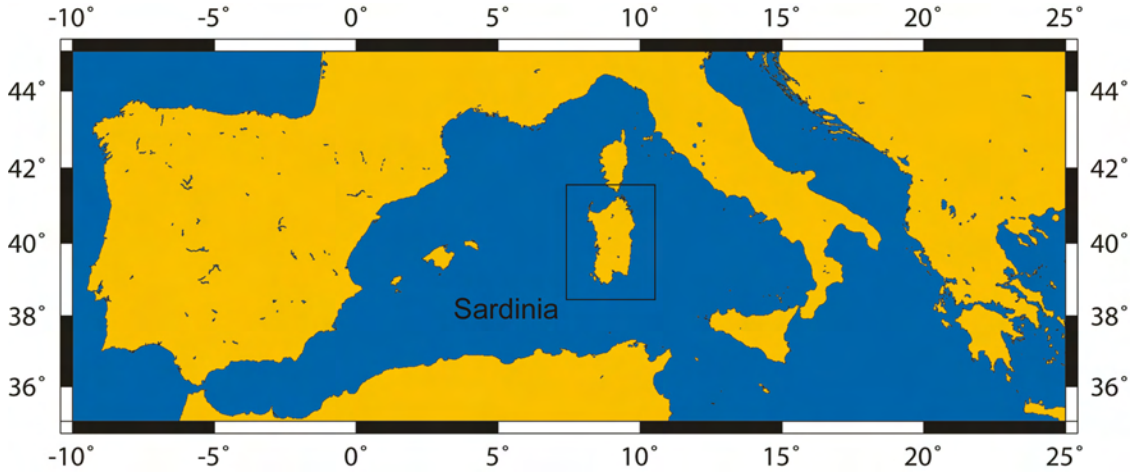

Fig. I.2. 1: Geographical position of Sardinia in the western Mediterranean Sea. Map produced with Online Map Creation provided by www.aquarius.ifm-geomar.de

PALAEOZOIC

Sardinia and Corsica, which together form the Corsic-Sardic Block, have been a part of Palaeo-Europe since Palaeozoic times. Approximately 75% of the island is formed by palaeozoic series (Fig. I.2.2), which are divided into several metamorphic and tectonic units. The two most important are the High Grade Metamorphic Complex (HGMC) and the Low to Medium Grade Metamorphic Complex (LMGMC). They are separated by the Posada Asinara Line, a suture in which remnants of oceanic crust give evidence for the subduction of the South Armorican Ocean. This subduction culminated in the continent-continent-collision between northern Armorica and southern Gondwana (CARMIGNANI et al., 1992, CONTI et al., 1999), resulting in the Variscan orogeny, which intensely deformed the ?Precambrian to late Devonian series. The degree of metamorphism increases from Southwest Sardinia (LMGMC) with low grade metamorphic rocks to gneisses and migmatites of the HGMC in

Northeast Sardinia. In the final stages of the Variscan orogeny, intrusions of large granite bodies with synchronous normal and strike-slip faulting occurred (CONTI et al., 1999). The faulting led to the formation of Upper Carboniferous to Lower Permian basins, which became filled up with clastic material and rhyolitic-rhyodacitic volcanics (COCOZZA & JACOBACCI, 1975, CARMIGNANI et al., 1992).

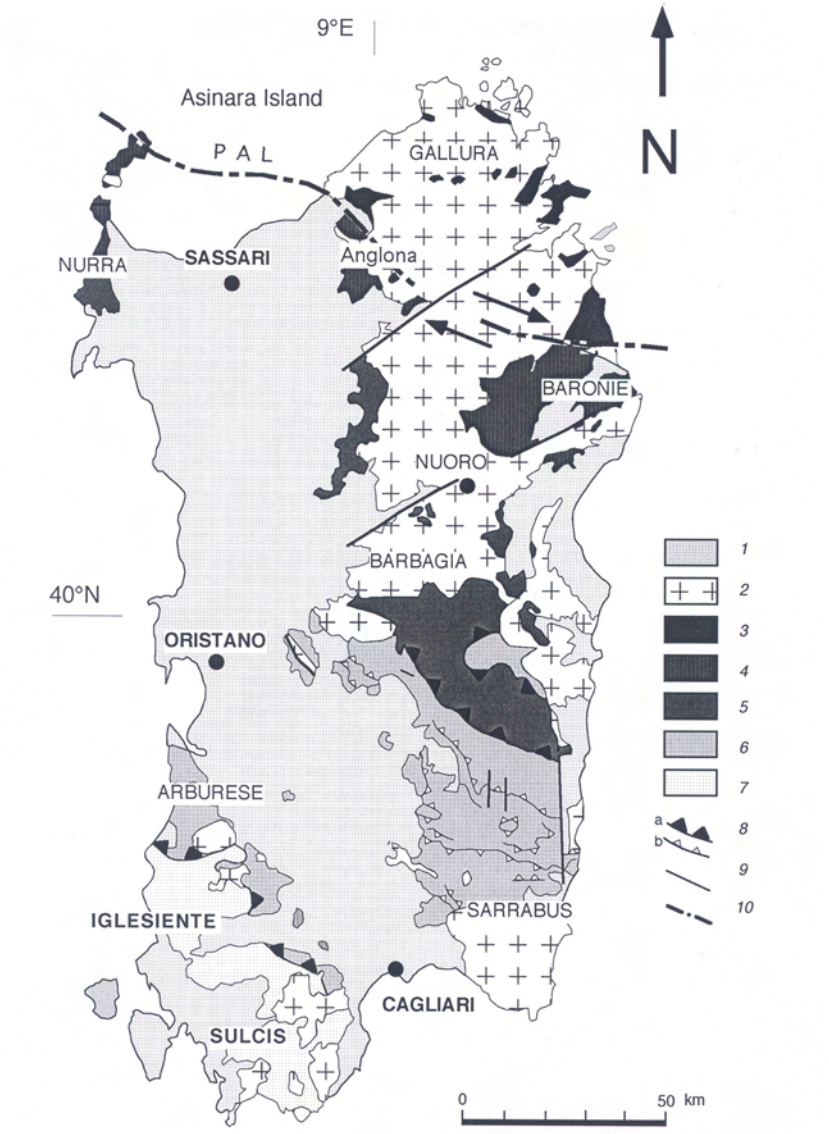

Fig. I.2. 2: Tectonic sketch map of Sardinia. 1= Post-Variscan cover deposits; 2= Variscan Batholith; 3= High Grade Metamorphic Complex (HGMC); 4= Internal nappes (low to medium-grade metamorphism (LMGMC); 5= Internal nappes (low-grade metamorphism); 6= External nappes; 7= External zone; 8= thrusts (a: main thrusts; b: minor thrusts); 9= faults; 10= PAL: Posada-Asinara line. Modified from CAROSI et al. (2004).

MESOZOIC

During the Mesozoic, Sardinia was characterized by regional extension, and was affected by several transgressions resulting in epicontinental shelf seas covering

the western and eastern part of the island (CARMIGNANI et al., 1989, CASULA et al., 2001). The Triassic is represented in Germanic Facies type.

Jurassic deposits are neritic, high-energy sediments locally intercalated with back reef/lagoonal deposits with a thickness of about 700m representing a large carbonate platform. Lower Cretaceous marine sediments conformably overlie Malm deposits. In Middle Cretaceous times, an important hiatus, accompanied with bauxite formation and erosional events between the Lower Aptian and Upper Cenomanian, was formed due to compressive tectonic activity (Austrian phase) in the northwestern part of the island. Based on palaeomagnetic data, COHEN (1980) postulates a possible counter clockwise rotation of 30° of the island together with Iberia at that time. The duration of the hiatus decreases towards the west and indicates a transgression from the west (CHERCHI, 1985, CASULA et al., 2001). From the end of the Cretaceous to the Upper Palaeocene, widespread continental deposits indicate an emersion affecting the whole island (CHERCHI, 1985).

CENOZOIC

Pre-rift stage: Palaeocene-Mid Oligocene (CASULA et al., 2001)

The existing continental conditions were interrupted by a short transgressive-regressive cycle during the Early Eocene (former Ilerdian), when Alveolinid and Orbitolites limestones were formed in south-western Sardinia. The limestones display a shallowing upward trend, and terminate in fresh water sediments bearing charophytes and pulmonate gastropods. Palynomorphs indicate a Lower Cuisian-Early Lutetian age (CHERCHI, 1985, CASULA et al., 2001). These deposits are unconformably overlain by conglomerates of the Cixerri Formation (Lutetian-Middle Oligocene) in southern Sardinia. The unconformity is triggered by a compressive phase (Pyrenean) in the Middle Eocene and affects Palaeozoic, Mesozoic and Lower Eocene strata (CASULA et al., 2001). The conglomerates contain Cretaceous clasts of the Pyrenaic-Provencal domain, and transport directions indicate the ongoing connection with the European continent up to the Upper Palaeogene (CHERCHI, 1985, CASULA et al., 2001).

Syn-rift stage: Mid Oligocene-Mid Burdigalian (Casula et al., 2001)

Due to the complex geodynamical processes resulting from the African-Eurasian collision and the Alpine orogeny, a number of back-arc basins opened in relatively short-time periods. One of these is the Western Mediterranean back-arc basin (also

called Provencal basin in GUEGUEN et al., 1998 or Liguro-Provencal back-arc basin in SPERANZA et al., 2002), which is linked to rollback in a N-W dipping subduction zone between the Adriatic domain in the Southeast and the Eurasian domain in the Northwest (Fig. I.2.3). This subduction was active since Early Oligocene times. Rifting culminated in the formation of oceanic crust and led to a drifting stage separating the Corsica-Sardinia microplate from Southern Europe in a counter clockwise rotation, which finished during the Early Miocene.

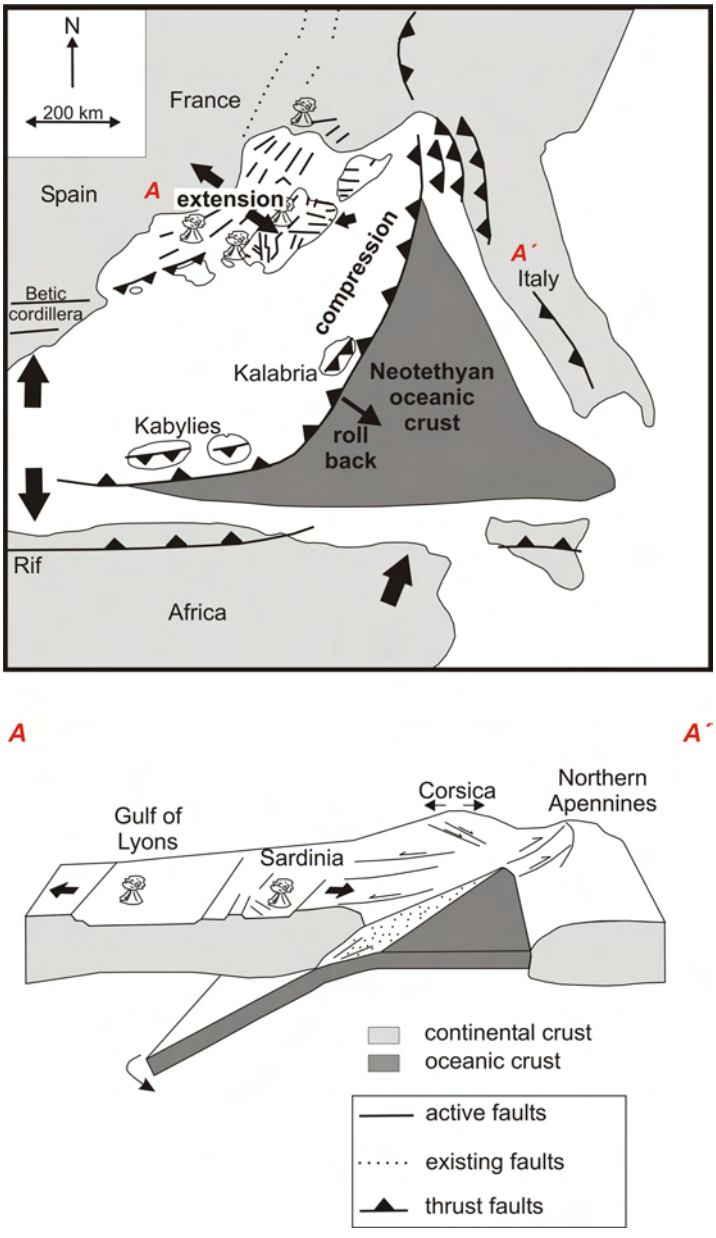

Fig. I.2. 3: Simplified palaeogeographic and tectonic reconstruction of the western Mediterranean realm during the Upper Oligocene (After SOWERBUTTS, unpublished PhD thesis, 1997).

Several authors discussed the beginning and ending of the rotation, amongst them COHEN (1980), MONTIGNY et al. (1981), CHERCHI & MONTADERT (1982), MARTINI et al.

(1992), VIGLIOTTI & LANGENHEIM (1995), GUEGUEN et al. (1998), GATTACCECA et al. (1999), SOWERBUTTS (2000), CASULA et al. (2001), DEINO et al. (2001), MONAGHAN (2001), and SPERANZA et al. (2002). The duration of the rotation is still being discussed. Whereas MONTIGNY et al. (1981), VIGLIOTTI & LANGENHEIM (1995) and GATTACCECA et al. (1999) propose an age between 20-21 Ma and 15-16 Ma, SPERANZA et al. (2002) assume that the rotation is younger than 19 Ma and did not end before approximately 16 Ma. In northern Sardinia, the multiphase structural movements, accompanied by extensive volcanism, led to the formation of two N-S oriented halfgraben systems.

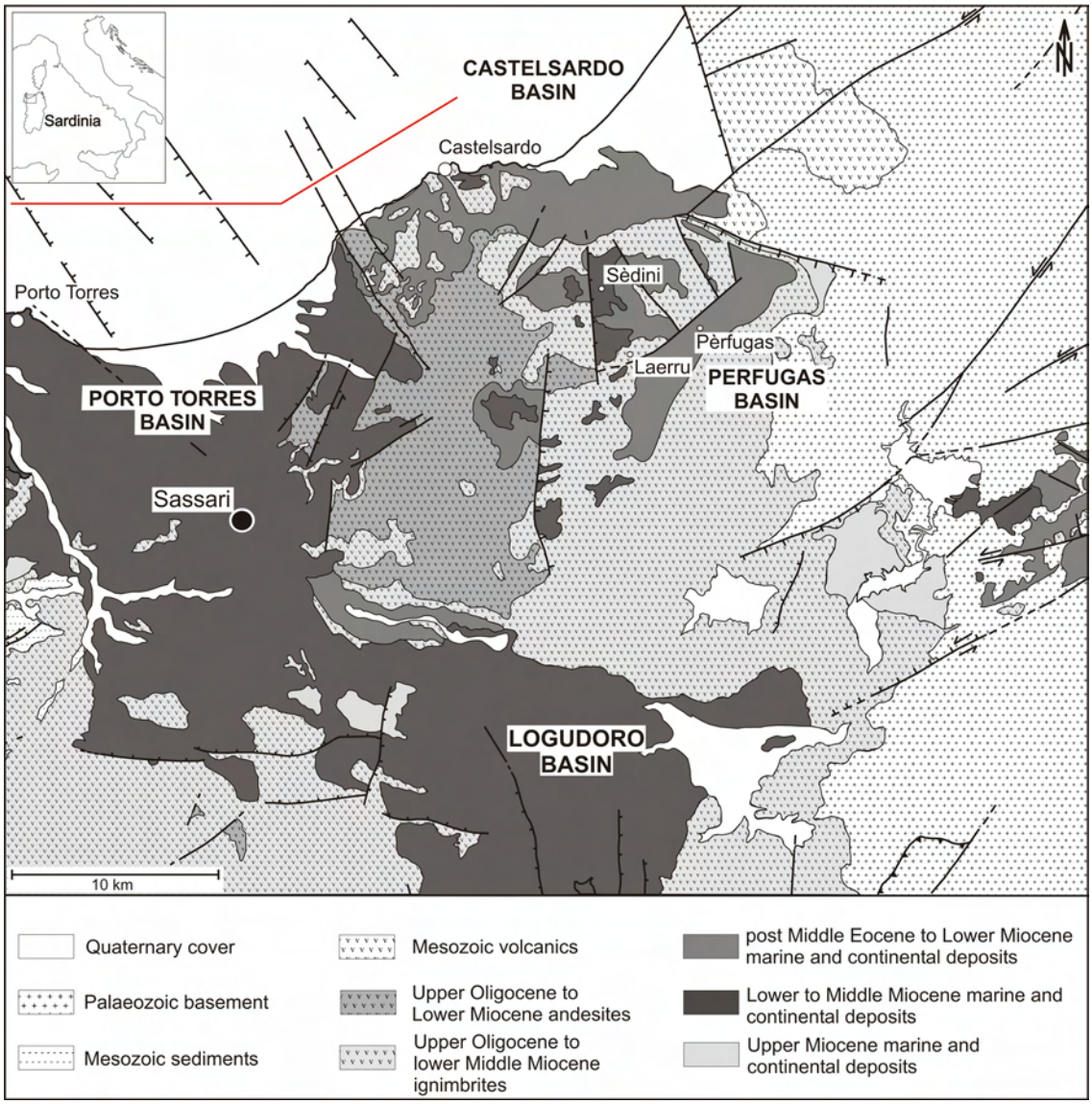

Fig. I.2. 4: Geological map of northern Sardinia with major structural elements. The Logudoro Basin, the Porto Torres Basin, the Castelsardo Basin, and the Perfugas Basin are halfgrabens with a Neogene sedimentary infill. The red line marks the position of the seismic line ES 125 shown in Fig. I.2.5. Based on THOMAS & GENNESSEAUX (1986), FUNEDDA et al. (2000), SOWERBUTTS (2000), and CARMIGNANI et al. (2001).

The western branch consists of the Porto Torres Basin in the North, separated from the southern Logudoro Basin by a transfer zone (THOMAS & GENNESSEAUX, 1986, FUNEDDA et al., 2000). The eastern branch contains the Castelsardo Basin to the north and the Perfugas Basin to the south (THOMAS & GENNESSEAUX, 1986, SOWERBUTTS, 2000; Fig. I.2.4). Faults in the Castelsardo Basin dip to the west, whereas they dip to the east in the Perfugas Basin. Displacement along listric, normal faults resulted in block rotation. Both areas are separated by a range of hillocks, located between the small town of Castelsardo and the village of Sedini, which may indicate buckling in an accomodation zone (FAULDS & VARGA, 1998).

Rift stratigraphy

Synsedimentary rifting in Sardinia is shown in THOMAS & GENNESSEAUX (1986) in a series of seismic sections measured offshore northern Sardinia (Fig. I.2.4). They identify seven seismic sequences, which can be correlated with the onshore stratigraphy (Fig. I.2.5). THOMAS & GENNESSEAUX (1986) use the time scale of LOWRIE & ALVAREZ (1981). The marine carbonates analyzed in this study, the Sedini Limestone Unit (QUESNEY-FOREST & QUESNEY-FOREST, 1984, THOMAS & GENNESSEAUX, 1986, ARNAUD et al., 1992, SOWERBUTTS, 1997, CASULA et al., 2001), and the marine succession of the Porto Torres Basin, are correlative to the seismic sequence 5.

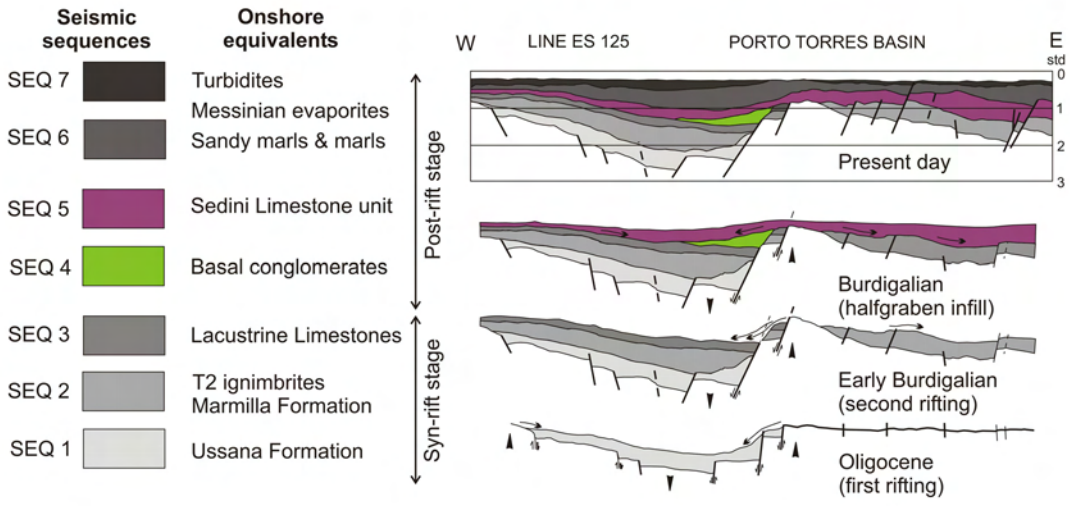

Fig. I.2. 5: Evolution of the Porto Torres Basin, from AGIP–ES 125 seismic line (position indicated as red line in Fig. I.2.4). Equivalent onshore deposits compiled from THOMAS & GENNESSEAUX (1986), and CASULA et al. (2001). First rifting occurred during Oligocene to Middle Aquitanian time, and second rifting during the early Burdigalian, after the rotation of Corsica and Sardinia. Modified from THOMAS & GENNESSEAUX (1986, Fig. 4). For datation of seismic sequences see Fig. I.2.6.

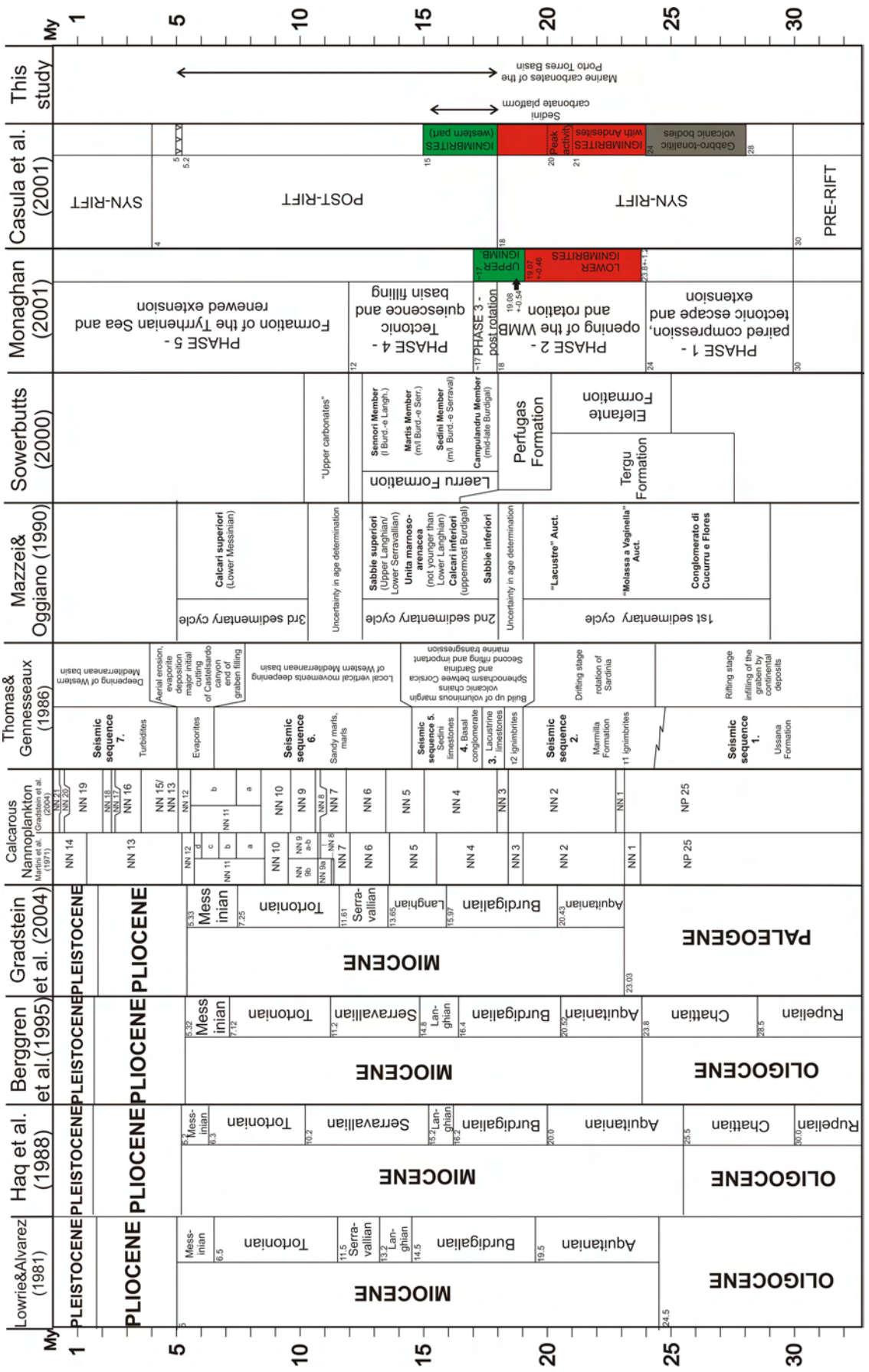

Fig. I.2. 6: Rift stratigraphy and associated lithologies on Sardinia. Compiled from authors mentioned in each column.

Seismic sequence 1 (Upper Oligocene to Aquitanian)

The initial rift began in a subaerial environment represented by continental deposits occurring along the rift walls visible in the seismic lines (THOMAS & GENNESSEAUX, 1986). Rapid subsidence led to progressive marine transgression resulting in great thickness of the sediments.

Seismic sequence 2 (Upper Oligocene to Early Burdigalian)

The second seismic sequence reflects a backstepping trend towards the graben margins during deposition (THOMAS & GENNESSEAUX, 1986, CASULA et al., 2001). Extensive magmatic activity is recorded by the occurrence of an ignimbritic layer (τ1, THOMAS & GENNESSEAUX, 1986), yielding a radiometric age of 20.7 Ma (EDEL, 1980). ASSORGIA et al. (1995) recognize this regional horizon within the lower ignimbrites (23.8 Ma to 19.07 Ma). Other authors (LECCA et al., 1997) identify an Aquitanian to Burdigalian volcano-sedimentary stage ranging from 24 to 18 Ma with peak activity during 21-20 Ma (CASULA et al., 2001).

The top of the second seismic sequence is characterized by a strong reflecting layer that has its onshore equivalent in a second regional ignimbritic layer (τ2, THOMAS & GENNESSEAUX, 1986). These ignimbrites are dated by EDEL (1980) as being 18.6 Ma in age. This second regional ignimbritic interval can be assigned to the upper ignimbrites ranging from 19.08 Ma (SOWERBUTTS, 1997) to approximately 17 Ma (LECCA et al., 1997). This volcanic series is called Upper Burdigalian to Langhian volcanic stage in CASULA et al. (2001). According to MONAGHAN (2001), the two ignimbritic layers belong to the Oligo-Miocene calc-alkaline series, which consists of basaltic to andesitic rocks, lava flows, dykes, pyroclastic breccias and the above mentioned dacitic to rhyolithic pyroclastic rocks and flows.

Seismic sequence 3 (Burdigalian)

The third seismic sequence rests unconformably on the τ2 layer. The onshore equivalents are lacustrine limestones (THOMAS & GENNESSEAUX, 1986). These lacustrine deposits occur in the literature as *Lacustre Auct*. or Perfugas Formation (SOWERBUTTS, 1997).

Seismic sequence 4 (Burdigalian)

The fourth seismic sequence of THOMAS & GENNESSEAUX (1986) is observed in footwall areas of faults in the Castelsardo and Porto Torres Basin. It is correlated with a "basal conglomerate of Burdigalian transgression".

Seismic sequence 5 (Burdigalian)

The fifth seismic sequence identified by THOMAS & GENNESSEAUX (1986) is a filling unit. However, local faults protrude into this sequence producing offsets (THOMAS & GENNESSEAUX, 1986; figs. 4 a and b). It comprises a succession of limestones, which occur onshore in the Porto Torres basin and in the Castelsardo basin. They are called Sedini Limestones (QUESNEY-FOREST & QUESNEY-FOREST, 1984, THOMAS & GENNESSEAUX, 1986, ARNAUD et al., 1992, SOWERBUTTS, 1997, CASULA et al., 2001), because they are exposed around the village of Sedini (Fig. I.2.4). The limestones are wackestones to boundstones forming a small carbonate platform of approximately 19 km^2 with thicknesses ranging between 10 to 60 m. The Sedini Limestone Unit is one of the emphases of this study and will be treated thoroughly in the following chapters.

Seismic sequence 6 (Langhian, Serravallian, Tortonian)

This seismic sequence lies upon an erosional surface or slightly unconformable on seismic sequence 5 and consists of sandy marls and marls. The top of seismic sequence 6 is another erosional surface related to the Messinian event. Deep submarine canyons have been incised during the Messinian in the continental shelf off northern Sardinia (THOMAS & GENNESSEAUX, 1986; Fig. 7).

Seismic sequence 7 (Pliocene, Quaternary)

This seismic sequence 7 overlies the Messinian erosional surface and is related to Pliocene and Quaternary turbidites (THOMAS & GENNESSEAUX, 1986).

The timing of rifting, as well as the duration and ending of drifting, is highly unclear. On the base of their seismic sections, THOMAS & GENNESSEAUX (1986) postulate a two-stage rifting with a first pulse of vertical movements from the Oligocene to Early Miocene and a second rifting event during the Burdigalian leading to another transgression (Fig. I.2.6). Indeed, in the seismic profiles, faults protrude the Burdigalian deposits and produce offsets, multiplying the already existing ones in the underlying deposits. CHERCHI & MONTADERT (1982) and CHERCHI & TREMOLIERES (1984) did not observe two such events in southern Sardinia, leading THOMAS & GENNESSEAUX (1986) to the conclusion that this double rifting is limited to the northern branch of the graben system only. CASULA et al. (2001) do not describe two phases of rifting in southern Sardinia either, whereas SOWERBUTTS (1997, 2000) respectively MONAGHAN (2001) does.

According to SOWERBUTTS (1997, 2000), and MONAGHAN (2001) five stages during rifting are postulated (Fig. I.2.6). The first stage, ranging from the middle to late Oligocene, represents the initial phases of extension and transtension and correlates with the eruption of the first volcanic arc rocks. A proto-rift consisting of E-W oriented grabens, reactivating Eocene trends, develops in south-western Sardinia, whereas a NW-SE trending graben structure occurs in South-central Sardinia, and N-S trending grabens and halfgrabens in north-western Sardinia.
The second stage lasts from the latest Oligocene to the early Burdigalian and represents a passive infill of the faulted topography. During the third stage in the Middle Burdigalian, a second main extension phase occurs on E-W and NW-SE to N-S trending high-angle, planar faults.
Stage 4 from late Burdigalian to Serravallian is characterized by post-rift topographic infill and thermal subsidence. Stage 5 from upper Serravallian to present day is a renewed extension accompanied by volcanism related to the formation of the Tyrrhenian Sea and results in extension on high angle, N-S oriented normal faults, reactivated NW-SE oriented faults in the Campidano region, and NE-SW trending faults in central northern areas.

To summarize, the Neogene succession of northern Sardinia was deposited in an extensive rift-drift regime that led to the formation of graben and halfgraben structures, as well as block rotation along normal faults. Extensive volcanism occurred, accompanied by clastic and lacustrine continental deposits. Progressive subsidence led to marine ingression. In the Middle Burdigalian to Langhian, fault-block carbonate platforms (*sensu* BOSENCE, 2005) developed on footwall highs or isolated highs formed by the faulted volcanic substrate (SOWERBUTTS, 1997, 2000, 2001, *this study*). Terrigenous input was low in the Perfugas Basin, whereas oscillating terrigenous input resulted in a mixed carbonate-siliciclastic succession in the Porto Torres Basin (VIGORITO et al. (2006), *this study*), and in the Logudoro Basin (MAZZEI & OGGIANO,1992, FUNEDDA et al. 2000, 2003). In the Porto Torres basin, syndepositional tectonics can be recognized by the occurrence of angular and corresponding erosional unconformities (see chapter II.2.).

I.3. Aim of Work

Carbonate Factories

Shallow-water carbonate sediments contain a variety of skeletal and non-skeletal grains. To describe their composition, or in which climatic environment they form, a number of terminologies have established (Fig. I.3.1). Most of them refer to the biota association, and the term to describe this is a combination of the occurring organisms. The "foramol"–association (*sensu* LEES & BULLER, 1972), for instance, consists of foraminifers and mollusks. Other terminologies refer to the prevalent climatic conditions during deposition, e.g. "non-tropical" (*sensu* NELSON, 1988), or the biogeographical province, in which the carbonates form, e.g. "warm-temperate" *sensu* BETZLER et al. (1997).

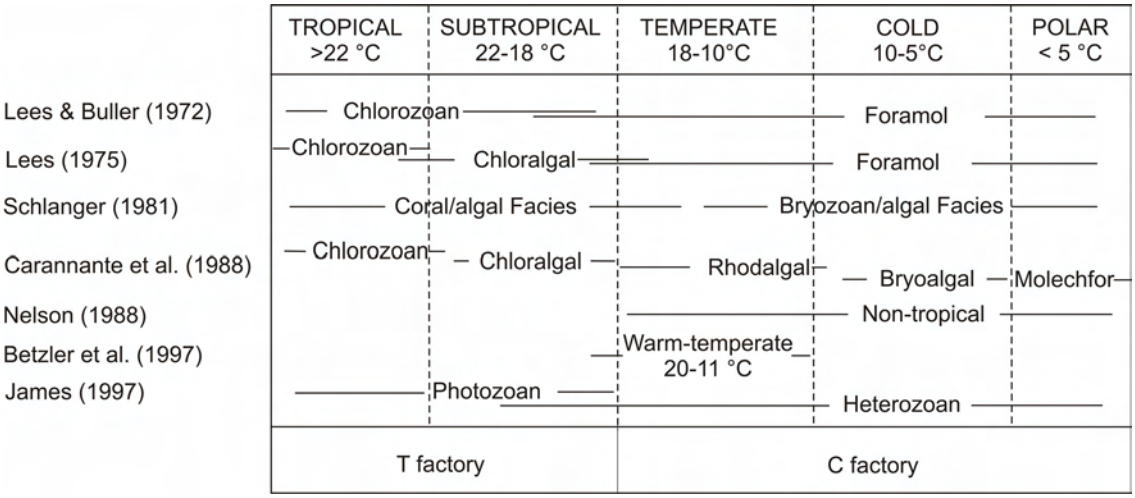

Fig. I.3. 1: Comparison of terminologies for carbonates formed in different climatic conditions. From Schlager (2005).

LEES & BULLER (1972) and LEES (1975) distinguish between a chlorozoan (Chlorophyta and Zoantharia), a chloralgal (Chlorophyta), and a foramol (Foraminifers and Mollusks) factory with respect to the skeletal grain composition (Fig. I.3.1). CARANNANTE et al. (1988) expanded this subdivision by substituting the foramol assemblage for the rhodalgal (Rhodophyta), the bryoalgal (Bryozoans and Rhodophyta), and the molechfor (Molluscs, Echinids and Foraminifers) lithofacies (Fig. I.3.1).

NELSON (1988) stated all carbonates formed below 18°C as "non-tropical" (Fig. I.3.1). BETZLER et al. (1997) defined the warm-temperate carbonate province ranging in water temperatures between 11 and 20°C (Fig. I.3.1). JAMES (1997) defined the

photozoan (phototroph organisms) assemblage and the heterozoan (heterotroph organisms) assemblage.

Figure I.3.1 shows that certain transitions exist between the subdivisions. LEES & BULLER (1972), and LEES (1975) state that foramol-type sediments can occur adjacent to chlorozoan and chloralgal sediments. CARANNANTE et al. (1988) pointed out the risk of misinterpretation when carbonate lithofacies are used as palaeolatitudinal indicators, for the same reason. Based on findings in the Lower-Middle Miocene of the Mediterranean and on the Recent Brazilian shelf, they proposed the rhodalgal lithofacies to be the transitional element between the chlorozoan/chloralgal and molechfor-type deposits.

An alternative classification of carbonate factories was suggested by SCHLAGER (2005, Fig. I.3.1), who differentiates between three types of factories named "T-factory" (tropical, top of the water column), "C-factory" (coolwater, controlled precipitation), and the "M-factory" (mud mount, micrite, not shown in Fig. I.3.1). The mode of the prevalent carbonate precipitation is considered as the controlling factor. The T- and C-factories show considerable transitions, as the C-factory can occur adjacent to the T-factory in deeper water or upwelling environments. The transition from C-factory to T-factory takes place beyond the subtropical latitudes with temperatures below 18°C and can extend over several thousand kilometers.

Platform Geometries

Geometries of carbonate build-ups are generally attributed to certain carbonate factories. According to SCHLAGER (2005), the C-factory forms carbonate ramps, as it has no ability to build wave-resistant rims. The same applies for warm-temperate carbonates (BETZLER et al., 1997). The T-factory forms rimmed platforms (c.f. rimmed shelf according to TUCKER & WRIGHT, 1990). Carbonate ramps often evolve into rimmed shelves (e.g. Wilson, 1975, READ, 1985, NELSON, 1988, HOMEWOOD, 1996, JAMES, 1997, BOSENCE et al., 1998, POMAR, 2001, BOSENCE, 2005, SCHLAGER, 2005). Such changes in platform geometry are thought to be the result of climatic and oceanographic fluctuations and a subsequent change in the type of carbonate factory from bioclastic, skeletal production to shallow-water, framebuilding, photozoan reef communities (BOSENCE, 2005). According to SCHLAGER (2005, p. 43), the ramp morphology is normally a transient stage. Carbonates with rim-building capacity have a strong tendency to prograde, steepen their slope and thus differentiate into a platform top, rim and steep slope.

Project Aims

This thesis is the result of the DFG-funded project TRANSCARB: Neogene transitional carbonates: the link between the tropical and the temperate carbonate province. The aim of this project was to characterize Miocene carbonate deposits at the transition from tropical to warm-temperate conditions, to analyze their biota assemblages, their facies distribution and their response to local and global sea-level fluctuations.

The development of facies models to pinpoint the characteristics of transitional systems helps to discriminate these from true "warm-water" or "cool-water" depositional systems. Hitherto, only little data exist for such systems. The Miocene of Sardinia is well suited for these purposes. The island was situated in the subtropical province during the Miocene. Rhodalgal-type deposits have been described by CHERCHI et al. (2000), GALLONI et al. (2001), MURRU et al. (2001), SIMONE et al. (2001), BASSI et al. (2006), and VIGORITO et al. (2005, 2006).

40% of worldwide hydrocarbon reservoirs are situated in Miocene carbonates of Southeast Asia (LONGMAN, 1993). The understanding of lateral and vertical facies variations, buildup geometries, and their interaction with basinal and tectonic settings, as well as relative sea-level fluctuations can provide useful information to defining optimum exploration targets (LONGMAN, 1993).

II. RESULTS

II.1. The Perfugas Basin

The Perfugas Basin is the first working area (Fig. I.2.4). The study area is located approximately 15km south of Castelsardo, between the villages of Sedini and Laerru, covering an area of about 19km^2. Figure II.1.a.1 shows a geological map, which is based on a mapping project of Hamburg University Diploma students (ALBERTSEN, 2005, GIENAPP, 2005 and NAGEL, 2005).

II.1.a. Facies and Stratigraphic Architecture of a Miocene Warm-Temperate to Tropical Fault-Block Carbonate Platform in Sardinia (Central Mediterranean Sea)[1]

ABSTRACT

A Miocene (Burdigalian) carbonate platform in northern Sardinia was studied in order to unravel its facies and stratigraphic architecture. The Sedini Limestone Unit formed at the western margin of the Perfugas Basin on a fault-bound topographic high. The 10–60m thick sedimentary succession contains two depositional sequences separated by a major erosional unconformity, and several high-frequency sequences reflecting the occurrence of higher-order base-level fluctuations. The deposits are massive limestones, bedded limestones and marlstones, which form a carbonate platform with an extension of about 19km^2. Sequence 1 consists of a homoclinal ramp with beaches, minor patch reefs, longshore bars, and finer-grained, outer-ramp sediments. Sequence 1 deposits were formed by a warm-temperate carbonate factory with abundant coralline algae, frequent larger benthic foraminifers (*Heterostegina sp.*, *Amphistegina sp.*, *Borelis sp.*), barnacles, bryozoans, molluscs, and minor corals. Sequence 2 documents a steepening of the carbonate platform slope. In the lower part of this sequence, a belt of submarine dunes separated platform-interior from deeper-water, bioclastic deposits. Dunes were locally stabilized by coralline-algal bindstones. In the upper part of sequence 2, the depositional system consisted of an extensive reef flat with a marked slope break formed by coralline-algal bindstones and rhodolithic clinoform beds dipping with up to 27°. The carbonate factory of sequence 2 is rich in reef-building zooxanthellate corals and therefore can be unequivocally assigned to a tropical carbonate factory. Spectacular outcrops in the Sedini Limestone Unit allow a detailed observation of the facies, the bedding geometries, and the stratigraphic architecture of carbonates formed at the transition from the temperate to the tropical realm.

[1] This chapter is based on: BENISEK, M.-F., MARCANO, G., BETZLER, C. and MUTTI, M. (submitted): Facies and stratigraphic architecture of a Miocene warm-temperate to tropical fault-block carbonate platform (Sardinia, Central Mediterranenan Sea).

INTRODUCTION

In neritic carbonates, palaeoceanography or climate determine the type of carbonate factory (CARANNANTE et al., 1988, NELSON, 1988, JONES & DESROCHERS, 1992, JAMES, 1997, SCHLAGER, 2005), with ambient water temperature as the major driver defining the carbonate-producing associations (JAMES, 1997, SCHLAGER, 2005), and additional factors influencing the type of carbonate factory such as nutrient input (HALLOCK & SCHLAGER, 1986). The tropical carbonate factory is dominated by photo-autotrophic organisms, symbiont-free heterotrophs are common but non-diagnostic (Schlager, 2005). In the cool-water factory, heterotrophic organisms dominate, and nutrient levels are generally higher than in the tropical factory. The transition between the tropical and the cool-water factories is gradual, and was termed warm-temperate carbonate province by BETZLER et al. (1997).

A modern example of warm-temperate carbonate sediments was described by COLLINS et al. (1993) and JAMES et al. (1999) from south-western Australia. Sea grass and macrophytes are rooted in sediments rich in coralline algae and larger benthic foraminifers above coralline-encrusted hardgrounds. Heterotroph elements such as bryozoans, molluscs, and small foraminifers are abundant. *Halimeda* is poorly calcified and is not a carbonate sediment source. Coral reefs occur as small fringing reef complexes, but also as shelf-edge reefs embedded in rhodolith gravel. Another example of modern warm-temperate sedimentation are the carbonates in the Gulf of California reported by HALFAR et al. (2004). Carbonate is produced in pocket bays and dominated by rhodoliths, with frequent molluscs and coral patches.

Lower and Middle Miocene Mediterranean neritic carbonate facies have biotic associations resembling these recent warm-temperate assemblages (ESTEBAN, 1996, PEDLEY, 1996, BRANDANO, 2003). The Neogene carbonates contain abundant heterozoan elements with intercalations of photozoan deposits (e.g. PEDLEY, 1996, CHERCHI et al., 2000, GALLONI et al., 2001). An intermediate, subtropical water temperature for these deposits can be deduced from the coral species and diversity. According to ROSEN (1999), Mediterranean coral associations indicate minimum sea surface water temperatures of 19°-21°C for the Aquitanian and Burdigalian, and of 18°-20°C for the Langhian and Serravallian. This is the cool end of the tropical province and the transitional zone to the warm-temperate province.

Here, we address facies models and sequence stratigraphy of Burdigalian warm-temperate and tropical carbonates which were deposited in the Sardinia rift basin (MARTINI et al. 1992, CHERCHI et al., 2000, BASSI et al., 2006). Carbonate

sedimentation is patchy and locally mixed with siliciclastic sediments. Outcrop quality is excellent. The carbonate factory mainly consists of coralline algae, bryozoans, molluscs, larger benthic foraminifers, and corals (CHERCHI et al., 2000, SIMONE et al., 2001, VIGORITO et al., 2006). Coral diversity is low, with *Porites*, *Tarbellastrea*, *Montastrea*, *Favites*, and *Thegioastrea* (CHERCHI et al., 2000, GALLONI et al., 2001). The carbonates were addressed as temperate and subtropical in origin by MURRU et al. (2001), BASSI et al. (2006), and VIGORITO et al. (2005, 2006).

The purpose of this contribution is to report on the facies of these warm-temperate carbonates, and to show their stratigraphic architecture. A turnover in platform geometry from a ramp *sensu* BURCHETTE & WRIGHT (1992) to a steep-flanked platform with slope angles of 25° is accompanied by a change from a warm-temperate to a tropical carbonate factory.

GEOLOGICAL SETTING AND STRATIGRAPHY

The Neogene sediments were deposited in halfgrabens that have been formed in the Oligo-Miocene. Halfgraben formation was related to the counter-clockwise rotation of the Corsica-Sardinian block due to the opening of the Western Mediterranean back-arc basin and subduction of Neotethyan oceanic crust to the east of Sardinia (e.g. CHERCHI & MONTADERT, 1982, THOMAS & GENNESSEAUX, 1986, FACCENNA et al., 2002, SPERANZA et al., 2002). In northern Sardinia, the multiphase structural movements, accompanied by extensive volcanism, led to the formation of two N-S oriented halfgraben systems. The western branch consists of the Porto Torres Basin in the North, separated from the southern Logudoro Basin by a transfer zone (THOMAS & GENNESSEAUX, 1986, FUNEDDA et al., 2000, Fig. I.2.4).

The eastern branch contains the Castelsardo Basin to the north and the Perfugas Basin to the south (THOMAS & GENNESSEAUX, 1986, SOWERBUTTS, 2000). Faults in the Castelsardo Basin dip to the west, whereas they dip to the east in the Perfugas Basin. Both areas are separated by a range of hillocks, located between the small town of Castelsardo and the village of Sedini (Fig. I.2.4), which may indicate buckling in an accomodation zone (FAULDS & VARGA, 1998). Basins in northern Sardinia contain marine Miocene siliciclastics and carbonates (POMESANO CHERCHI, 1971, ARNAUD et al., 1992, MARTINI et al., 1992, SOWERBUTTS, 2000, MONAGHAN, 2001, VIGORITO et al., 2006).

Based on outcrop studies in the Castelsardo and Perfugas basins, SOWERBUTTS (1997, 2000) distinguishes 3 tectonic phases. The first, late Oligocene phase is the rift formation, followed by a late Chattian to early Aquitanian second phase of E-W

to NW-SE oriented faulting. A third phase of N-S to NNW-SSE striking faulting occurred during the early Burdigalian. The relief, which was flooded during the Burdigalian, was shaped by the third tectonic phase and deposition of a series of dacitic ignimbrites between 19 and 17 Ma (LECCA et al., 1997). The ignimbrites are overlain by the Perfugas Fm. (SOWERBUTTS, 2000, i.e. "Lacustre" *Auct.*), which consists of volcanoclastics and lacustrine sediments. Siliciclastic sediments were formed in a fluvial to alluvial environment after the lacustrine and volcanoclastic deposits.
Marine carbonates, denominated Sedini Limestone (THOMAS & GENNESSEAUX, 1986), overlie the lacustrine and alluvial deposits and the volcanics (Figs. II.1.a.1, II.1.a.2).

ARNAUD et al. (1992) assign the carbonates to the TB 2.1 and TB 2.2 cycles (i.e., latest Aquitanian and Burdigalian, HAQ et al., 1988). According to SOWERBUTTS (2000), this sedimentary unit is late Burdigalian to Langhian in age (18-15 Ma). Calcareous nannoplankton associations indicate that deposits were formed in the upper part of NN4 and the lowermost part of NN5 (C. MÜLLER, pers. comm. 2006). The Sedini Limestone Unit consists of two depositional sequences separated by an erosional unconformity. Deposits are massive limestones, bedded limestones and marlstones that form a carbonate platform with an extension of approximately 19km^2 (Fig. II.1.a.1). This study analyzes the Burdigalian to Langhian limestone succession (Fig. II.1.a.2) in the Perfugas Basin.

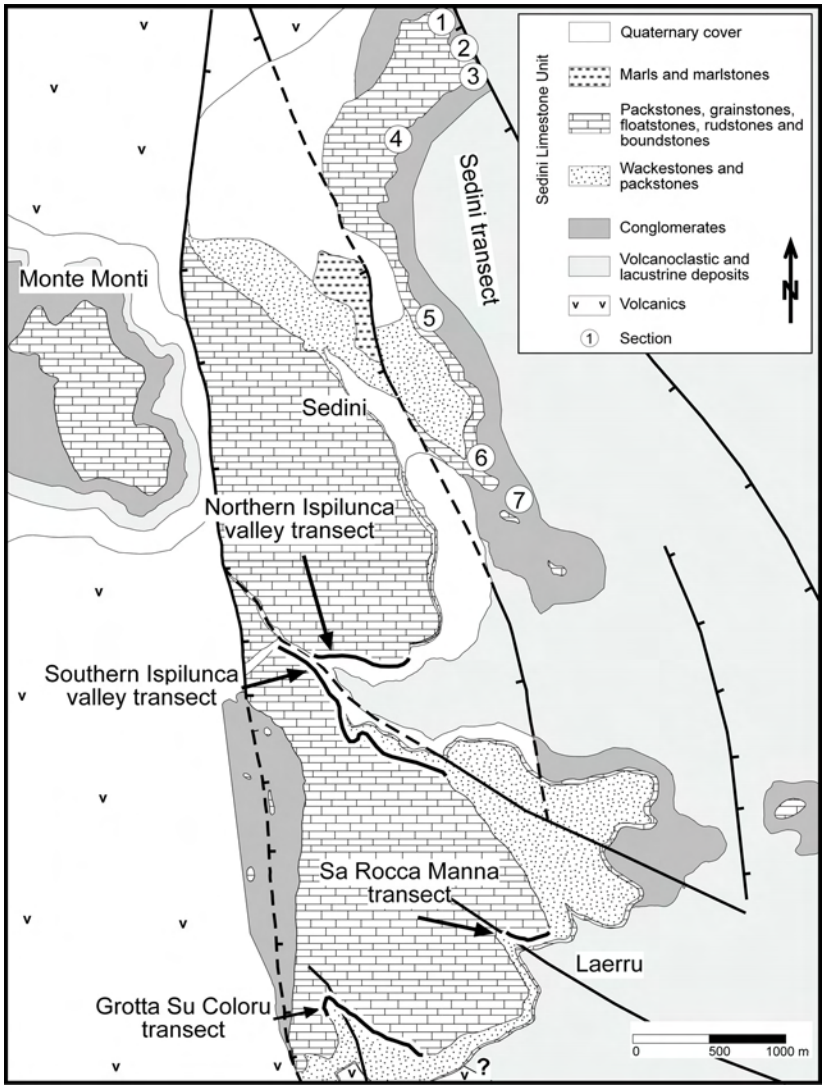

Fig. II.1.a. 1: Geological map of the working area showing distribution of main lithologies with location of the transects discussed in the text. Numbers refer to sections included in the Sedini transect. Based on ALBERTSEN (2005), GIENAPP (2005), and NAGEL (2005).

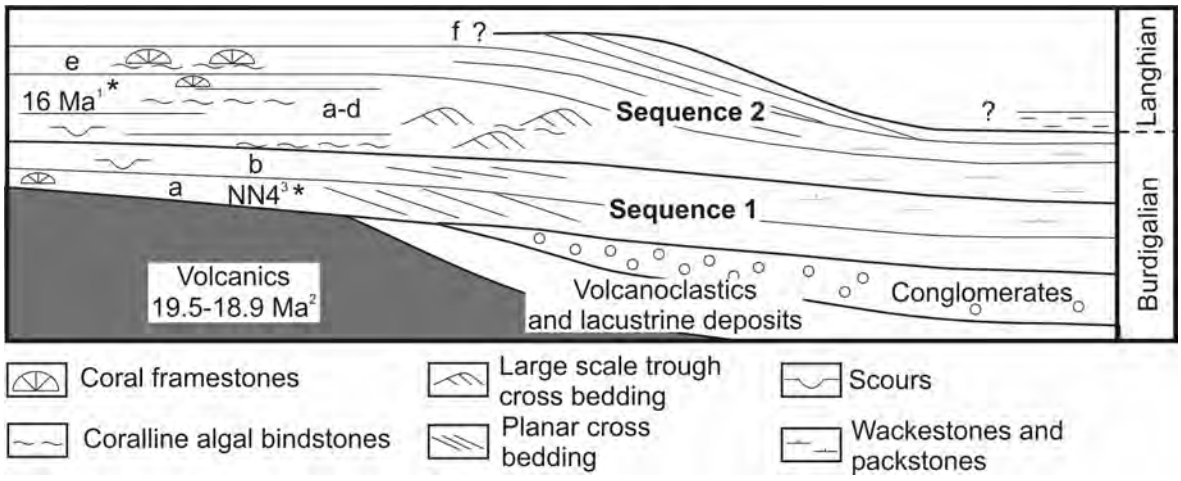

Fig. II.1.a. 2: Miocene stratigraphy of the northern part of the Perfugas Basin in the area of Sedini and Laerru. Age information compiled by following sources: 1: Sowerbutts (1997), 2: Beccaluva et al (1997), 3: Calcareous Nannoplankton (C. MÜLLER, pers. comm. 2006).

THE SEDINI LIMESTONE UNIT

The Sedini Limestone Unit (THOMAS & GENNESSEAUX, 1986) is a 10-60m thick succession situated between Sedini and Laerru, south of Castelsardo (Fig. I.2.4). The stratigraphic architecture of the deposits is shown in Fig. II.1.a.2, Fig. II.1.a.1 presents a detailed geological map. Overlying the volcanic rocks, there is a volcanoclastic and lacustrine unit, followed by cross-bedded fluvial conglomerates. Marine deposits are carbonates, which consist of packstones to rudstones with boundstones, and fine-grained wackestones and packstones. A small carbonate platform is dissected by a series of NNW-SSE running faults (Fig. II.1.a.1). Offsets indicate postsedimentary activity of these faults. It cannot be excluded that these movements occurred as reactivations of older structures because the fluvial conglomerates, and the lowermost marine carbonates wedge out along faults. Such a process of local fault reactivation is imaged in the seismic line published by THOMAS & GENNESSEAUX (1986, Fig. I.2.5) in the Castelsardo Basin to the north. In this line, the sequence that corresponds to the Sedini Limestone Unit drapes a fault block relief, but some of the faults also propagate into this sequence. Mapping shows that the youngest marine deposits in the study area are partially silicified bedded marls and marlstones with frequent sponge spicules, benthic foraminifers and fish remains located to the North-northeast of the village of Sedini (Fig. II.1.a.1).

SELECTED TRANSECTS

Geometries, facies and stratigraphy of the carbonate platform are well exposed in a series of ravines cross-cutting the carbonate body. For this study, five transects along valleys and cliffs were selected (Fig. II.1.a.1). Photo panoramas were taken from four of the transects and, where accessible enough, sections were measured. In the case of the Sedini transect, no such photo panorama could be made, owing to the wide extent of this transect and the degree of vegetation cover.

Fig. II.1.a. 3 (next page): Northern Ispilunca valley transect with interpretation of erosional surfaces, sequences, and depositional geometries. Bars and numbers S5-S8 indicate position of lithological sections. Roman numerals refer to erosional surfaces.

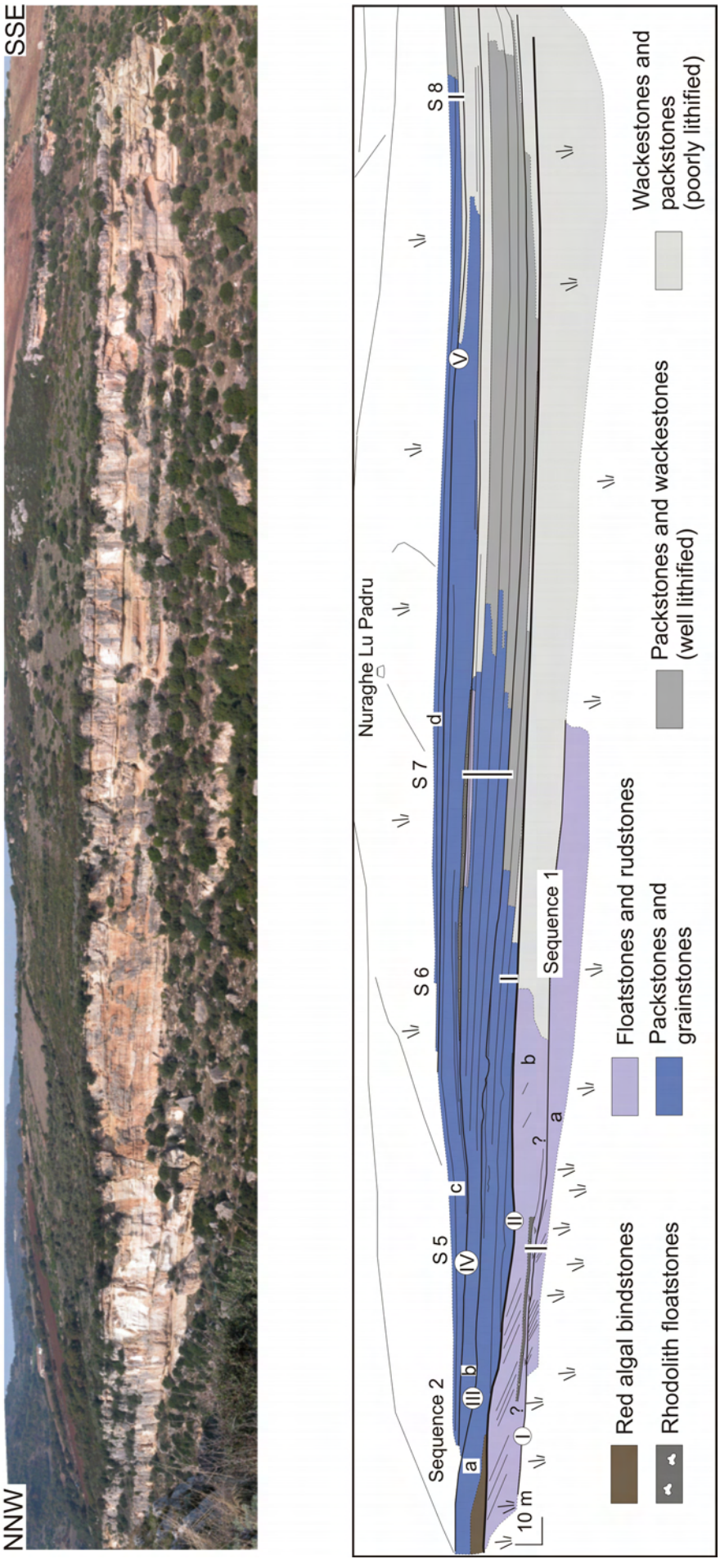
SSE
NNW
Nuraghe Lu Padru
S 8
S 7
S 6
S 5
d
c
b
a
V
IV
III
II
I
?
Sequence 2
Sequence 1
10 m
Red algal bindstones
Rhodolith floatstones
Floatstones and rudstones
Packstones and grainstones
Packstones and wackestones (well lithified)
Wackestones and packstones (poorly lithified)

Ispilunca Valley Transects

The Ispilunca valley crosscuts the Sedini Limestone Unit in a Northwest–Southeast direction (Fig. II.1.a.1). The northern and southern cliffs of this valley provide excellent insight into the internal geometries of most of the succession.

Northern Ispilunca Valley Transect

The transect is roughly oriented NNW-SSE, approximately 40m high and 520m long. It contains the lower and middle part of the Sedini Limestone Unit, the basal contact between the conglomerates and the carbonates is not exposed. The cliff is partially accessible and four sections were measured. The location of these sections is shown in Fig. II.1.a.3.

Section S5 is 5m long and comprises 4.20m of floatstones and rudstones with large-scale, straight-crested foresets arranged in simple sets (ANASTAS et al., 1997) in its base. The dip of the cross-beds is to the east. The floatstones and rudstones contain frequent branches of coralline algae, rhodoliths (3-5cm), *Heterostegina sp.* and *Amphistegina sp.* as main components. Other components are bivalves, echinids and bryozoans. The top of the cross-bedded interval is truncated (surface indicated with roman letter "I" in Fig. II.1.a.3) and overlain by a 30-40cm thick interval with medium-scale, trough cross-bedding. This interval is followed by a 40-50cm thick floatstone with abundant rhodoliths and barnacles. A further floatstone to rudstone interval with large-scale, straight-crested foresets overlies the rhodolith floatstone. One erosive surface (I), divides Section S5 into two sequences. A detail of this situation is shown in Fig. II.1.a.4. To the SSE, the upper cross-bedded interval interfingers with poorly lithified wackestones and packstones.

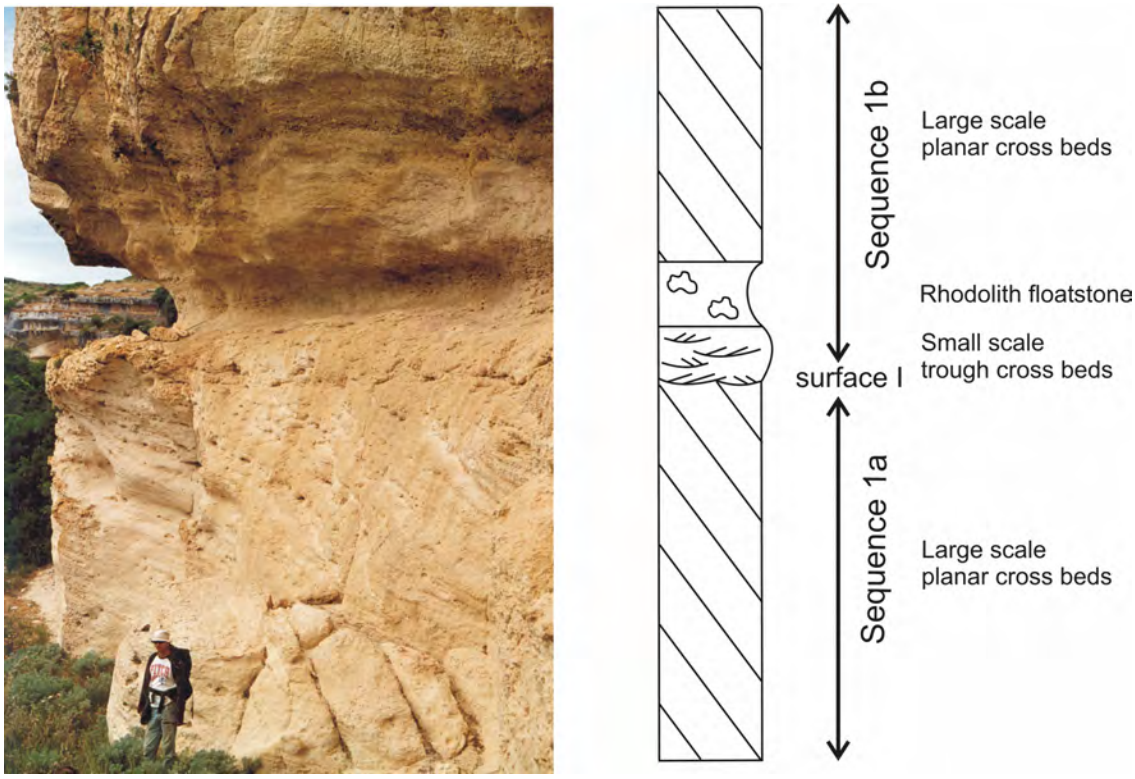

Fig. II.1.a. 4: Large-scale, planar cross-bedding in deposits of sequences 1a and 1b in the northern Ispilunca valley transect. Note that the topmost part of the lower planar cross-beds is reworked and overlain by an interval with trough cross-bedding. The boundary between sequences 1a and 1b is placed at the base of the trough cross-bedded interval.

Section S6 is 4.50m long and contains 1.50m of poorly lithified, bioturbated wackestones and packstones with echinids and bivalves in its base. Above a sharp surface, indicated as "II" in Fig. II.1.a.3, a 3m thick interval of packstones and grainstones with abundant echinid debris follows. To the SSE, these packstones and grainstones grade into wackestones and packstones. To the NNW, the packstones and grainstones onlap surface II. Here, the deposits display small-scale, trough cross-bedding and cut-and-fill-structures. Further to the NNW, surface II is directly overlain by 2 m thick coralline-algal bindstones (Fig. II.1.a.5), which contain encrusting forms of *Sporolithon sp.*, *Lithophyllum sp.*, *Mesophyllum sp.* and *Neogoniolithon sp*. Other components are bivalves (e.g. *Spondylus sp.*, *Pecten sp.*, *and Isognomon sp.*), bryozoans, larger benthic foraminifers, encrusting foraminifers, echinid spines, and complete echinids.

Fig. II.1.a. 5: Coralline-algal bindstone of sequence 2a. Outcrop is located at the northern termination of the Ispilunca valley.

Section S7 is 18.50 m long and starts with a 50cm thick bioturbated wackestone and packstone with complete echinids, rare small rhodoliths, and bivalves. Above a sharp surface (III), 4m of packstones and grainstones with coralline-algal branches, echinid and bivalve debris, bryozoans, *Heterostegina sp.*, *Amphistegina sp.,* and rare coral fragments follow (Fig. II.1.a.6).

To the NNW, surface III is characterized by channel-shaped cut-and-fill structures. Above this interval, 14m of packstones and grainstones (with intercalated floatstones and rudstones) with rhodoliths, pectinid fragments, barnacles, bryozoans, some coral fragments, and miliolid foraminifers occur. A sharp surface (IV) is overlain by a 50cm thick and 60m wide lense of floatstones and rudstones with rhodoliths and oysters. Overlying packstones and grainstones drape this lense. To the SSE, the deposits of S7 grade into strongly bioturbated, bedded wackestones and packstones with fragmented bivalves, bryozoans, echinids, and complete irregular echinids, which occur mostly at the base of fining-upward cycles. As shown in Fig. II.1.a.3, these deposits show different degrees of lithification, ranging from well to poorly lithified. Poorly lithified limestones are finer-grained and less sorted than the well-lithified deposits.

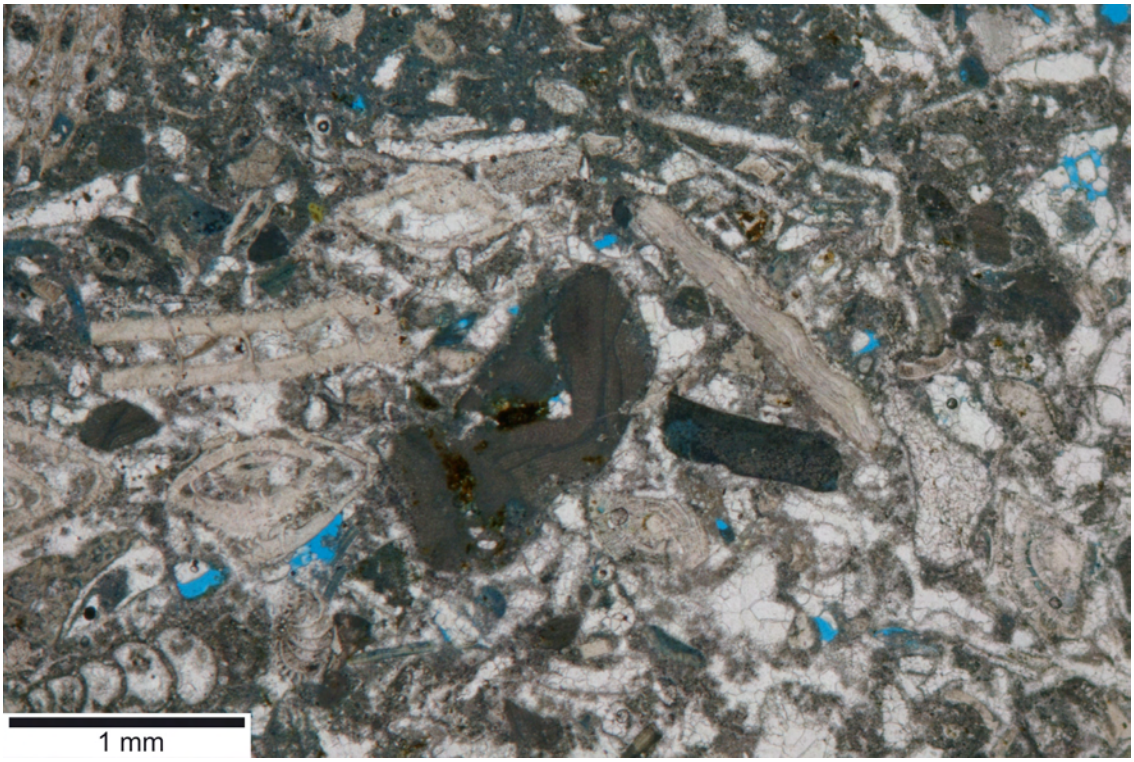

Fig. II.1.a. 6: Packstone with the larger benthic foraminifer *Amphistegina sp.*, and debris of the larger benthic foraminifer *Heterostegina sp.*, bivalve debris, coralline-algal debris and other bioclasts. Sequence 2b, northern Ispilunca valley transect, section S7.

Section S8 is 10m thick. The base is surface V. Above this surface, 1.50m of bioturbated wackestones and packstones occur, followed by 50cm of a rhodolith floatstone and 8m of packstones and grainstones with abundant echinid fragments, coral fragments, and coralline-algal debris. To the SSE, the packstones and grainstones grade into well lithified wackestones and packstones.

Interpretation

In the northern Ispilunca valley transect, six sediment packages occur, subdivided by five surfaces. The most prominent of these is surface II, an erosional feature cutting down into the underlying deposits up to 5m. We interpret this surface as a sequence boundary triggered by a relative sea-level fall, dividing the succession of the northern Ispilunca valley into two sequences (1 and 2). Both sequences furthermore consist of high-frequency sequences (1a, b and 2a-d).

Large-scale cross-bedded floatstones and rudstones in sequences 1a and 1b are interpreted to have formed in submarine bars. Bars migrated to the east, the floatstones and rudstones interfinger with finer-grained, bioturbated deposits. Preservation of bioturbation and the occurrence of well-preserved, complete echinids are interpreted to represent an environment below regular wave-base.

In the upper part of sequence 1a, the well-defined contact between the straight foresets and the trough cross-bedded interval is interpreted to reflect a change of the hydrodynamic conditions. Migration of the bar system was interrupted, and the top of the bar was reworked. Trough cross-beds indicate that this reworking has been triggered by wave action. It is proposed that this is a consequence of a wave-base lowering, most probably triggered by a relative sea-level fall.
A subsequent deepening of the depositional system is recorded by the rhodolith floatstones (NALIN et al., 2007), which locally drape the underlying, trough cross-bedded deposits. Reinstoration of a submarine bar system is indicated by the occurrence of the straight crested bars overlying the coralline-algal interval.

Sequence 2 is subdivided into four higher-frequency sequences (2a-2d) by surfaces III-V. The lowermost deposits are infills of the erosional topography created by the sequence boundary (II). Coralline-algal bindstones, which directly overlie the sequence boundary in the westernmost part of the outcrop, reflect a deepening after the relative sea-level lowstand, which triggered formation of the sequence boundary. According to BOSENCE (1991), the occurrence of the coralline-algal genera *Sporolithon sp.*, *Lithophyllum sp.*, *Mesophyllum sp.* and *Neogoniolithon sp.* in the coralline-algal bindstones of sequence 2a points to water depths of 40m. The lateral and downdip change from limestones to marlstones and marls indicates a change from hydrodynamically more agitated to quieter waters, which is interpreted as a deepening from a position around storm wave-base to below storm wave-base towards the SSE. This is indicated by the cut-and-fill-structures in the packstones and grainstones of sequences 2a and b, which are interpreted to be caused by storms. The equivalent, finer-grained packstones and wackestones occurring in the SSE are well bedded and locally contain tempestite layers, and are therefore thought to have been deposited in a deeper and quieter environment below storm wave-base.

Fig. II.1.a. 7 (next page): Southern Ispilunca valley transect with position of the sequence boundary (II), and the high-frequency sequence limits (roman numerals). As most of this outcrop is inaccessible, no lithological information is provided. Position of accessible coral reefs is indicated.

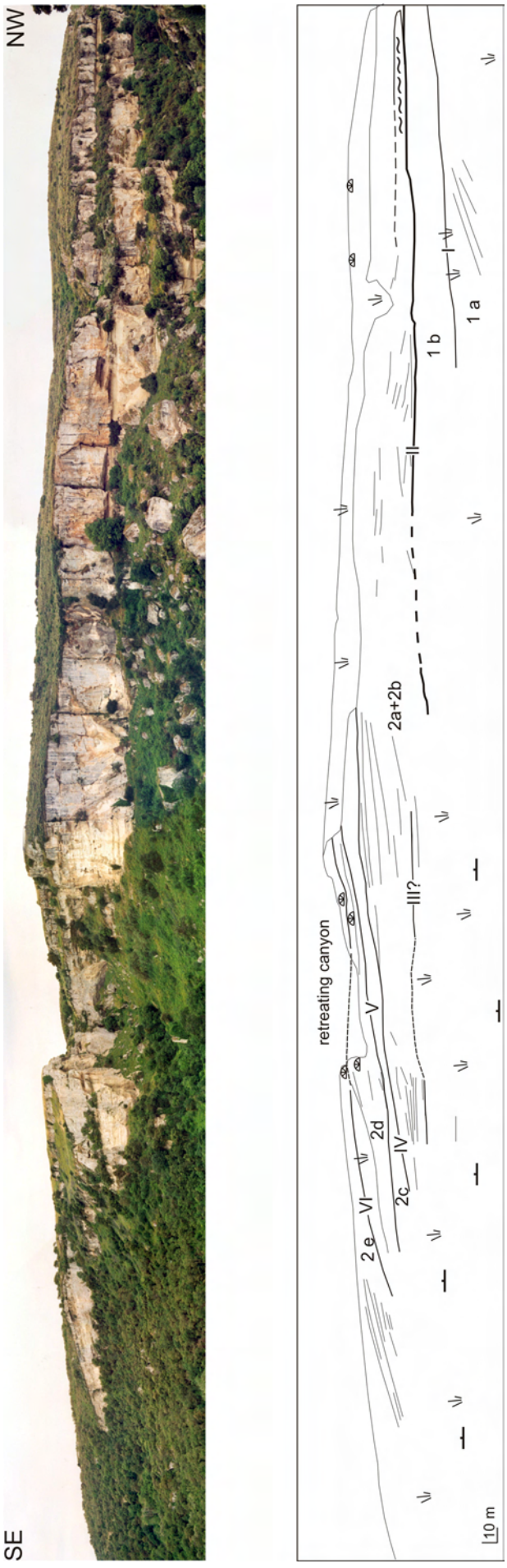
NW
SE
retreating canyon
1 a
1 b
2a+2b
III?
V
2d
IV
2c
VI
2 e
10 m

Southern Ispilunca Valley Transect

The southern Ispilunca valley transect is oriented Northwest-Southeast, has a length of approximately 1500m, and is approximately 40-50m high. The steep cliff is only accessible at several places and therefore, mainly depositional geometries are shown in Fig. II.1.a.7. We visually correlated the surfaces with the ones occurring in the northern Ispilunca valley transect at the north-western termination of the valley, where it is only 50m wide.

The basal contact of the limestones to the underlying conglomerates is not exposed in this transect. In the lowermost portion of the cliff (1a), floatstones and rudstones comprising large-scale cross-beds with straight foresets dipping to the east are exposed. The floatstones and rudstones are composed of echinid and coralline-algal debris, and *Amphistegina sp.* as main components. Additional content are bivalves and bryozoans. Sediment package 1b physically corresponds to the second set of cross-beds observed in the northern Ispilunca valley transect. However, it is a massive to poorly bedded sediment package in this transect. The two units are separated by surface I, which cannot be traced further to the southeast because of the vegetation cover. Above surface II, which displays a SE oriented, downward flexure, a thick package with large-scale, trough cross-bedding (2a+2b) occurs. In the North-West, this surface is directly overlain by coralline-algal bindstones. In the south-eastern part of this package, there is evidence for a dividing surface, which cannot be traced further to the north-west. This surface is tentatively correlated to surface III of the previously described transect. The large-scale, trough cross-beds are truncated by surface IV. This surface is cut by the recent topography and cannot be traced further to the north-west. However, it displays an inclined geometry. The following unit (2c) displays no visible sedimentary structures, but drapes the moderate slope defined by the lower bounding surface IV. Surface V is the lower bounding surface of a gently inclined, wedge-shaped sediment package (2d), which in its upper portion contains small coral reefs associated with oyster framestones at their base. Deposits of the package 2e overlying surface VI, are clinoforms dipping with up to 25° to the ESE. Clinoforms contain abundant rhodoliths, and locally are rhodolith rudstones. Upslope, clinoform floatstones and rudstones interfinger with coralgal boundstones up to 6 m thick. Corals form crusts alternating with crustose coralline algae. These coral deposits occupy the entire plateau at the top of the cliff, laterally extending for almost 1km, and locally form framestones (Fig. II.1.a.8).

Fig. II.1.a. 8: Coral framestone of sequence 2e at the northern end of the southern Ispilunca valley transect.

Interpretation

Surface II subdivides this succession into two sequences (1 and 2). The erosional character of the sequence boundary, however, is more pronounced in the northern Ispilunca valley transect. Above the sequence boundary, a gradual increase in inclination of both surfaces and depositional geometries documents a steepening of the depositional relief throughout the evolution of the carbonate platform. Steepening coincides with the inception of boundstones, e.g. the coralline bindstones of sequence 2a+b and the coral reefs of sequences 2d and 2e. In addition to coralline-algal bindstones, sequence 2a+b consist of large-scale, trough cross-bedded packstones and grainstones, which are interpreted as a system of submarine dunes.

During the deposition, a platform geometry formed, with submarine dunes at the platform margin locally stabilized by boundstones and framestones. At the latest stage of carbonate platform development (sequence 2e), the depositional system consisted of a reef flat with a marked slope break and fore-reef bioclastic and rhodolithic limestones.

The increase of slope inclination appears much more pronounced in the southern than in the northern Ispilunca valley transect. This is the consequence of transect orientation, which in the northern transect is oblique to the platform slope.

Sa Rocca Manna Transect

This transect is located along a cliff 1.8km SSE of the Ispilunca Valley (Fig. II.1.a.1). Being almost completely accessible, it was investigated in detail, and seven sections were measured. The WNW-ESE oriented cliff is 200m wide and 20m high (Fig. II.1.a.9).

In its lower part, the cliff consists of a 17m thick interval of packstone and grainstone beds dipping up to 15° to the east. These deposits grade into flat-bedded, biodetritic wackestones and packstones, which further to the east grade into finer grained deposits and marlstones. Packstones contain fragments of echinids, bivalves, as well as branches of coralline algae. Molluscs are preserved as molds, mostly with micritic rims. Coral detritus is a minor component. The amount of coralline-algal debris increases upsection. Wackestones and packstones are rich in benthic foraminifers, bryozoans, and serpulids. Marlstones contain planktic foraminifers, echinids, bryozoans, and bivalves, which are preserved as molds. In the zone with inclined bedding, 2m thick and 5–6m wide coralline-algal bindstone lenses with *Lithophyllum sp*., *Mesophyllum sp*. and *Sporolithon sp*. occur (Fig. II.1.a.9). A 50cm thick, bioclastic floatstone bed with bivalves, rhodoliths, and coral fragments overlies the echinid packstones and the flat-bedded wackestones and packstones. The bed can be traced over a distance of approximately 110m (Fig. II.1.a.9).

Fig. II.1.a. 9 (next page): Sa Rocca Manna transect with interpretation of stratigraphic architecture in high-frequency sequences 2d–2f. Letters a–e in the photograph refer to detail photos in Fig. II.1.a.10.


ESE
WNW
a
b
c
d

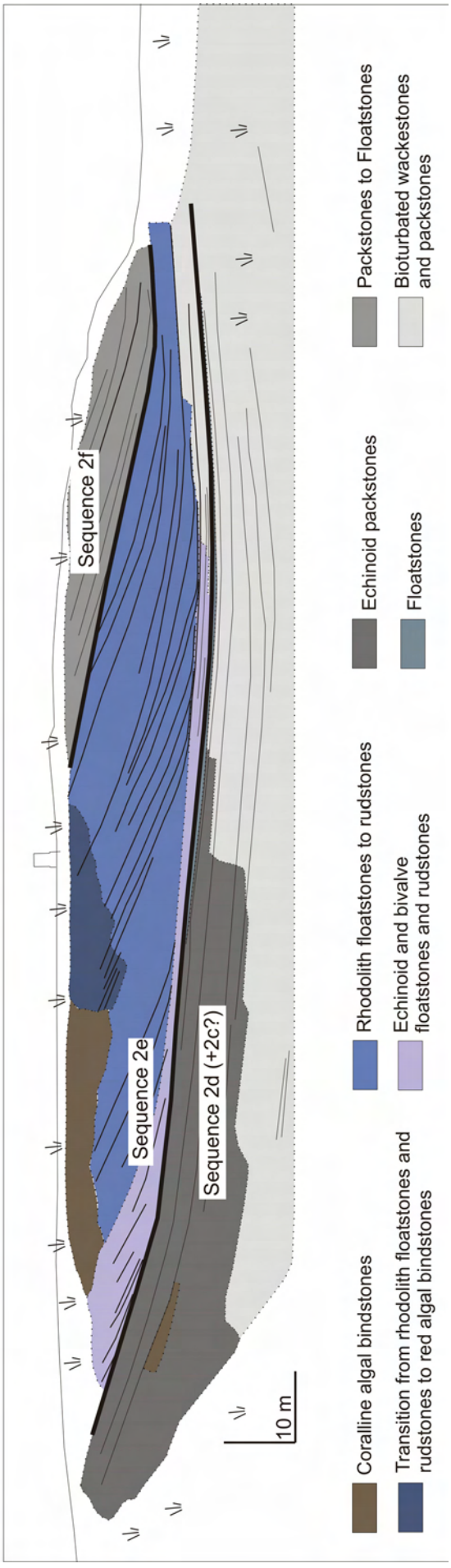
Sequence 2f
Sequence 2e
Sequence 2d (+2c?)
10 m
Coralline algal bindstones
Transition from rhodolith floatstones and rudstones to red algal bindstones
Rhodolith floatstones to rudstones
Echinoid and bivalve floatstones and rudstones
Echinoid packstones
Floatstones
Packstones to Floatstones
Bioturbated wackestones and packstones

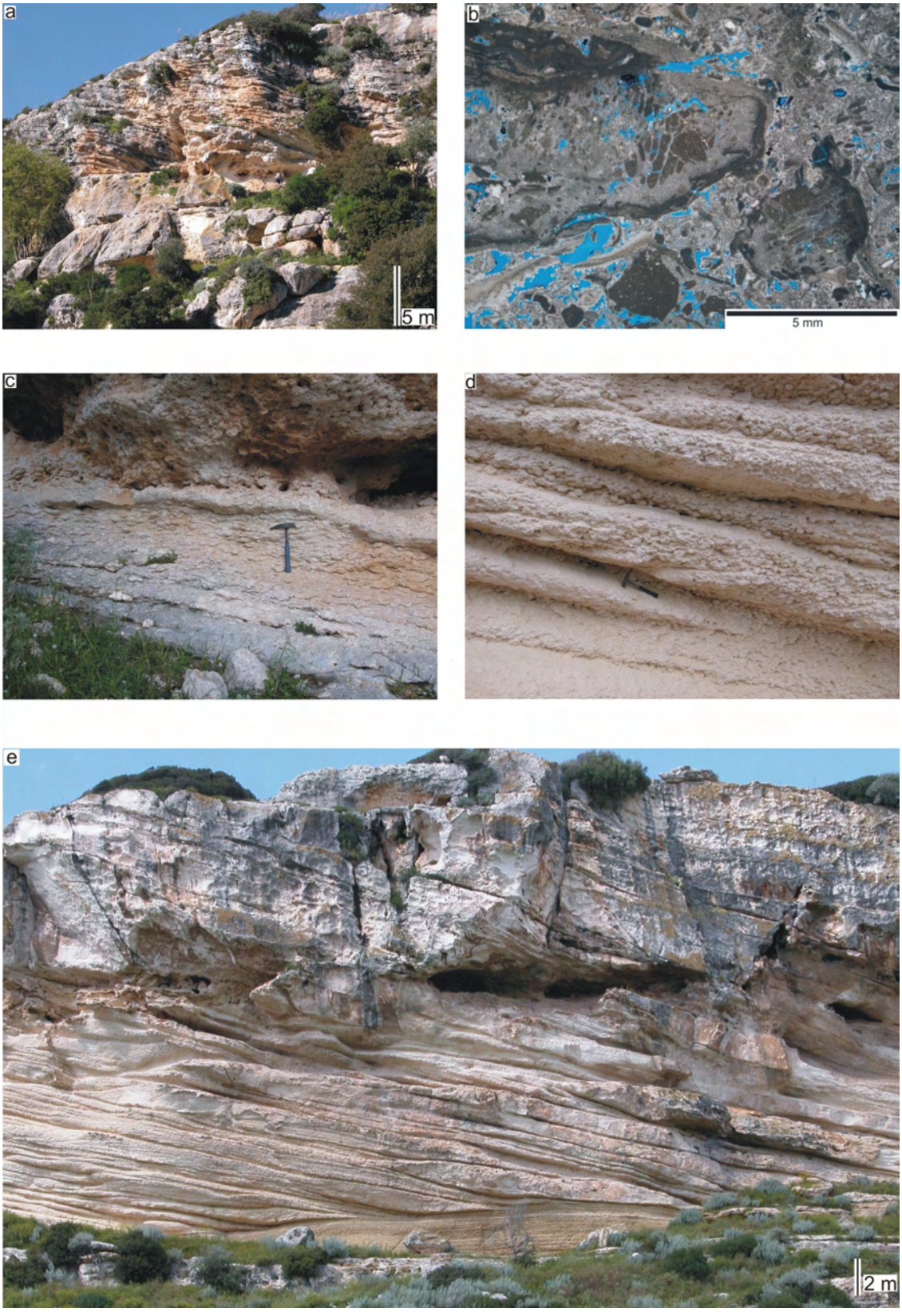
a
5 m
b
5 mm
c
d
e
2 m

Fig. II.1.a. 10 (previous page): Details of the Sa Rocca Manna transect.
a: Change from packstones and grainstones of sequence 2c/d to steeply dipping large-scale, planar cross-bedded echinid and bivalve floatstones and rudstones. The surface separating both units is the boundary between high-frequency sequences 2d and 2e. **b:** Thin section photograph of large-scale cross-bedded floatstones and rudstones with coralline-algal encrusted coral debris. **c:** Transition from a coralline-algal bindstone to rhodolithic floatstones and rudstones in the topset area of the rhodolthic clinoforms. This facies forms the platform edge in sequence 2e. **d:** Rhodolithic clinoforms. Note subhorizontal internal layering. **e:** View of the clinoforms, which are approximately 20m high. Note that each clinoform bed passes into an only few centimetres thick, planar floatstone bed. There is no indication of slumping, channels or any type of redeposition in this transect.

The top of this lower sedimentary unit is located at a surface, at which a significant increase in dip of the beds up to 15-20° occurs (Figs. II.1.a.9, II.1.a.10a). Above this surface, a 30cm thick layer of fine-grained packstones is overlain by floatstones and rudstones with abundant echinid and bivalve debris, as well as debris of corals (Fig. II.1.a.10b). The fine-grained packstones are the bottom-set deposits of the steeply dipping, coarse-grained limestones.

Floatstones and rudstones are overlain by a 2m thick coralline-algal bindstone in the north-western part of the outcrop. To the south-east, topset bindstones get enriched in rhodoliths (Fig. II.1.a.9). Downslope, this bindstone grades into a rhodolith rudstone arranged in 20m high clinoforms dipping with up to 27° to the south-east. A detailed view of the topsets of the clinoforms is shown in Fig. II.1.a.10c. Topset beds have wavy surfaces. Rhodoliths are ellipsoidal to discoidal, and up to 10cm large. They are closely packed and have been fused in a later stage by continued coralline-algal encrustation.

Clinoform beds have complex internal geometries, and each of the clinoform beds is a composite body (Fig. II.1.a.10d) with a subhorizontal internal layering, similar to rudimentary stratifications described in rhodolithic deposits in New Zealand (BURGESS & ANDERSON, 1983). Some of the clinoform beds wedge out upslope (Fig. II.1.a.10e). The bottomset of the clinoforms is depicted in Fig. II.1.10e. Each clinoform bed terminates in a 5 to 10cm thick layer of bivalve rudstone grading into an echinid floatstone away from the slope. In the bivalve rudstone, well-preserved pectinids occur. The bottomsets climb up during formation of this sediment package.

Along the clinoforms, rhodolith size decreases downslope from approximately 10 to 5cm. Upslope, rhodoliths predominate, while towards the bottomsets, the amount of matrix between the rhodoliths increases. Rhodoliths in the upper part of the clinoforms are both sphaeroidal and ellipsoidal, the amount of ellipsoidal rhodoliths increases downslope. In thin sections, the rhodoliths are composed of alternating layers of coralline algae, encrusting foraminifers, and celleporiform bryozoans. Coralline-algal growth is laminar, warty and fruticose, resulting in frequently branched rhodoliths and some laminar concentric rhodoliths (*sensu* BOSENCE, 1983a, and WOELKERLING et al., 1993). Rhodoliths with both growth patterns also occur.
The upper limit of the sediment package is defined by a toplap configuration (Fig. II.1.a.9). The youngest sedimentary unit in this transect is a bioclastic packstone to floatstone with large-scale, planar cross-beds which are only preserved in a small wedge. Beds of this unit downlap onto the unit`s lower bounding surface.

Interpretation
Physical tracing of sediment bodies and geometries between the Ispilunca Valley transect and the Sa Rocca Manna transect shows that this outcrop contains sequence 2 deposits. It is not unequivocally testable if the lower part of the cliff only contains sequence 2d, or if it also includes part of sequence 2c. Sequence 2e makes up the middle part of the succession. An additional high-frequency sequence 2f forms the youngest deposits of the cliff.

Facies and depositional geometries of sequence 2c/d are similar to the facies described in the Ispilunca Valley transects, with coralline-algal bindstones and large-scale, trough cross-bedded, submarine dune deposits. The bindstones are embedded in the large scale, trough cross-bedded deposits and are interpreted to act as sediment stabilizers. The limit between sequences 2c/d and e reflects a turnover of the carbonate factory and depositional system. The Sa Rocca Manna sequence 2e deposits are interpreted to have been formed along the slope of the reef-bearing carbonate platform. Inner platform facies with coral framestones, however, are not exposed in Sa Rocca Manna, but 800m north-westerly of the outcrop. Upper-slope deposits are coralline algal-bindstones grading into a rhodolithic slope (Figs. II.1.a.9, II.1.a.10c). Subhorizontal internal layering of the composite clinoform bodies indicates that these bodies were not formed by sole off-platform shedding of rhodoliths. It is proposed that rhodoliths also grew in-situ along the slope, which resulted in a subhorizontal internal layering. In-situ rhodolith accumulation on slopes is described in the large-scale, rhodolithic clinobeds of

Menorca (OBRADOR et al. 1992, POMAR, 2001, POMAR et al., 2002, BRANDANO et al., 2005) and on fore-reef slopes reported in BOSENCE (1983b).

Toplaps of rhodolith clinoforms in the last progradational episodes of sequence 2e indicate post-depositional erosion before formation of sequence 2f. Deposits of sequence 2f are not discussed any further, because of the poor control of this unit due to missing outcrops.

Grotta Su Coloru Transect

This 1km long cliff along the eastern flank of the valley with the Grotta Su Coloru (Figs. II.1.a.1, II.1.a.11a, d) has a NW-SE orientation and is 40-50m high. Most of the cliff, which consists of the lower part of the Sedini Limestone Unit, is not accessible. Therefore no sections were measured.

The base of the Sedini Limestone succession is not exposed in this cliff. At its north-western termination, the lower part of the cliff consists of bedded packstones to wackestones (Figs. II.1.a.11a, b, c). Above a sharp surface, these are overlain by low-angle, planar cross-beds dipping towards the south-east that interfinger with medium-scale, trough cross-bedded grainstones and packstones (Fig. II.1.a.11b). These grade into planar-bedded wackestones and fine-grained packstones towards the south-east (Fig. II.1.a.11a).

This succession is followed by a 3m thick interval of finer-grained, bioturbated, bioclastic packstone (Fig. II.1.a.11b). At the south-eastern end of the Grotta Su Coloru transect, this interval thickens to 6.5m of bioturbated wackestones and packstones with *Thalassinoides* burrows at the top (Fig. II.1.a.11a). Fine-grained packstones are truncated by erosional incisions (Figs. II.1.a.11 b, c) that are 4–5m broad, cutting down to 1.5m. Infills of the erosive depressions consist of pectinid packstones to floatstones arranged in medium-scale, trough cross-beds (Fig. II.1.a.11b). Overlying the pectinid packstones to floatstones, there is a 3m thick interval of large-scale, low-angle planar cross-bedded packstones and grainstones dipping towards the NE (Fig. II.1.a.11c).

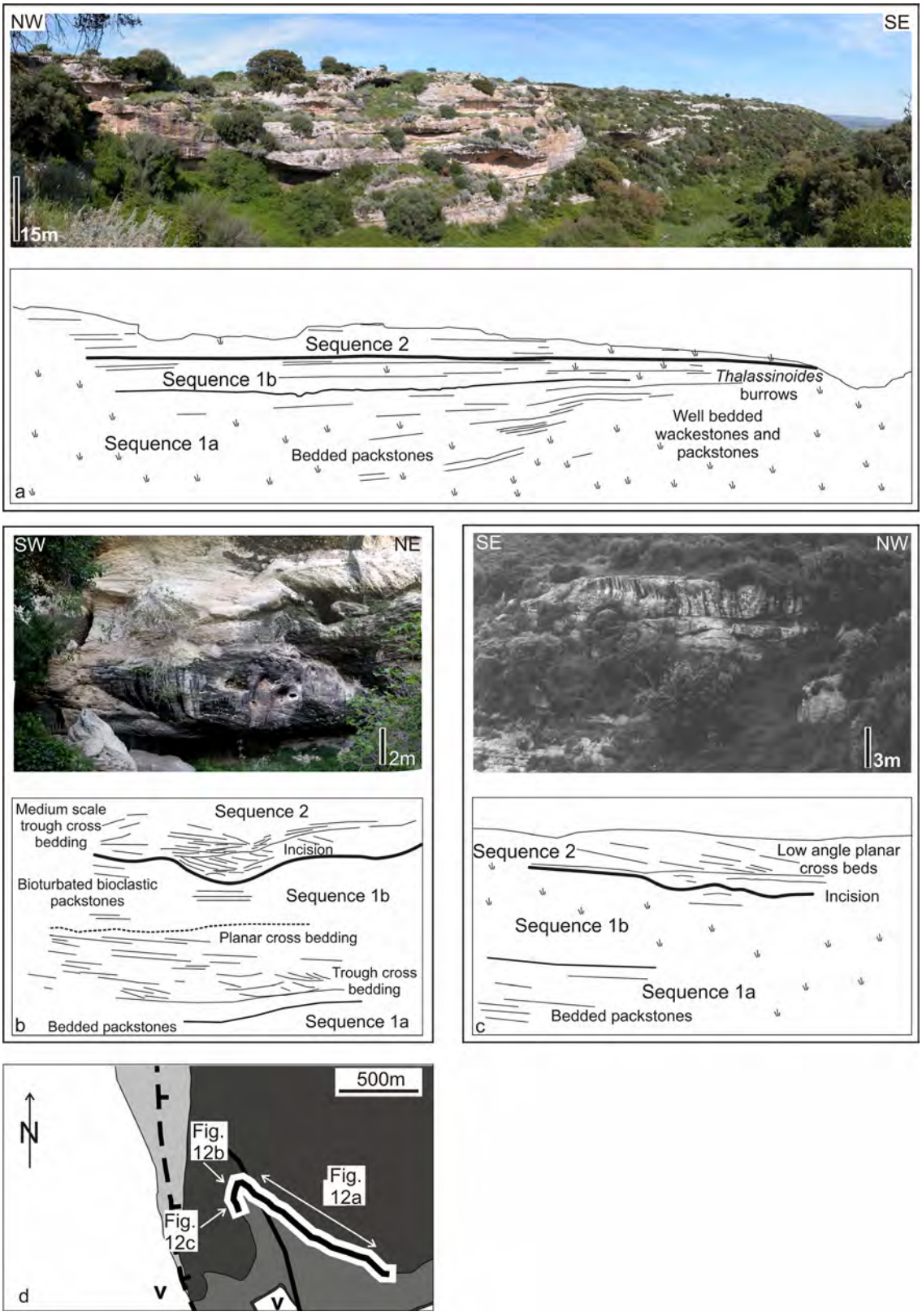

Fig. II.1.a. 11: Grotta Su Coloru transect. **a:** Eastern valley-cliff (approximate height is 40-50m). **b:** Sedimentary structures at the entrance of the Grotta Su Coloru. Height of the wall is approximately 11m, location is shown in the map (d). **c:** Channel incision and low-angle planar cross-bedding in packstones and grainstones in the upper part of the western valley-cliff. Sediment package with cross-beds is approximately 3m thick. Location is shown in the map (d). **d:** Geological map of the Grotta Su Coloru valley (detail of Fig. II.1.a.1) with locations of details shown in Fig. II.1.a.11 a-c.

Interpretation

Most of the Grotta Su Coloru transect consists of sequence 1 limestones, with the lower part of sequence 2 at the cliff's top. High-frequency sequence 1a is separated from high-frequency sequence 1b by a sharp surface (Figs. II.1.a.11b, c). Lateral facies variations in sequence 1b are typical for a beach depositional system (Fig. II.1.a.11b). Low-angle, planar cross-bedding indicates sedimentation in the foreshore area, trough cross-bedding is representative of the shoreface area. Planar-bedded wackestones and fine-grained packstones with *Thalassinoides* burrows (Fig. II.1.a.11a) are interpreted to have formed in a quieter hydrodynamic environment, below fairweather wave-base.

As the contact between the sequence 1a wackestones (Figs. II.1.a.11a, b, c) and the overlying interval of sequence 1b beach deposits (Fig. II.1.a.11b) is a sharp surface, it is suggested as reflecting a forced regression. An increase of the accomodation space during deposition of sequence 1b is reflected by the turnover from beach sediments (Fig. II.1.a.11b) to the bioturbated, finer-grained wackestones to packstones above the trough cross-bedded deposits (Figs. II.1.a.11b, c).

A renewed base-level lowering is indicated by the incision of channels (Figs. II.1.a.11b, c) at the top of the bioturbated limestones. This limit is interpreted to represent the limit between sequences 1 and 2. The later infill of these channels with the medium scale, trough cross-bedded pectinid packstones and floatstones show that the top of the succession at the Grotta valley transect records a base-level rise. Subsequent infill resulting in a reduction of accomodation space is indicated by low-angle, planar cross-bedded packstones and grainstones (Fig. II.1.a.11c). The sedimentary structures identify these deposits as the foreshore area of a beach depositional system.

Sedini Transect

The Sedini transect is 4 km long, and runs in an approximate North-South direction along the cliff below the village of Sedini (Fig. II.1.a.1). It is 6m thick in the North and thickens to 17m in the South. It was reconstructed using seven sections (Figs. II.1.a.1, II.1.a.12). The transect, for its length and vegetation cover, is not documented by photographs.

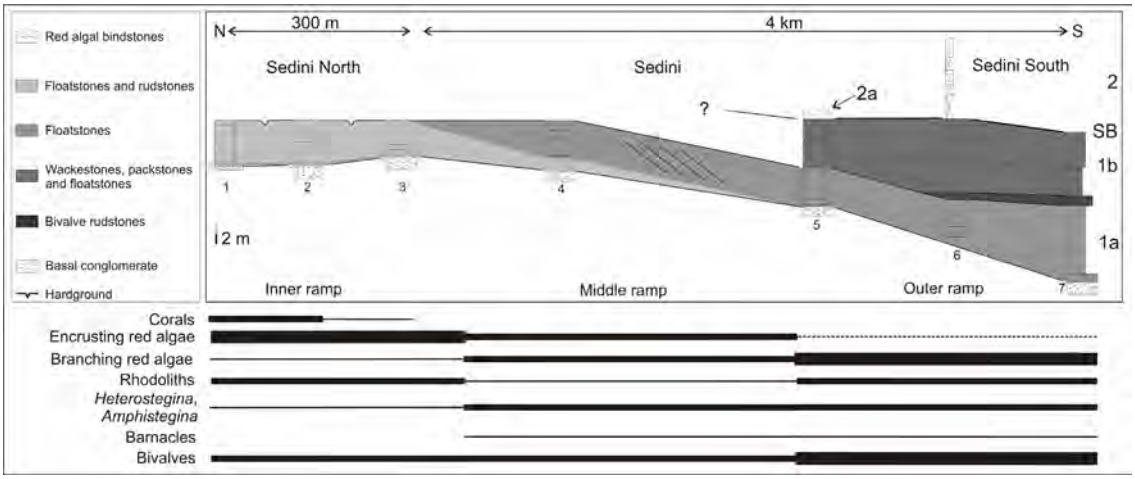

Fig. II.1.a. 12: Sedini transect. Location of lithological sections is shown in Fig. II.1.a.1. Bars indicate relative abundance of selected biota, ranging from rare to very abundant. Note the occurrence of a hardground at the top of the three northern sections. Coralline-algal bindstone at the top of section 5 is interpreted as the lowermost part of sequence 2a.

Most of the sections record the transition between the Sedini Limestone Unit and the underlying fluvial conglomerates. This transition consists of a conglomerate grading upsection into limestones with minor amounts of quartz, feldspar and biotite. The lower part of the limestones contains abundant reworked siliciclastics, with granite boulders up to 15cm in size. In sections 1-3, a layer with thick-shelled oysters occurs in the upper part of the conglomerates. Overlying limestones are floatstones to rudstones containing coralline-algal branches, rhodoliths, bivalves, echinids, bryozoans, and barnacles. In section 1, deposits also contain coral fragments, and the large benthic foraminifer *Borelis sp.* (Fig. II.1.a.13). Some layers contain frequent intraclasts, and the top of the floatstones to rudstones is bored by *Lithophaga* (Fig. II.1.a.14).

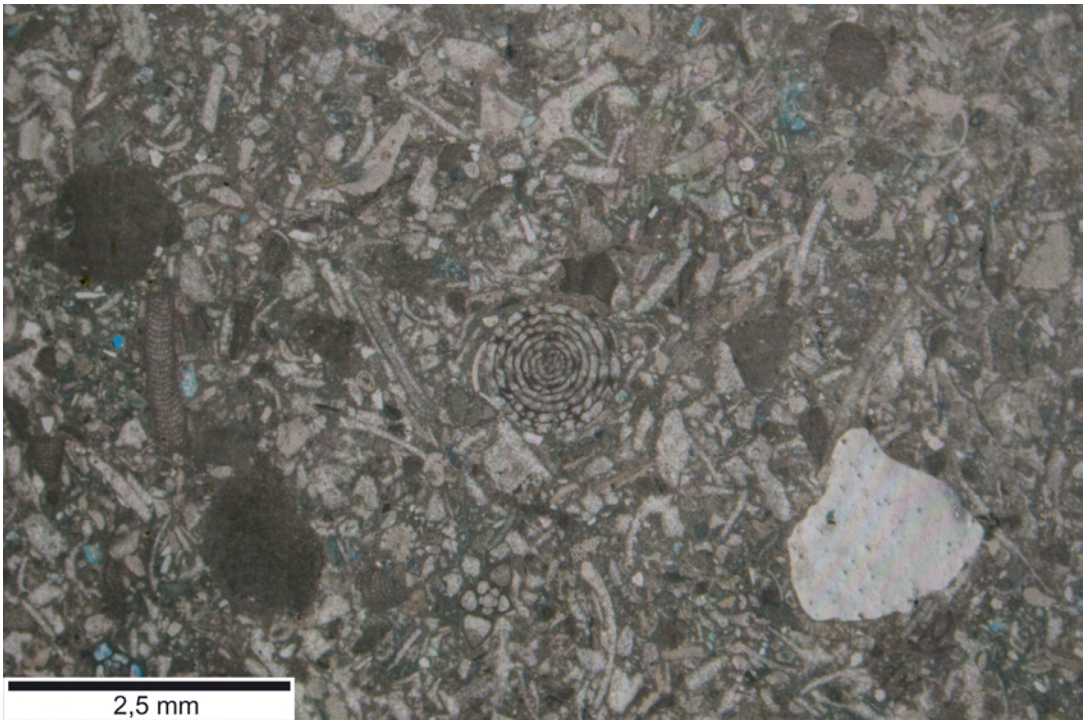

Fig. II.1.a. 13: Packstone with the larger benthic foraminifer *Borelis sp.*, coralline-algal debris and other bioclasts in Sequence 1a in the northern part of the Sedini transect (section 1).

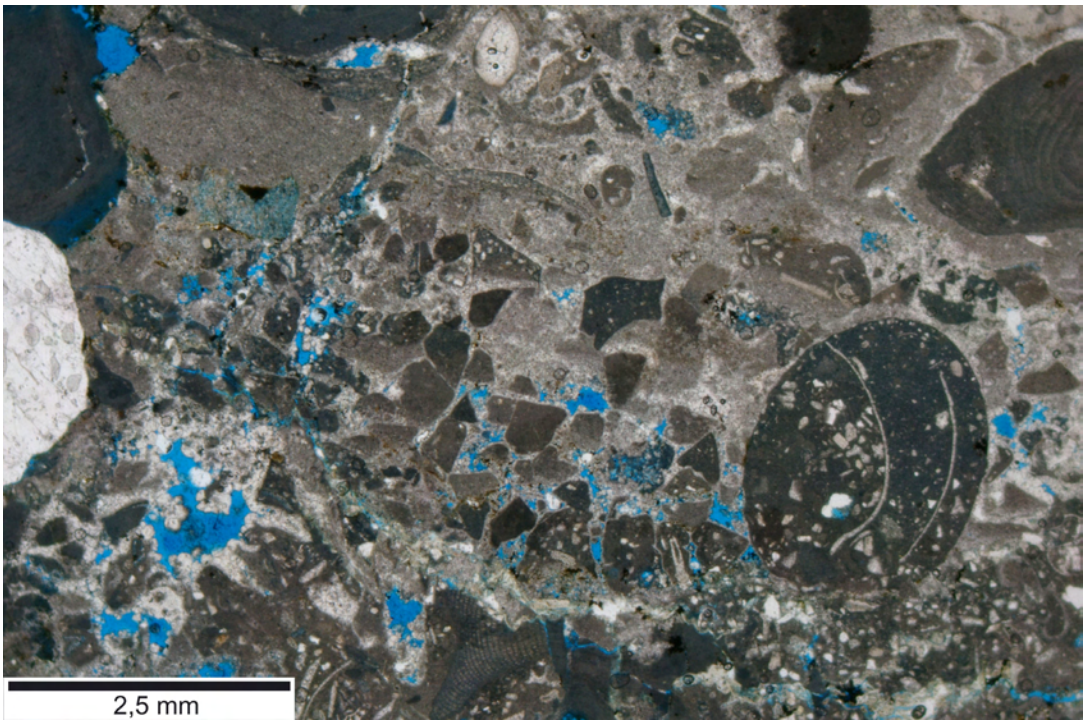

Fig. II.1.a. 14: Floatstone with coralline-algal debris, intraclasts and a *Lithophaga* boring in Sequence 1a in the northern part of the Sedini transect (section 1).

The lower part of section 4 comprises floatstones and rudstones with bivalves, barnacles, echinoderm debris, and coralline algae. A 40cm deep, and 2m broad incision infilled with oysters and barnacle fragments occurs in this interval. In the middle part of section 4, there is a layer with irregular echinids. The upper part of section 4 is made of floatstones and rudstones with very abundant branches of coralline algae and encrusting coralline algae. In addition, bivalves, echinids, and the larger benthic foraminifers *Amphistegina sp.* and *Heterostegina sp.* occur. To the south, the degree of fragmentation of the coralline algae increases.

Floatstones and rudstones dominated by coralline-algal branches make up the lower parts of sections 5–7 (Fig. II.1.a.15). Limestones in all sections are strongly bioturbated, with exception of an outcrop in the area between sections 4 and 5, where a 3.5m thick body of large-scale cross-beds dipping 15° to the east is exposed.

Fig. II.1.a. 15: Rudstone of coralline-algal branches in sequence 1b in the Sedini transect, section 7. Diameter of coin 22 mm.

In the middle part of sections 6 and 7 there is a 1m thick floatstone to rudstone layer with coarse bivalve detritus in section 6, and well-preserved, thick-shelled oysters

in section 7. In section 7, this layer also contains in-situ barnacles and intraclasts. Barnacles and clasts are encrusted by coralline algae. Further bioclasts are branches of coralline algae, echinids and larger benthic foraminifers (*Amphistegina sp.* and *Heterostegina sp.*). The floatstone to rudstone layer disappears between sections 6 and 5.

Above the rudstone to floatstone layer, in sections 6 and 7, well-sorted, bioclastic wackestones and packstones with abundant echinid debris occur. Limestones coarsen upwards, and are rich in coralline algae in the upper part of the sections. The upper part of section 5 is made up of a coarsening-upward package of packstones and floatstones containing abundant coralline-algal branches, rhodoliths and bivalves. The top of section 5 consists of a coralline-algal bindstone. The upper part of section 6 contains a ca. 7m thick succession of wackestones (Fig. II.1.a.12). The contact between the wackestones and the underlying floatstones is not exposed.

Interpretation

The Sedini transect consists of sequence 1 deposits, with a very minor part of sequence 2 in the upper part of sections 5 and 6 (Fig. II.1.a.12). The limit between sequences 1a and 1b is below the floatstone to rudstone layer that contains thick-shelled oysters and in-situ barnacles. In the northern part of the transect, this boundary is a hardground with *Lithophaga* borings. The hardground can be traced between sections 1 and 3.

The facies changes in sequence 1a are interpreted to reflect a North–South directed increase of the water depth along a ramp morphology. The inner ramp consists of shallow-water deposits, with coral fragments, red-algal encrustations, intraclasts and the larger benthic foraminifer *Borelis sp*. The middle ramp environment is characterized by the occurrence of the larger benthic foraminifers *Heterostegina sp.* and *Amphistegina sp.*, accompanied by fragments of coralline algae. This facies resembles the *Calcarenite biancastra a macroforaminiferi* of CIVITELLI & BRANDANO (2005). This assemblage is typical for tropical and subtropical environments at water depths between 40 and 70m (BRANDANO, 2003). In the middle to outer ramp, the occurrence of large-scale, tabular cross-beds indicates the presence of longshore bars, similar to those in the northern transect of the Ispilunca Valley. Incisions in the lower part of section 4 are interpreted as channel incisions, triggered by bottom currents.

Formation of a hardground at the top of sequence 1a attests for an interruption of sedimentation. Between sections 1 and 3, the ichnogenus *Gastrochaenolites* gives evidence for early lithification, in sections 6 and 7 in-situ barnacles and thick-shelled oysters reflect occurrence of a lithified sea floor. Above the hardground, fine-grained packstones and wackestones indicate sedimentation in relatively deep water. The lower sequence 1b is interpreted to reflect the consequence of a relative sea-level fall followed by a sea-level rise, leading first to the establishment of a hard-bottom community and then to deposition of deeper-water, finer-grained material. Coarsening-upwards of the overlying sediments of sequence 1b is interpreted as a shallowing of water depth.

Occurrence of the bindstone in the topmost part of section 5 shows a renewed formation of a stable substrate, later colonized by encrusting coralline algae. The bindstone is interpreted to pertain to sequence 2a; the lower bounding surface of the bindstone is thought to correspond to the sequence boundary between sequences 1 and 2. Wackestones in the uppermost part of section 6 are outer platform deposits of sequence 2.

DISCUSSION

The Sedini Limestone Unit is a well-exposed example of a fault-block carbonate platform (*sensu* BOSENCE, 2005) with a complex stratigraphic architecture. Several unconformities, the temporal changes in carbonate factory, and changes of the depositional geometries, subdivide the Sedini Limestone Unit into two depositional sequences and several higher-frequency sequences (Fig. II.1.a.16).

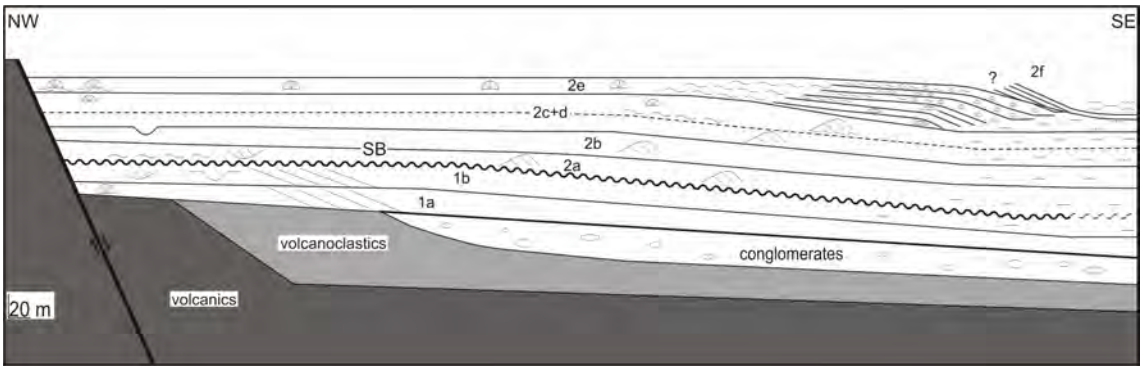

Fig. II.1.a. 16: Stratigraphic architecture of the Sedini Limestone Unit, with a carbonate ramp in sequence 1 and a turnover from a ramp to a steep-flanked platform in sequence 2.

Carbonate Platform Facies and Stratigraphy

The lower sequence 1 of the Sedini Limestone Unit is a carbonate ramp depositional system that was deposited in an embayment opening to the south-east (Fig. II.1.a.17). The inner ramp consists of different facies associations. In the South-West (Grotta Su Coloru Transect), beach deposits formed, with foreshore and shoreface bedding passing into planar-bedded wackestones and packstones (Fig. II.1.a.17). In the North-East (Sedini Transect) small patch reefs grew along the shoreline (Fig. II.1.a.17). Corals are fragmented, and occur together with encrusting coralline algae, rhodoliths, and intraclasts. Reef debris deposits interfinger with floatstones and rudstones consisting of branches of coralline algae, bivalves, larger benthic foraminifers, and bryozoans. Sedimentary structures are small troughs and channels.

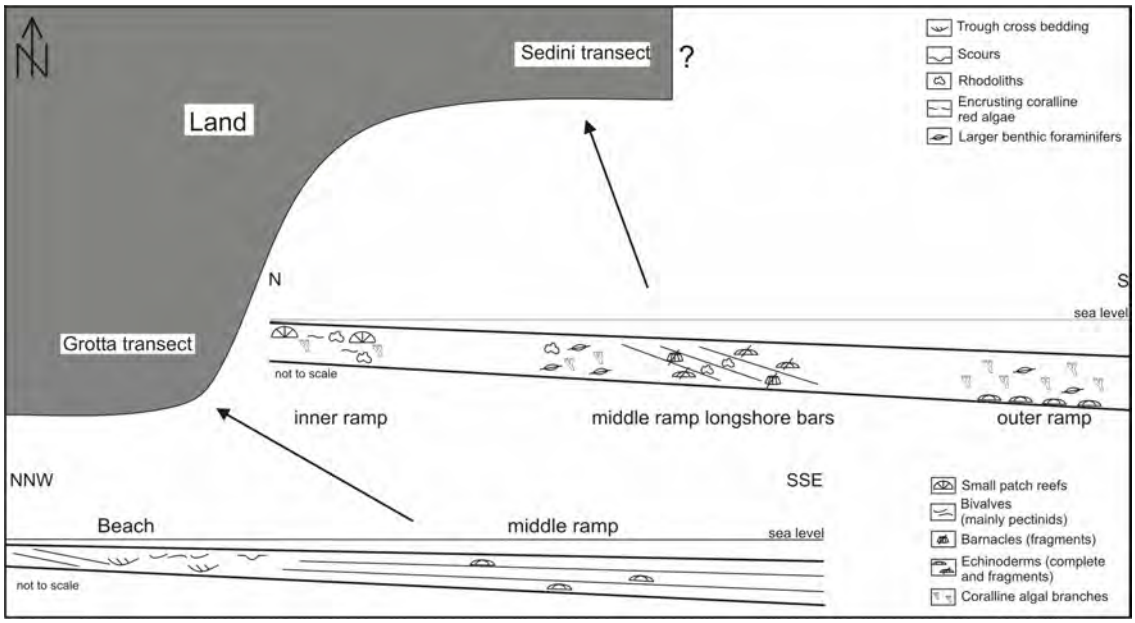

Fig. II.1.a. 17: Palaeoenvironmental interpretation of the study area during formation of sequence 1. Not to scale.

In the middle to outer ramp, deposits are floatstones and rudstones containing branches of coralline algae, small rhodoliths, fragmented echinids, and bivalves. Sedimentary structures are large-scale cross-beds with straight foresets, which are interpreted as longshore bars moved by East-directed currents. Subordinate directions are south-east to north-east. Small-scale, trough cross-bedding in the topset area indicates partial reworking at the top of the bars by wave action. The outer ramp is represented by packstones and floatstones dominated by branches of coralline algae. Further bioclasts are echinids, bryozoans, and bivalves.

Deposits of sequence 2 document an evolution from the ramp to a platform with a defined slope break (Fig. II.1.a.16). During the early stages of platform growth, in sequences 2a – 2d, the inner platform facies consists of coralline-algal bindstones. The lowermost coralline-algal bindstones overlie the sequence boundary and form a wedge that pinches out into a proximal direction (Fig. II.1.a.7). In the mid-platform environment, submarine dunes occur. Dunes are locally stabilized by 0.4–0.5m thick coralline-algal bindstones (2a–2d). Off-platform, the dunes grade into bedded, fine-grained, bioclastic packstones and wackestones.

In sequences 2d and 2e, the inner platform contains coral reefs. Reef deposits are framestones, up to six meters thick (Fig. II.1.a.8), and form a reef flat with a surface of approximately 4km^2. Towards the platform edge, coralline algae are more abundant and form a bindstone at the slope break (Figs. II.1.a.9, II.1.a.10c). Slope deposits at this platform stage are rhodolith rudstones arranged in a series of spectacular clinoform beds, 20m high and dipping with up to 27° basinwards (Figs. II.1.a.9, II.1.a.10d, e). Although slope angles are steep, there are no breccia, slumps or debris-flow deposits, and each clinoform terminates in a floatstone and rudstone bed only a few centimetres thick (Fig. II.1.a.10e). This minor off-platform shedding is interpreted as a consequence of the persistent coralline-algal incrustations that stabilized the slope.

The latest stage of the platform evolution of the Sedini Limestone Unit is only poorly recorded. In one of the transects (Sa Rocca Manna), it is documented that rhodolith formation at the slope ends at the upper limit of the high-frequency sequence 2e. The youngest carbonates of sequence 2f are bioclastic deposits. Neritic carbonate sedimentation in the Perfugas Basin seems to have terminated after formation of this last platform sediment package. The last marine deposits of the area are marls with sponge spicules, which, however, crop out at only one locality overlying fine-grained packstones and wackestones forming the basin deposits of sequence 2 (Figs. II.1.a.1, II.1.a.2).

Turnover in Geometry

Carbonate ramps and rimmed platforms are often closely related in time (e.g. WILSON, 1975, READ, 1985, BOSENCE, 2005). A common succession in the geological record is the up-section change from ramps to reef-rimmed platforms at different scales ranging from small platforms of km-size (e.g. MARTIN & BRAGA, 1994, BRACHERT et al., 1996) to bodies several hundred kilometers large such as e.g. the Great Bahama Bank (EBERLI & GINSBURG, 1987, 1989, BETZLER et al., 1999). It was evoked that palaeoceanographical or climate fluctuations trigger such geometrical

changes (MARTIN & BRAGA, 1994, BETZLER et al., 1995, BRACHERT et al., 1996), though ramp to platform turnovers may be largely a consequence of the stratigraphic architecture (HOMEWOOD, 1996). Landward stepping units, which form during base-level rises, have a residual bathymetry at the seaward end, and following seaward steps will leave to clinoform formation. According to SCHLAGER (2005), the turnover in geometries is a consequence of the tropical carbonate factory by itself, as it has the tendency to prograde and to steepen its slope. The ramp stage is understood as a transient stage due to delayed rim development during a rapid transgression.
In the Sedini Limestone Unit, change of buildup geometry goes along with a change of the carbonate factory, and seems to be especially related to the advent of sediment binding by coralline algae in the sequence 2. The lower sequence 1 in general is dominated by coralline algae. Other representative components are larger benthic foraminifers (frequent *Heterostegina sp.*, abundant *Amphistegina sp.*, and rare *Borelis sp.*), barnacles, bryozoans, and molluscs. Corals are scattered, and only recorded in the nearshore deposits of the Sedini transect. Micritic rims are rare in sequence 1 deposits (MARCANO et al., in prep.). These features assign the factory to the upper limit of the warm-temperate realm as defined by BETZLER et al. (1997). Similar Miocene carbonate depositional systems at the transition from the warm-temperate to the tropical realm were described from the Apennines e.g. by BRANDANO (2003) or CIVITELLI & BRANDANO (2005). They accumulate on carbonate ramps, because the carbonate factory does not produce any wave- or current-resistant rim structure. The carbonate factory of sequence 2 is rich in reef-building zooxanthellate corals and therefore can be unequivocally assigned to a tropical carbonate factory (JAMES, 1997). Coral reefs formed a reef flat, and extensive coralline-algal incrustations stabilized the platform edge and slope. Prograding submarine dunes became locally stabilized by coralline-algal encrustations and early cements (MARCANO et al., in prep.) and therefore increasingly acted as a wave resistant rim as described in SCHLAGER (2005), forming a steep-flanked platform in the late stage.

CONCLUSIONS

A sedimentological and stratigraphical model for a fault-block-carbonate platform is presented. This platform evolves from a ramp to a steep-flanked platform. The geometrical turnover goes along with a change of the carbonate factories from warm-temperate to tropical. The warm-temperate ramp contains small patch reefs,

beaches, longshore bars as well as outer ramp, bioclastic, and coralline-algal packstones to rudstones. The overlying steep-flanked platform stage contains coral reef framestones forming a reef flat, rhodolithic slope deposits and deeper-water peri-platform fine-grained carbonates. Rhodolith beds are spectacularly exposed, and facies can be traced from the topset to the bottomset of individual clinoform beds. Steepening of the depositional relief of the carbonate platform is gradual and linked to the inception of coralline-algal bindstones. This study presents a further example for the close relation between carbonate factory and stratigraphic architecture of carbonate platforms.

II.1.b. Coralline-Algal Assemblages of a Burdigalian Platform-Slope: Implications for Carbonate Platform Reconstruction (Northern Sardinia, Western Mediterranean Sea)[1]

ABSTRACT

The rhodolithic slope deposits of a Burdigalian carbonate platform in Sardinia were analyzed to reconstruct facies and palaeobathymetry. There is a distinct red-algal growth zonation along the platform-slope. The clinoform rollover area consists of coralline-algal bindstones, which downslope change into a rhodolith facies where rhodoliths are locally fused by progressive encrustation. Mid-slope rhodoliths are moderately branched, and downslope rhodoliths have fruticose protuberances, resulting in branching rhodolith growth patterns. There is a sharp change from the rhodolitic facies to the basinal, bivalve-dominated facies at the clinoform bottomsets. Red-algal genera identified include *Sporolithon sp., Lithophyllum sp., Spongites sp., Hydrolithon sp., Mesophyllum sp., Lithoporella sp., Neogoniolithon sp.*, and other Mastophoroids and Melobesioids. Genera and subfamilies show a zonation along the clinoforms, allowing palaeobathymetric estimates. The clinoform rollovers formed at a water depth of around 40m, the bottomsets around 60m. Results from geometrical reconstruction show that coral reefs in the inner platform formed in water depths of around 20m. Therefore, the Sedini carbonate platform is an example of a reef-bearing carbonate platform, in which the rim or the platform-interior reefs do not build up to sea level. If outcrop conditions do not allow a detailed view of platform geometries, such geometry may be misinterpreted as the shallow-water rim of a platform. The example of the Sedini carbonate platform also indicates that a mere geometrical reconstruction of platform geometries in subsurface data may lead to misinterpretations, because the edge of the platform does not necessarily indicate sea-level position.

[1] This chapter is based on BENISEK, M.-F., MARCANO, G., BETZLER, C., and MUTTI, M. (to be submitted): Coralline-Algal Assemblages of a Burdigalian Platform-slope: Implications for Carbonate Platform Reconstruction (Northern Sardinia, Western Mediterranean Sea)

INTRODUCTION

Coralline algae are important contributors to Mediterranean Neogene neritic carbonates, and a peak in coralline-algal abundance in the Neogene carbonate platforms occurs in the early to Middle Miocene (ESTEBAN, 1996, HALFAR & MUTTI, 2005). A number of studies describe these Mediterranean Miocene coralline-algal occurrences, amongst them the assemblages in Malta (BOSENCE & PEDLEY, 1982, BOSENCE, 1983c), Southern Spain (e.g. BRAGA & MARTIN, 1988, BRAGA & AGUIRRE, 2001), Menorca (OBRADOR et al., 1992, BRANDANO et al., 2005) and Crete (KROEGER et al., 2006). Red algae form crusts, boxworks, and rhodolithic beds. They build biostromes (BOSENCE & PEDLEY, 1982, BOSENCE, 1983c), and occur as dispersed branches and rhodoliths in biodetritic limestones (BRAGA & MARTIN, 1988, ESTEBAN, 1996, BRAGA & AGUIRRE, 2001, KROEGER et al., 2006).

Beds of densely packed rhodoliths are found in middle to outer sectors of distally steepened ramps (CARANNANTE & SIMONE, 1996), from marginal shelf sectors and as re-deposits in submarine channels (BASSI et al., 2006). Rhodolith beds from a Tortonian distally steepened carbonate ramp in Menorca are also described as forming large-scale slope clinobeds with a length of 100 to 200m (OBRADOR et al., 1992, BRANDANO et al., 2005). Rhodoliths along these clinoforms grew in-situ. Ramp slope rhodolith clinoforms shorewards interfinger with middle ramp cross-bedded dolograinstones, and towards the basin pass into finer-grained sediments.

A different depositional system with rhodolithic clinoforms occurs in a Burdigalian carbonate platform in northern Sardinia. Rhodolith clinoforms form along the slope of a coral-reef bearing carbonate platform. Good outcrop conditions permitted detailed inspection of the coralline-algal zonation along a set of clinoform beds. Palaeobathymetric estimations delivered by the coralline-algal platform-slope assemblages permit further insight into facies relationships and the anatomy of Miocene Mediterranean carbonate platforms.

GEOLOGICAL SETTING

The Western Mediterranean back-arc basin opened due to subduction of Neotethyan oceanic crust in a NW-dipping subduction zone during the long-range structural reorganisation of the Mediterranean realm beginning in the Palaeogene. As a result, Sardinia, together with Corsica, separated from southern Europe and

moved to its present position performing an approximately 23° counter-clockwise rotation (e.g. CHERCHI & MONTADERT, 1982, THOMAS & GENNESSEAUX, 1986, FACCENNA et al., 2002, SPERANZA et al., 2002). The structural processes triggered formation of a series of N-S oriented halfgrabens (Porto Torres Basin, Logudoro Basin, Castelsardo Basin, and Perfugas Basin), which were filled with an Oligo-Miocene volcano-sedimentary succession (figs. I.2.4, II.1.a.1). At the flanks of the basins, fault-block carbonate platforms formed during the Burdigalian (THOMAS & GENNESSEAUX, 1986, MAZZEI & OGGIANO, 1992, SOWERBUTTS, 1997).

The carbonate platform studied is the Sedini Limestone Unit (ARNAUD et al., 1992, THOMAS & GENNESSEAUX, 1986), situated in the Perfugas Basin. HAGEN et al. (2005) presented a sequence-stratigraphic subdivision of the carbonate platform succession into two depositional sequences (Fig. II.1.a.2) overlying volcanics (19.5–18.9Ma old, BECCALUVA et al., 1985) and volcanoclastics together with lacustrine sediments. The up to 60m thick carbonate platform succession consists of packstones to rudstones with boundstones and fine-grained wackestones and packstones (Fig. II.1.a.1). Sequence 1 consists of a carbonate ramp with small coral patch reefs, beaches, longshore bars and finer grained outer-ramp deposits containing calcareous nannoplankton of Zone NN4 (C. MÜLLER, pers. comm., 2006). Sequence 2, which according to SOWERBUTTS (1997) yields an $^{87}Sr/^{86}Sr$ age of 16Ma, is characterised in its lower part by the occurrence of coralline-algal bindstones and large-scale trough cross-bedded packstones and grainstones (Fig. II.1.b.1), which are interpreted as submarine dunes. The late platform stage consists of a reef flat composed of coral reefs (figs. II.1.a.2, II.1.b.1) and an associated steep coralline-algal dominated platform-slope (figs. II.1.b.1 and II.1.b.2). Thus, the carbonate platform architecture changes from a ramp geometry to a steep-flanked platform.

METHODS

The slope of the Sedini carbonate platform was investigated by measuring sections. The stratigraphy and depositional geometries were studied with geological mapping, physical tracing, interpretation of large-scale photo panoramas, and with LIDAR-measurements. Growth patterns and growth forms of red algae in thin sections are described using the definitions of WOELKERLING et al. (1993) and BOSENCE (1991). Determination of coralline-algal genera was performed applying the identification key of BRAGA et al. (1993). Using BOSENCE´s (1991) application of

present-day coralline-algal bathymetric distribution for Neogene genera, a palaeobathymetric reconstruction of the platform-slope is proposed.

RESULTS

Sedini Carbonate Platform Edge and Slope

The late carbonate platform-slope stage (Sequence 2) is well exposed in two ravines running more or less perpendicular to the platform edge (figs. II.1.b.1, II.1.b.2). The southern flank of the Ispilunca valley provides a 1.5km long section through the platform (figs. II.1.b.1), with bioclastic sand bars and coral reefs in the platform interior (figs. II.1.b.1b, c), and clinoform slope deposits with rhodolithic and bioclastic limestones (figs. II.1.b.1c). Correlation of strata in the platform interior shows that the Sequence 2d and 2e clinoforms lie approximately 20m lower than the platform-interior coral reefs.

The flank of the Sa Rocca Manna ravine, which is the most accessible outcrop and the focus of this study, displays the transition from the platform edge to the basin over a distance of 200m (Fig. II.1.b.2). The lower part of this succession contains echinid packstones with minor, up to 8m wide and up to 1.50m high coralline-algal bindstone lenses. The packstones interfinger with finer-grained, bioturbated wackestones and packstones to the south-east, i.e. basinwards.

Above a sharp surface, planar cross-bedded echinid and bivalve floatstones to rudstones occur, downlapping onto this surface which was defined as the limit of a high-frequency sequence by HAGEN et al. (2005). The floatstones and rudstones are overlain by coralline-algal bindstones. Bindstones display a faint layering, which dips slightly basinwards. Distally, the bindstones merge into bedded rhodolith floatstones to rudstones. Beds have a basinward dip of 25°. The bottomsets of the inclined beds consist of echinid and bivalve floatstones to rudstones.

The coralline-algal bindstones laterally change into a transitional facies, consisting of rhodolith floatstones to coralline-algal bindstones, which form the topset deposits of steep (up to 27°) rhodolithic clinoforms. The bottomsets of the clinoforms consist of echinoid and bivalve floatstones and rudstones, and bioturbated wackestones and packstones. The clinoform package is 21m thick and terminated by an erosion surface. This surface is overlain by a sediment package composed of bioclastic packstones to floatstones with inclined bedding. Deposits contain minor corals and rhodoliths.

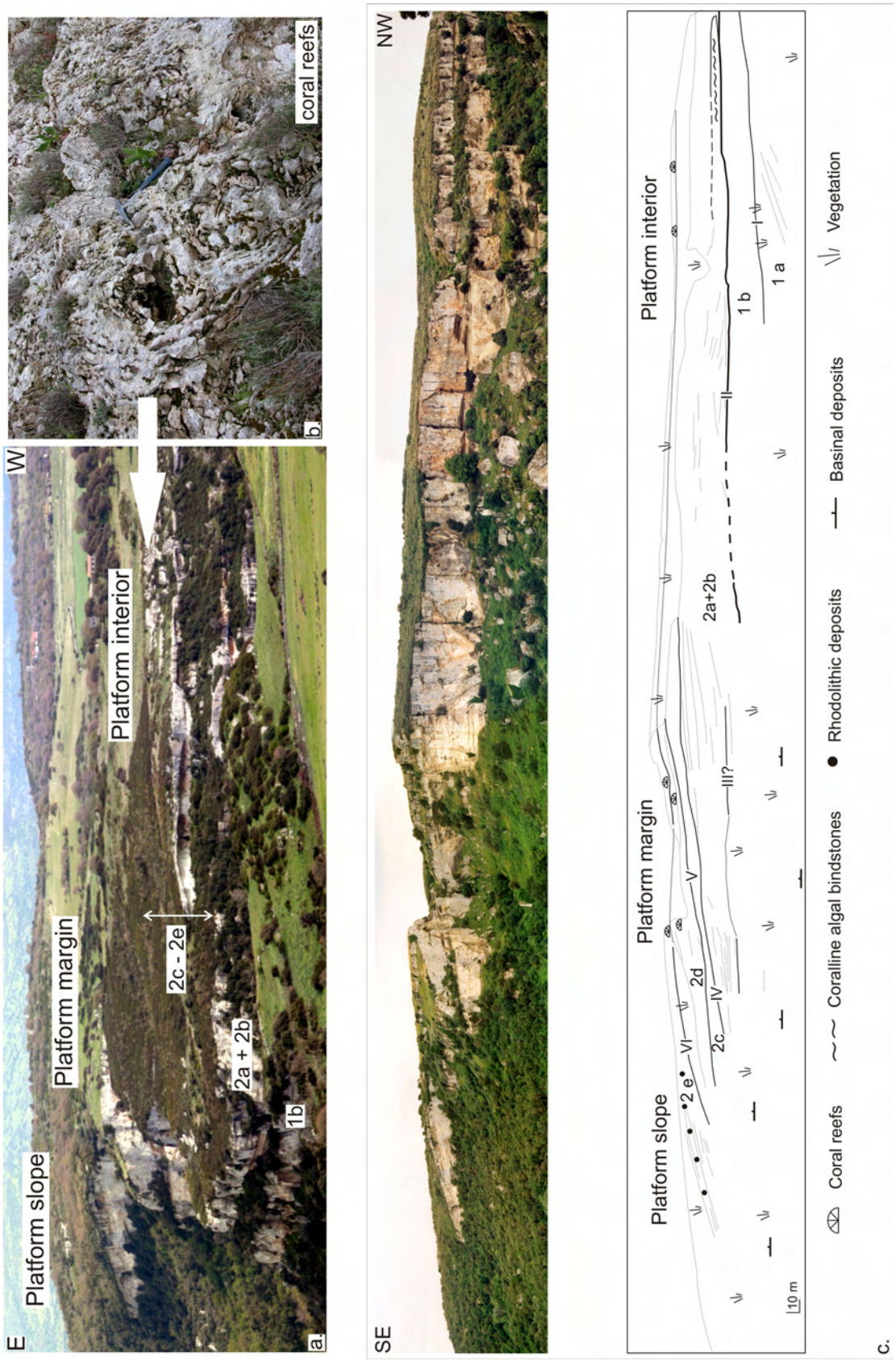

Fig. II.1.b. 1: **a.** View of the southern part of the Sedini carbonate platform from NW to SE, showing transition from flat-lying, platform-interior deposits to the steeply dipping platform-slope. The cliff in the left-hand part of the photograph is depicted in detail in c**. b.** Platform-interior coral reefs**. c.** Flank of the Ispilunca ravine with stratigraphic interpretation. Roman numbers refer to high-frequency sequence boundaries, delimiting high-frequency sequences 1a–2e.

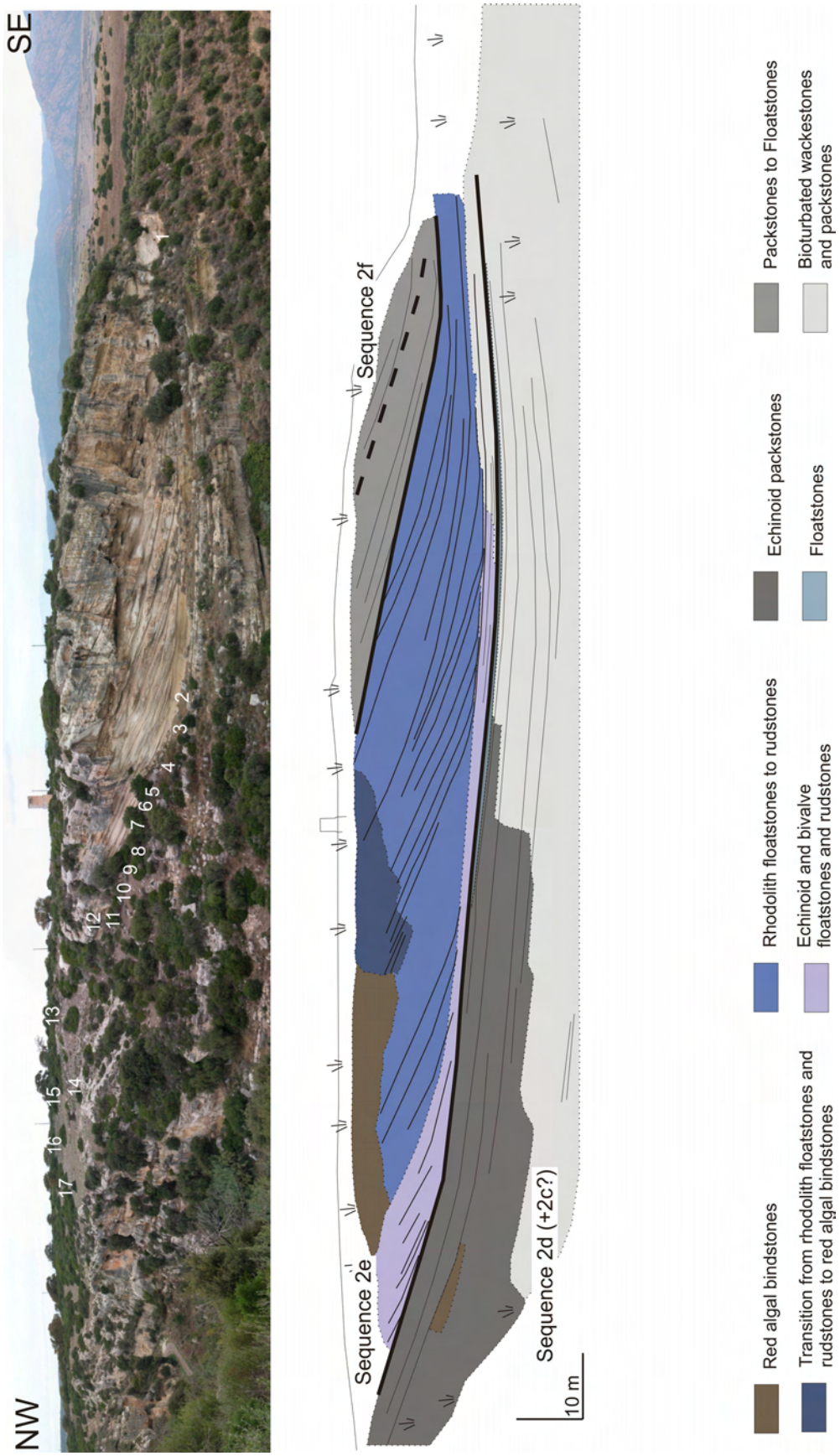

Fig. II.1.b. 2: Cliff of the Sa Rocca Manna ravine with facies distribution (see Fig. II.1.a.1 for location). The clinoforms dip with angles of up to 27° and form the slope of the Sedini carbonate platform. Numbers in the outcrop photograph refer to samples analyzed in this study (fig. II.1.b.6, table 1).

Clinoform architecture

Individual clinoform beds are 25 to 30cm thick. Along clinoform beds, there are differences in the red-algal growth-patterns and growth-forms (Fig. II.1.b.3, Tab. 1). In the bindstone, coralline algae produce robust frameworks with some delicate tendency (*sensu* BOSENCE, 1991). Growth forms are layered to foliose with warty and fruticose protuberances (*sensu* WOELKERLING et al., 1993). Coralline-algal crusts are often broken, and breaks are healed with cement (figs. II.1.b.3, II.1.b.4a).

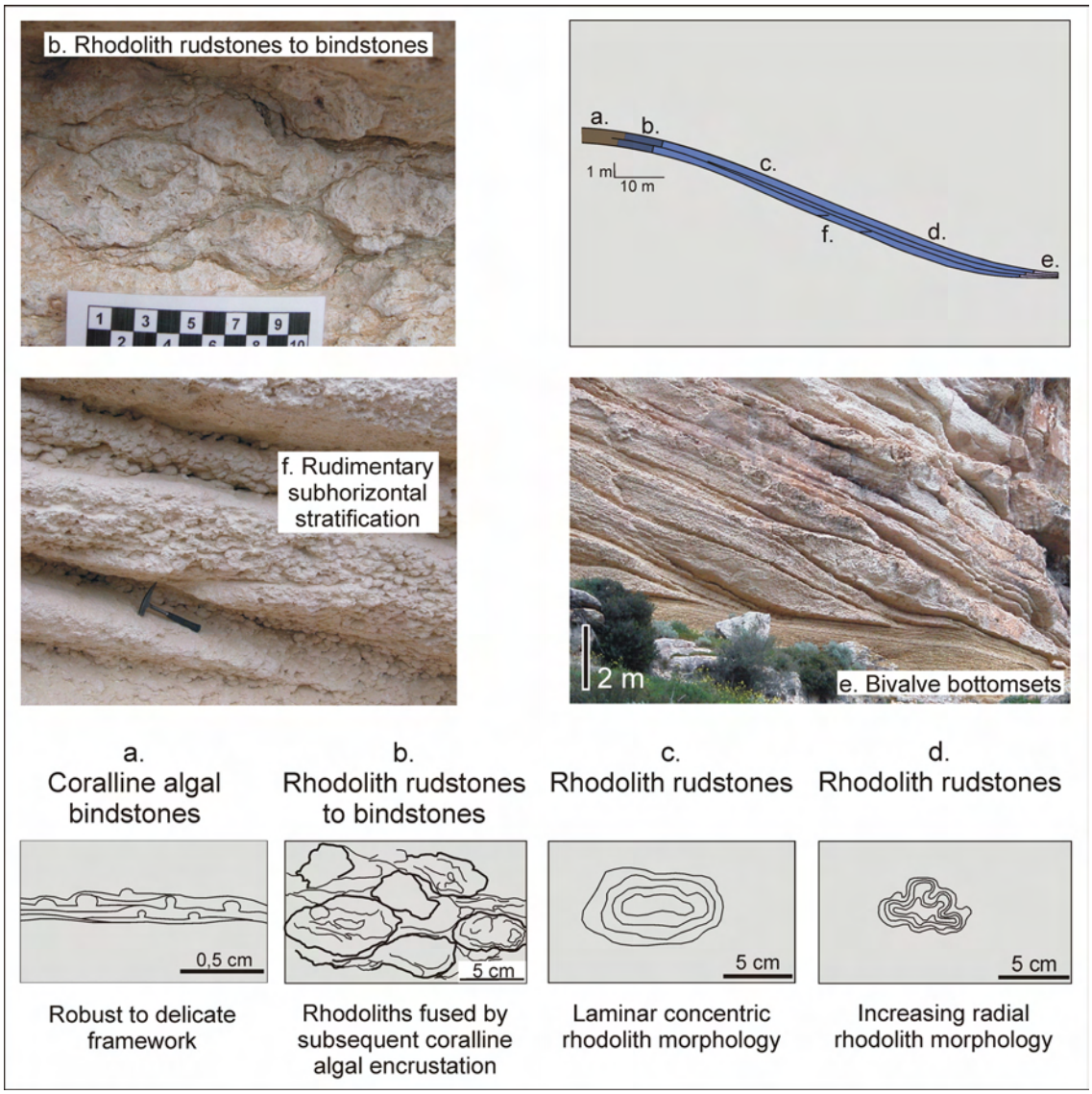

Fig. II.1.b. 3: Details of clinoform beds. Along each clinoform bed, there is a distinct facies zonation. Facies a are bindstones, facies b is a transitional facies from bindstone to rhodolithic rudstones. Facies b, c, and d are rhodolithic facies, each characterized by different rhodolithic growth-forms. Note pinching out of the rhodolithic facies at the clinoform bottomsets (e).

At the clinoform break, there is a change in growth-pattern from encrusting to rhodolithic. Rhodoliths are 10–15cm large, and are ellipsoidal to discoidal with

laminar-concentric morphologies (figs. II.1.b.3, II.1.b.4b). They are closely packed, and locally single rhodoliths are fused by continued coralline-algal encrustation. Downslope, in the foreset area, the deposits grade into rhodolithic rudstones. Rhodolith shape is discoidal to sphaeroidal and rhodolith size decreases from 10-15cm to 5-10cm in diameter. Rhodolith structures are moderately branched (figs. II.1.b.3, II.1.b.4c). The amount of matrix between rhodoliths increases downslope. At the lower termination of clinoform beds, occurrence of fruticose protuberances in the rhodoliths slightly increases, resulting in more radial branched growth forms (figs. II.1.b.3, II.1.b.4d). Coralline crusts along the slope are intensely bored.

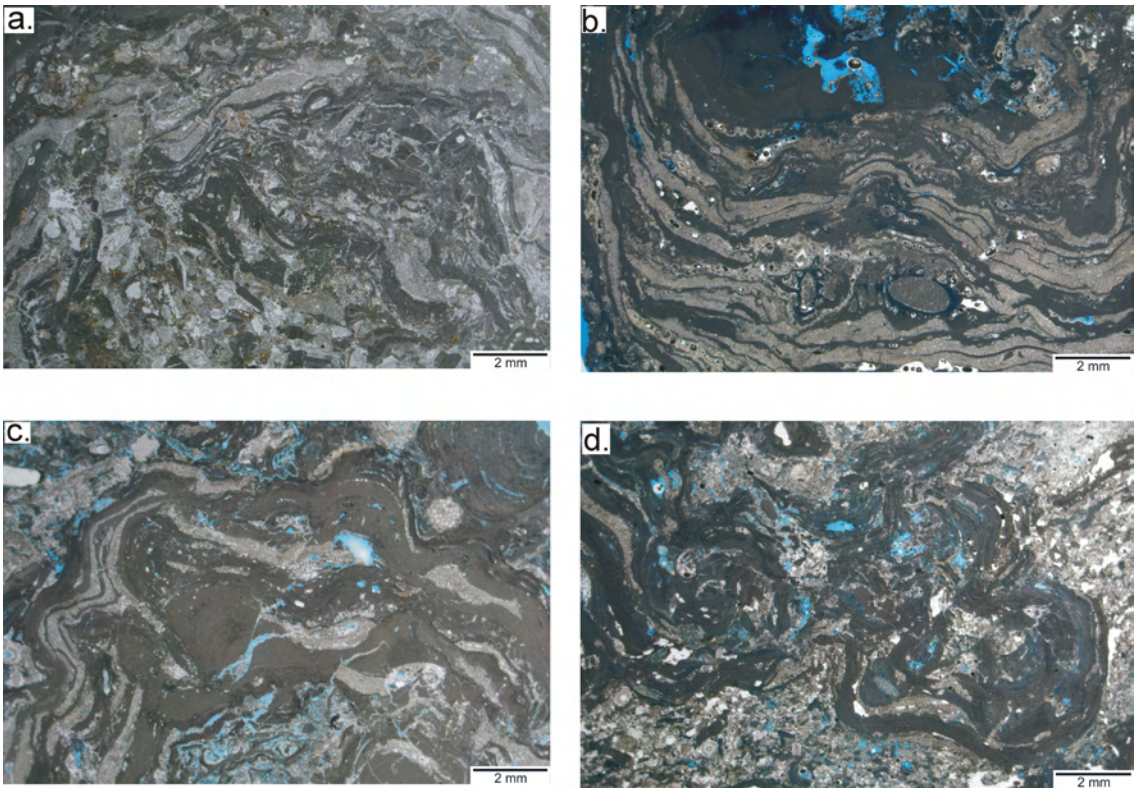

Fig. II.1.b. 4: Coralline-algal growth-forms and Rhodolith morphologies in the clinoform beds. **a.** bindstone, **b.** rhodolith with laminar concentric structure at the transition from the bindstones to the rhodolith rudstones, **c.** moderately branched rhodolith of the upper platform-slope, **d.** branched rhodolith of the lower platform-slope.

Each clinoform bed terminates in an approximately 10cm thick bottomset layer. Bottomset layers contain minor red algae and are enriched in bivalves, mainly pectinids and oysters. Bivalves are often preserved with both valves, therefore indicating that components were not reworked. Basinwards, the fossil content of the layers decrease and deposits are wackestones to fine-grained packstones.

Clinoform beds are separated by several mm to cm thick, fine-grained, bioclastic packstone drapes. In the older part of the slope succession, clinoforms beds are mostly regular (figs. II.1.b.2, II.1.b.5). In the younger part, clinoform beds are irregular, and truncations occur (Fig. II.1.b.5), some with a trough-shaped geometry. In individual clinoforms beds, there is a rudimentary stratification (figs. II.1.b.3, II.1.b.5). This stratification is horizontal to subhorizontal.

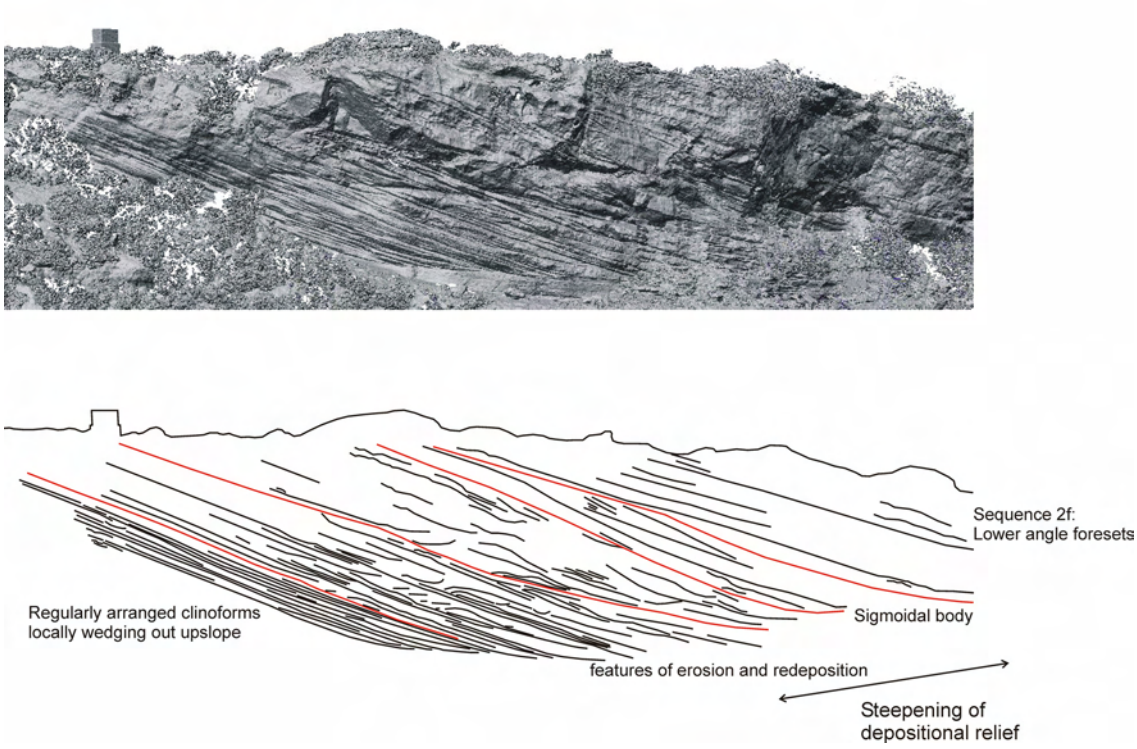

Fig. II.1.b. 5: LIDAR image of a part of the Sa Rocca Manna transect. Line drawing shows internal geometries of clinoforms in the outcrop.

Coralline-algal genera

Figure II.1.b.6 and Tab. 1 provide an overview of the distribution of some coralline-algal genera and subfamilies along the carbonate platform-slope. The position of the samples is shown in Fig. II.1.b.2.

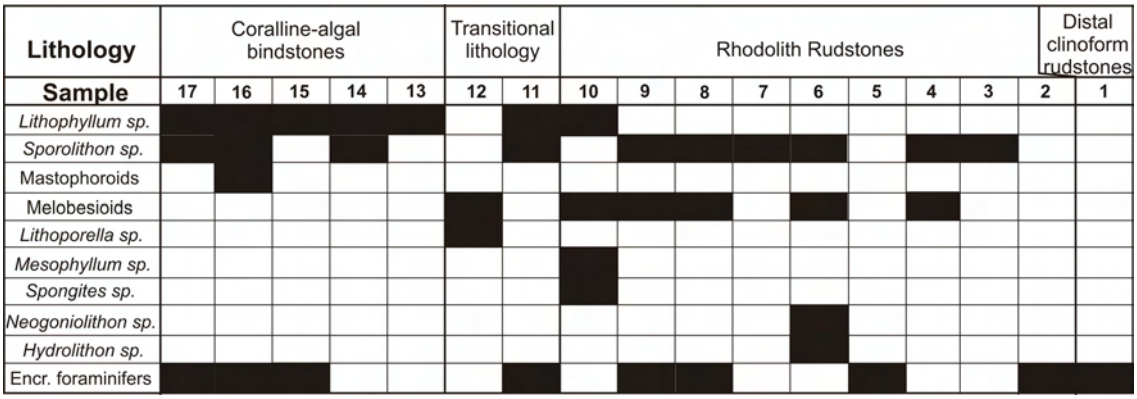

Fig. II.1.b. 6: Coralline-algal subfamilies and genera along a clinoform bed. Distribution of genera and subfamilies shows a downslope enrichment of Melobesioid coralline algae. See text for discussion.

The distribution of the algae along the slope is not uniform. The coralline bindstones (samples 13-17) contain *Sporolithon sp.* and Mastophoroids. Where preservation allows, Mastophoroids are attributable to the genus *Lithophyllum sp.* Encrusting foraminifers are present in samples 15–17. The slope samples 12-2 were taken in intervals of 1-2m along the same clinoform bed. In the transitional facies between the bindstones and the rhodolith floatstones to rudstones, red algae are *Lithoporella sp.* and melobesioids (sample 12), as well as *Lithophyllum sp.* and *Sporolithon sp.* (sample 11). Encrusting foraminifers are present in this facies.

Samples 10 to 2 are from the rhodolith rudstones. *Lithophyllum sp., Mesophyllum sp., Spongites sp.* (Fig. II.1.b.7a), and Melobesioids occur in sample 10. Samples 9-3 contain *Sporolithon sp*. (Fig. II.1.b.7b) and other Melobesioids (Fig. II.1.b.7c), in addition sample 6 contains *Neogoniolithon sp.* and *Hydrolithon sp.* (Fig. II.1.b.7d). Encrusting foraminifers are usually abundant in the rhodolith floatstones to rudstones, and they form extensive encrustations in samples 5 and 2. Red algae are present in these samples; they lack, however, reproductive conceptacles and other features required for subfamily and genus determination (BRAGA pers. comm., 2007).

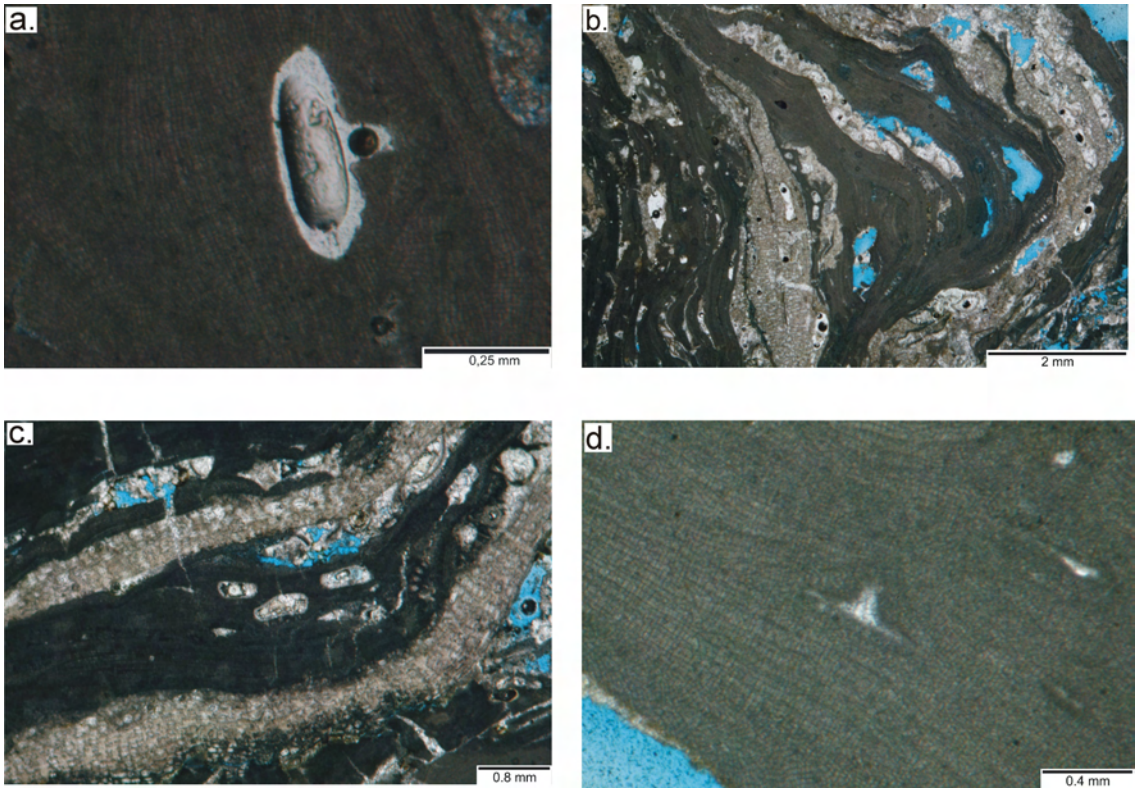

Fig. II.1.b. 7: Selected thin-section photographs of coralline-algal genera and subfamilies identified in the Sa Rocca Manna transect. **a.** *Spongites sp.*, **b.** *Sporolithon sp.*, **c.** melobesioid coralline algae, **d.** *Hydrolithon sp.*

DISCUSSION

Palaeobathymetry of the Clinoform Beds

The outcrop at the flank Sa Rocca Manna ravine is interpreted as documenting the edge of a carbonate platform, and contains the transition from the upper slope to the platform interior deposits (bindstones), the slope deposits with rhodoliths, the toe of slope deposits with bivalves, and fine-grained basinal deposits. Water depth of the Sedini carbonate platform edge can be pinpointed by two lines of evidence. The red-algal genera allow an absolute depth-assignment and the Rhodolith morphologies a relative depth zonation.

Lithophyllum sp. and *Sporolithon sp.* occur in the bindstones and the transitional facies to the rhodolithic deposits at the clinoform rollovers. The abundance of *Lithophyllum sp.* decreases downslope, where *Mesophyllum sp.* and other Melobesioid genera are more abundant (Fig. II.1.b.6). BOSENCE (1991), relying on analyses of Recent Pacific and Caribbean red-algal associations, proposes a bathymetric zonation based on taxonomic variations of red-algal associations. According to BOSENCE (1991), this zonation is also valid for Neogene carbonates.

Following this zonation, the clinoform-break deposits were formed in water depths between 40-60m. This assignment relies on the occurrence of *Sporolithon sp.* Downslope, the coralline-algal assemblage corresponds to the depth range of 40-100 m.

In a number of studies, Rhodolith morphologies are inferred to change with water depth. BRAGA & MARTIN (1988) showed in Tortonian nearshore rhodoliths, that there are depth-related differences in structure and composition. Rhodoliths are massive in shallower water and crusts are more columnar in deeper waters. Species diversity increases with water depth. BOSENCE (1991) discussed how the morphology changes from concentric crusts to radial branching growth forms with increasing water depths in living rhodoliths. Although the activity of dwelling organisms, which repeatedly turn rhodoliths around, was stressed as a major contributor of concentric, algal incrustations (e.g. PRAGER & GINSBURG, 1989, MARRACK, 1999) the outcrop of the Sa Rocca Manna ravine provides a further well-documented example of a water depth related differentiation of rhodolith growth forms (figs. II.1.b.3, II.1.b.4).

Coralline-algal bindstone crusts in the clinoform rollovers are robust, reflecting moderate to high turbulence, although delicate morphologies also occur (figs. II.1.b.3, II.1.b.4a). The transitional facies between bindstones and rhodoliths at the slope break reflects a transitional energetic environment, resulting in the formation of both laminar concentric rhodoliths and coralline-algal frameworks (figs. II.1.b.3, II.1.b.4b). Mid-slope rhodoliths are slightly more concentric than downslope rhodoliths (figs. II.1.b.3, II.1.b.4c). Downslope, rhodoliths tend to have more fruticose protuberances, leading to slightly more radial branched rhodoliths (figs. II.1.b.3, II.1.b.4d), rather than concentric forms. The increasing amount of matrix supports the hypothesis of downslope decreasing energy.

Further evidence for higher hydrodynamic energy at the clinoform rollovers may be indicated by the occurrence of breaks in the coralline crusts. Breaks are interpreted to reflect the action of events with a strengthening of physical reworking of the sea floor, such as storm events. The healing of crusts, without complete destruction of primary structures, is taken as evidence that such conditions occurred episodically.

Implications for Platform Architecture

Figure II.1.b.8 shows a model of the facies architecture of the late stage Sedini carbonate platform, documenting that this platform consists of a reef flat with a fore-reef rhodolithic slope. The clinoform rollover area was stabilized by robust to delicate coralline-algal encrustation. The upper slope was populated by rhodoliths, locally fused by progressive encrustation. Rhodoliths, which grew in-situ along the slope, represent the entire clinoform deposits, except for the bottomsets, where well-preserved bivalves dominate. The variations in growth pattern and growth form of the red algae reflect a downslope decreasing gradient in hydrodynamic energy. A water depth value of around 40m is postulated for the platform edge based on the red-algal assemblages, whereas a water depth of around 60m is postulated for the basinal deposits based on geometrical reconstruction. From the geometrical reconstruction of the platform-slope and the inner platform area (Fig. II.1.b.1), there is also evidence that the platform-interior coral reefs thrived in water depths of approximately 20m.

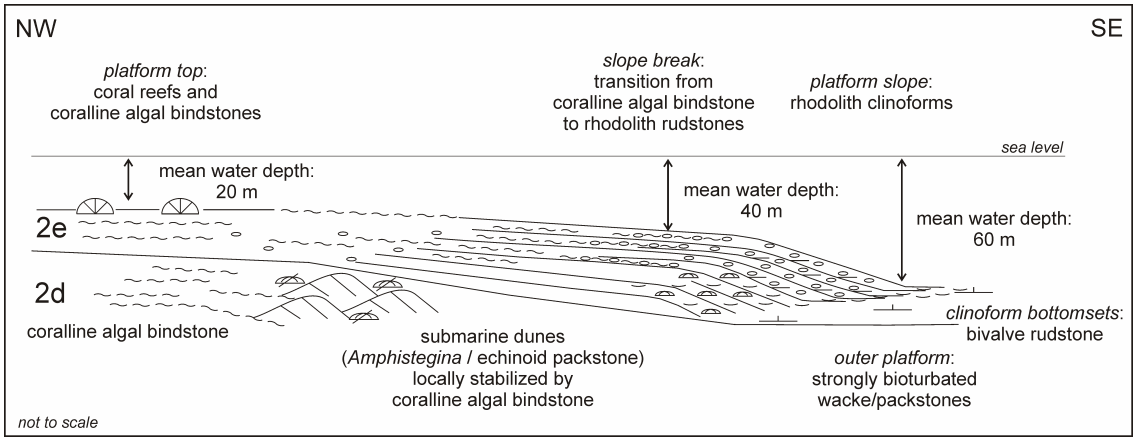

Fig. II.1.b. 8: Model of the Sedini carbonate platform with distribution of facies. See text for discussion.

Therefore, the Sedini carbonate platform provides a case of a steep-flanked carbonate platform with a relatively deep, coral-reef bearing platform-interior and rhodolithic platform-margin facies. Occurrence of a depositional system with such characteristics corroborates a hypothesis postulated by POMAR & HALLOCK (2007), that reef-building, neritic corals in some cases did not build up to sea level during Middle Miocene times. The peculiar geometry of the Sedini carbonate platform does not conform to the usual model of a flat-topped, rimmed geometry typical of a tropical carbonate factory (see SCHLAGER, 2005 for discussion), which builds up to sea-level. Although it is not testable which mechanism ultimately controlled the

Sedini carbonate platform geometry, it is also conceivable that ambient water conditions were a major controlling factor of platform shape. According to ROSEN (1999), and BOSELLINI & PERRIN (2008), Burdigalian coral associations of the Mediterranean area point to minimum sea-surface palaeotemperatures between 19°-20°C. This is at the cool end of tropical conditions, i.e. at the transition to temperate waters, where shallow-water carbonates form ramps because no wave resistant constructions occur, and where carbonate production rates are low (BETZLER et al. 1997, JAMES et al. 1999).

CONCLUSIONS

The Burdigalian Sedini carbonate platform contains platform-interior coral reefs and rhodolithic clinoform slope-deposits. There is a distinct red-algal growth zonation along the platform-slope. The clinoform rollover area consists of rhodophyte bindstones. Downslope, this facies changes into a rhodolith facies, where rhodoliths are locally fused by progressive encrustation. Mid-slope rhodoliths are more concentric than downslope rhodoliths with fruticose protuberances. At the clinoform bottomsets, there is a sharp change from the rhodolitic facies to the basinal, bivalve-dominated facies. Red-algal genera and subfamilies show a zonation along the clinoforms, which allows palaeobathymetric estimates of the rhodolith clinoforms. The clinoform rollovers formed at a water depth of around 40m, the bottomsets around 60m. Results from geometrical reconstruction show that the inner platform coral reefs formed in water depths of around 20m. Therefore, the Sedini carbonate platform is an example for a reef-bearing carbonate platform, where the rim or the platform-interior reefs do not build up to sea level. This geometry may be controlled by ambient seawater temperatures, which are transitional between tropical and temperate temperatures. The case of the Sedini carbonate platform has implications for the interpretation of carbonate platforms developing under similar ecological conditions. If outcrop conditions do not allow a detailed view of platform geometries, the clinoform rollover area may be misinterpreted as the shallow-water rim of a platform. The Sedini carbonate platform is small, and the succession only several ten meters thick. Thus, details are below conventional seismic resolution. However, it teaches that a mere geometrical reconstruction of platform geometries in seismic data may lead to misinterpretations, because the edge of the platform does not necessarily indicate sea-level position. This may be characteristic for transitional carbonate platforms.

II.1.c. Facies Description

The following chapter with brief descriptions summarizes the different lithofacies of the Sedini Limestone Unit. Lithofacies delimitation relies on texture, composition, sedimentary structures, and sediment geometries. Seventeen Facies are differentiated, which occur in two depositional sequences. Location of sections and transects named in the Facies description part is shown in Fig. II.1.c.1.

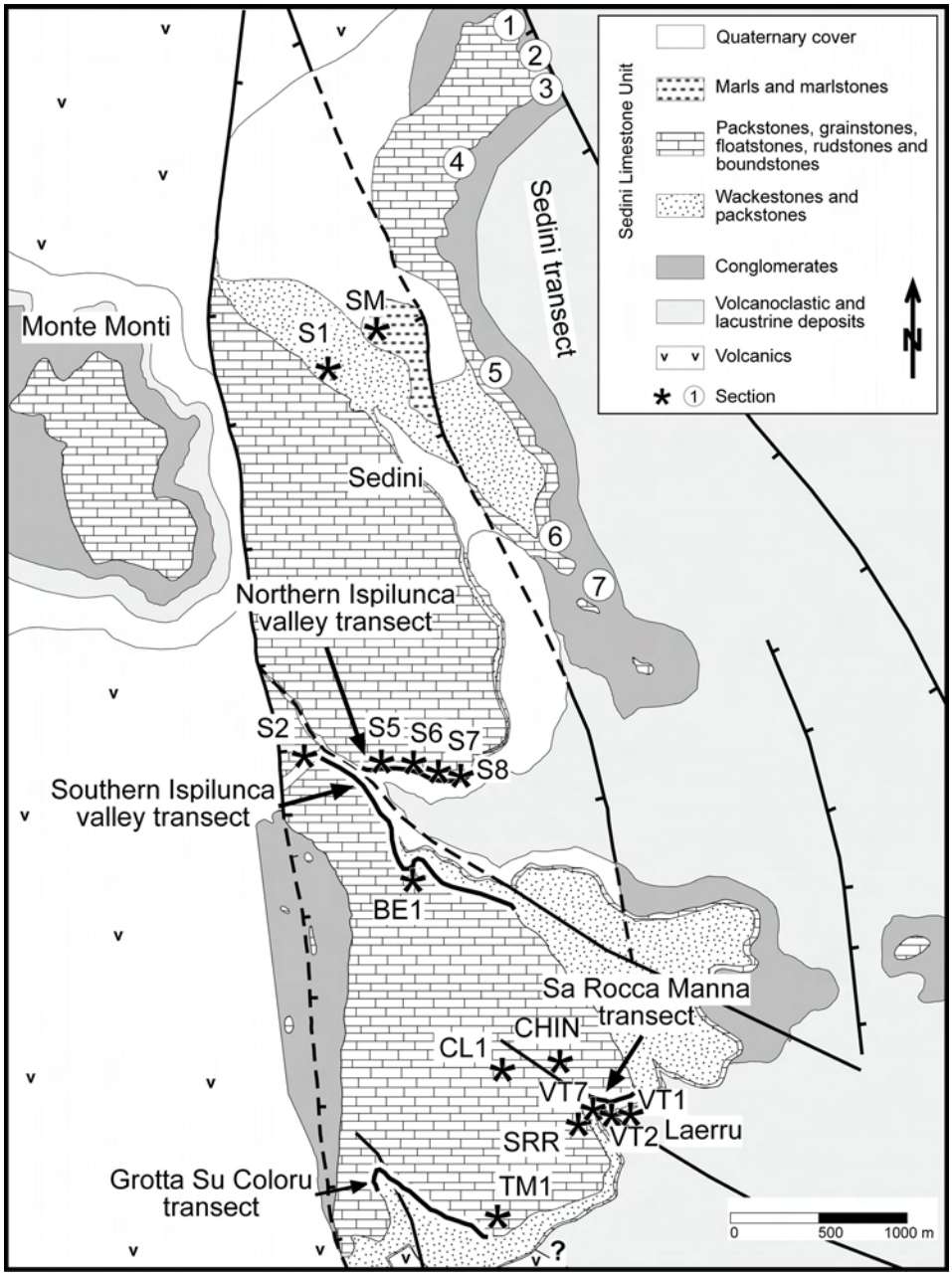

Fig. II.1.c. 1: Geological map of the study area in the Perfugas Basin with localities and transects discussed in the following chapter.

Facies 1: Coral-Bearing Floatstones and Rudstones

This Facies is restricted to Sequence 1, where it occurs in outcrops in the northern part of the carbonate platform (sections 1, 2, 3, and 4), along a cliff north of the village Sedini. Deposits are massive white-grey floatstones and rudstones arranged in up to 4m thick massive to poorly bedded, bioturbated packages. Locally, this Facies contains a significant amount of siliciclastics, where it overlies alluvial conglomerates. At these localities, the siliciclastic content and grain size decreases upsection. Main components are encrusting coralline algae and coralline-algal debris. Coralline algae have warty and fruticose growth forms and are thought to be remnants of open branched rhodoliths. Coral fragments and the large benthic foraminifer *Borelis sp*. (Fig. II.1.c.2.) are also constituents of this Facies, as well as *Heterostegina sp*. Locally, the small benthic foraminifer *Quinqueloculina sp.* and other miliolid foraminifers, as well as encrusting foraminifers occur. Other components are gastropods and barnacles. Coral debris and bivalves are usually preserved as molds, micritic rims do not occur. Coral remnants are often encrusted by coralline algae. Coralline algae have warty and fruticose growth forms and are thought to be remnants of open branched rhodoliths.

Throughout the sections containing Facies 1, borings occur. Intraclasts, up to 5cm in diameter, are frequent components in these deposits. Figure II.1.c.3 shows a thin section photograph of such a component, which is subangular to rounded and incrusted by red algae. The intraclast consist of a breccia with up 5mm large mudstone to wackestone clasts embedded in a blocky spar.

Facies 1 occurs in sections located in the northernmost part of the Sedini carbonate platform, where shallow-water carbonates wedge out. For this reason, and because the Facies bears abundant shallow-water allochems, it is interpreted as shallow-water Facies. Corals, *Borelis sp.*, *Quinqueloculina sp.*, other miliolid and encrusting foraminifers point to a reefal environment. The fact that all corals are only preserved as fragments is an evidence for a high-energy environment with the dominating processes being frequent reworking and growth. Occurrence of intraclasts and borings at several levels indicate that deposits underwent early lithification and reworking of early lithified clasts.

This Facies shows similarities to modern deposits in south-western Australia. The Southwest Australian Shelf is situated in transitional conditions between tropical in the North and warm temperate in the South. The Carnavon ramp in the North contains local fringing reef complexes in the Inner ramp, which occur adjacent to coarse-grained deposits composed of coralline algae, molluscs, foraminifers (such as *Amphistegina sp*., *Heterostegina sp*., and larger Milioline taxa) echinoids, serpulids,

and bryozoans. Seawards of these fringing reefs, hardgrounds and incipient hardgrounds are common (JAMES et al., 1999). The occurrence of *Heterostegina sp*. points to sea-grass meadows in the proximity (CHAPRONIERE, 1975; WILSON et al., 1997).

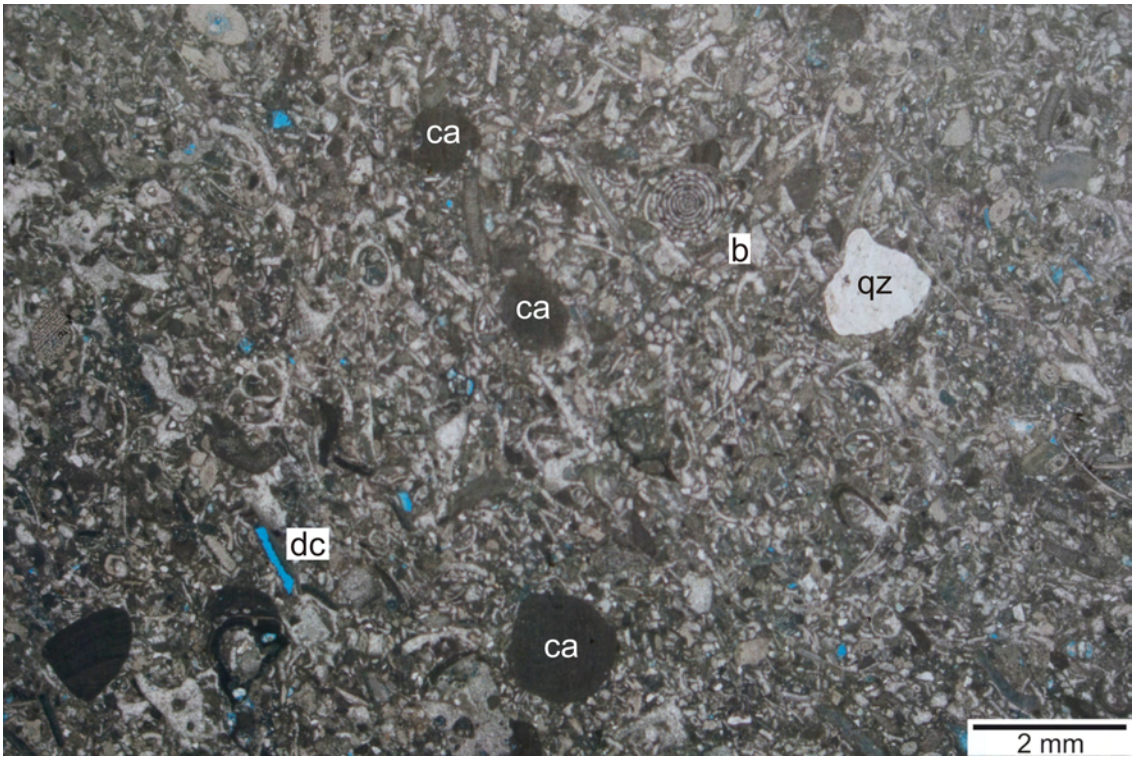

Fig. II.1.c. 2: Thin section photograph of Facies 1. Packstone to floatstone with the larger benthic foraminifer *Borelis sp*. (b), coralline-algal debris (ca). Note the dissolved component (dc). Sample 18-2.1.

Facies 2: Trough Cross-Bedded and Planar Cross-Bedded Echinid Grainstones and Packstones

Trough cross-bedded and planar cross-bedded, well-sorted echinid grainstones and packstones with pectinid bivalve debris occur in the southernmost part of the Sedini carbonate platform, in outcrops of the Grotta Su Coloru (GSC) transect (Fig. II.1.a.11b). Other components in these deposits are small bivalve fragments, branches of coralline algae and small benthic foraminifers, such as *Elphidium sp*. Planar cross-beds dip with 2–5 ° basinwards, and in their lower part merge into medium scale trough cross-beds. The cross bedding of this Facies is interpreted as foreshore and shoreface bedding of beach deposits.

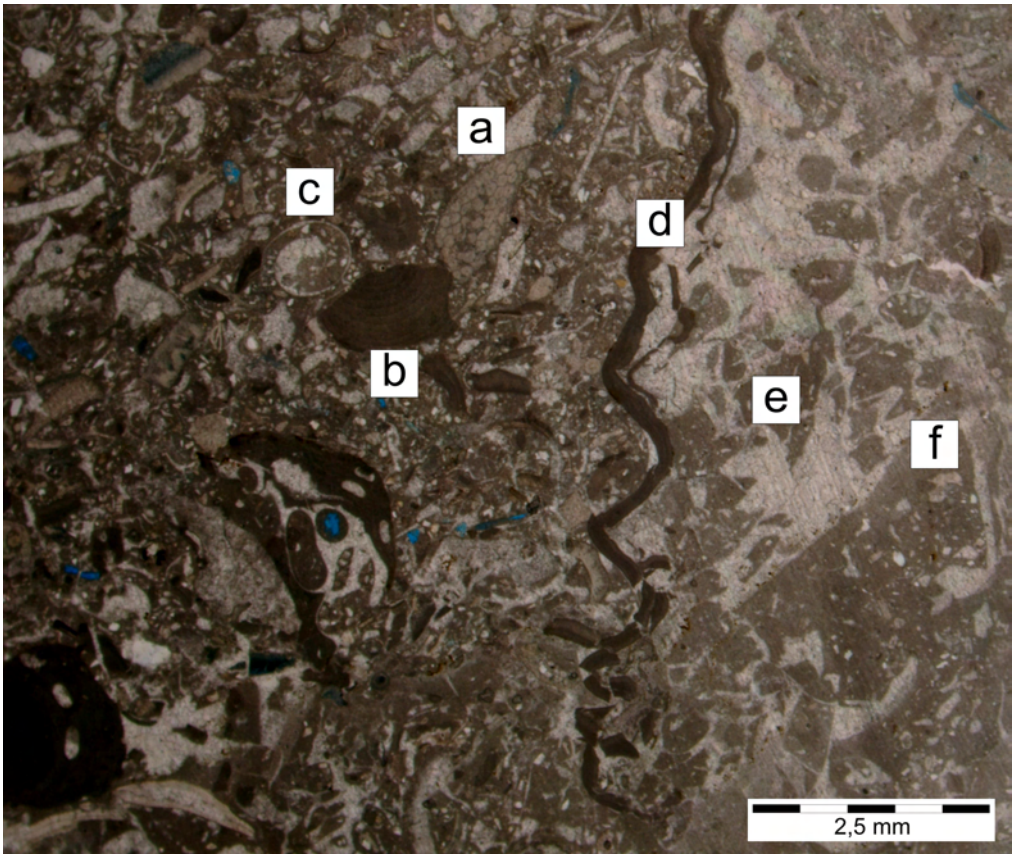

Fig. II.1.c. 3: Intraclast encrusted by coralline red algae. a: Bryozoan, b: Coralline-algal debris, c: Gastropod, d: Encrusting coralline algae, e, f: Brecciated components within the intraclast. Sample 1-1.2.

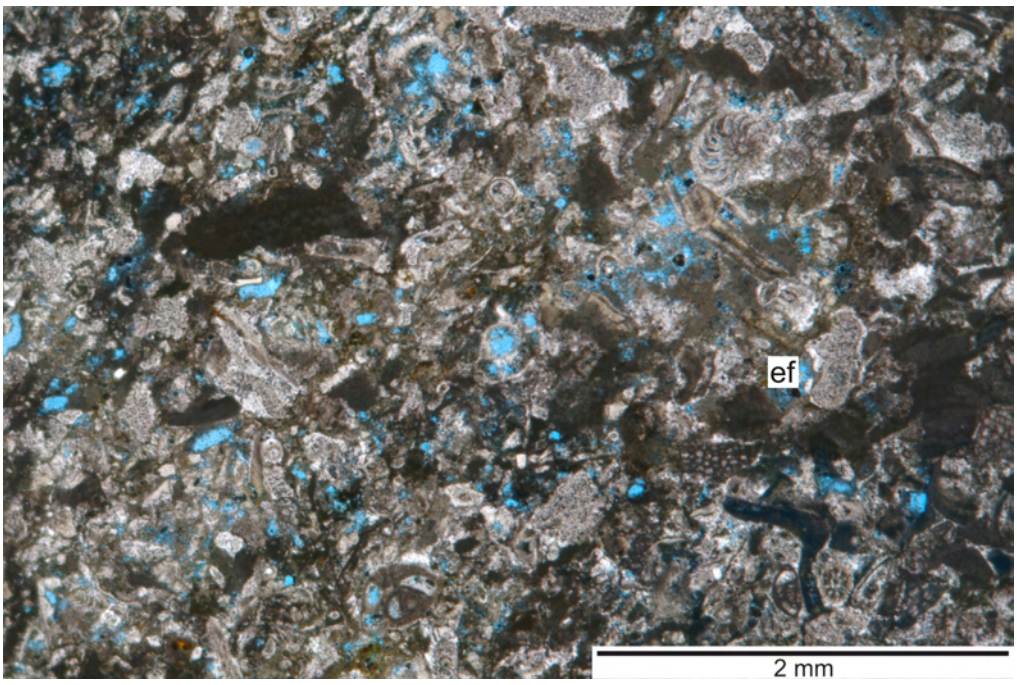

Fig. II.1.c. 4: Facies 2. Note abundant echinid fragments. Sample GSC-beach.

Facies 3: Hardground with Lithophaga Borings

This Facies occurs at the top of the northern Sedini transect sections. It appears as intensely bored and brecciated limestone. Borings occur in components but as well in the matrix, the Facies contains encrusted intraclasts and *Lithophaga* borings (Fig. III.1.a.5). Deposits are interpreted as hardgrounds, because borings and intraclasts indicate early lithification.

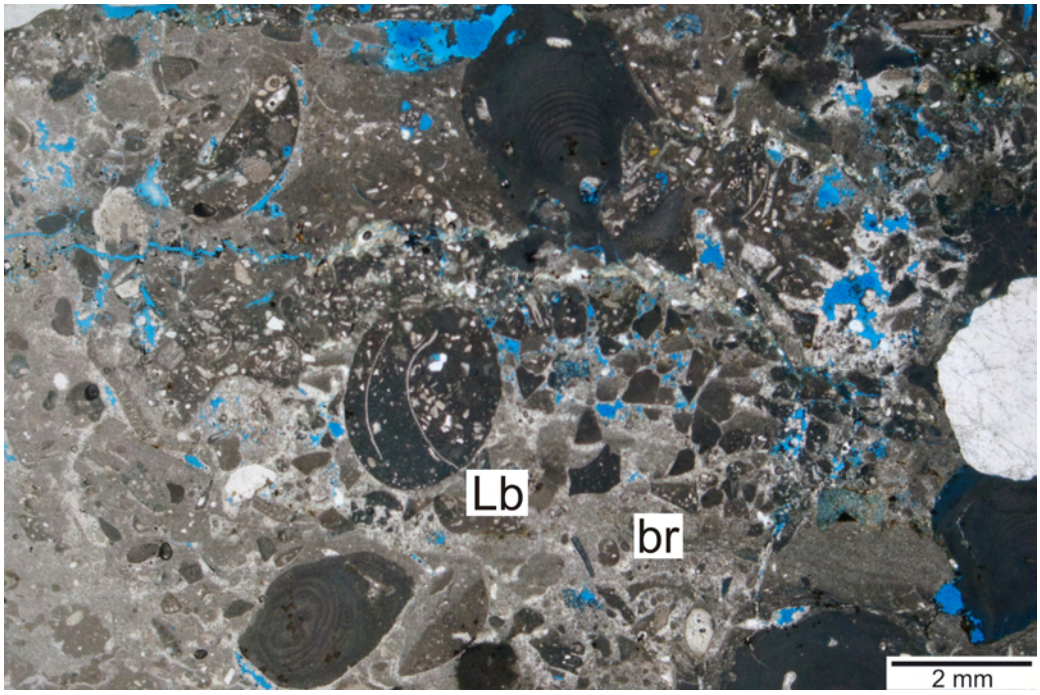

Fig. II.1.c. 5: Hardground overlying sequence 1a. Note brecciated parts and *Lithophaga* borings (Lb). Sample 2-4.3.

Facies 4: Coralline-Algal Debris Floatstones and Rudstones

This Facies are floatstones and rudstones characterized by very abundant coralline-algal branches (Fig. II.1.a.15). Most of the branches are attributed to corallines, some with joints, indicating that these branches are derived from geniculate coralline algae. Whether all of these branches are from geniculate corallines is not straightforward, but probable. The Facies also contains fruticose and warty protuberances, which are the remnants of branched rhodoliths (Fig. II.1.c.6). Red algae in well-preserved, warty to fruticose rhodoliths can be assigned to the coralline-algal genus *Sporolithon sp*. Other coralline-algal genera have not been determined, due to bad and fragmented preservation. Other components in this Facies are *Amphistegina sp.*, *Heterostegina sp*. and small benthic foraminifers, echinid fragments, bivalve fragments and bryozoans. The samples are moderately

sorted, and no sedimentary structures occur. This Facies occurs in sections 4 – 7 in the Sedini Transect.

Facies 4 is interpreted to have formed in minimum water depths of 40m, which is indicated by the occurrence of *Sporolithon sp.* (BOSENCE, 1991). Growth forms of rhodoliths point to a medium to low energy hydrodynamic setting. However, the occurrence of well preserved *Amphistegina sp.* and *Heterostegina sp*. record the vicinity of sea-grass meadows (CHAPRONIERE, 1975, WILSON et al., 1997), which are restricted to the photic zone.

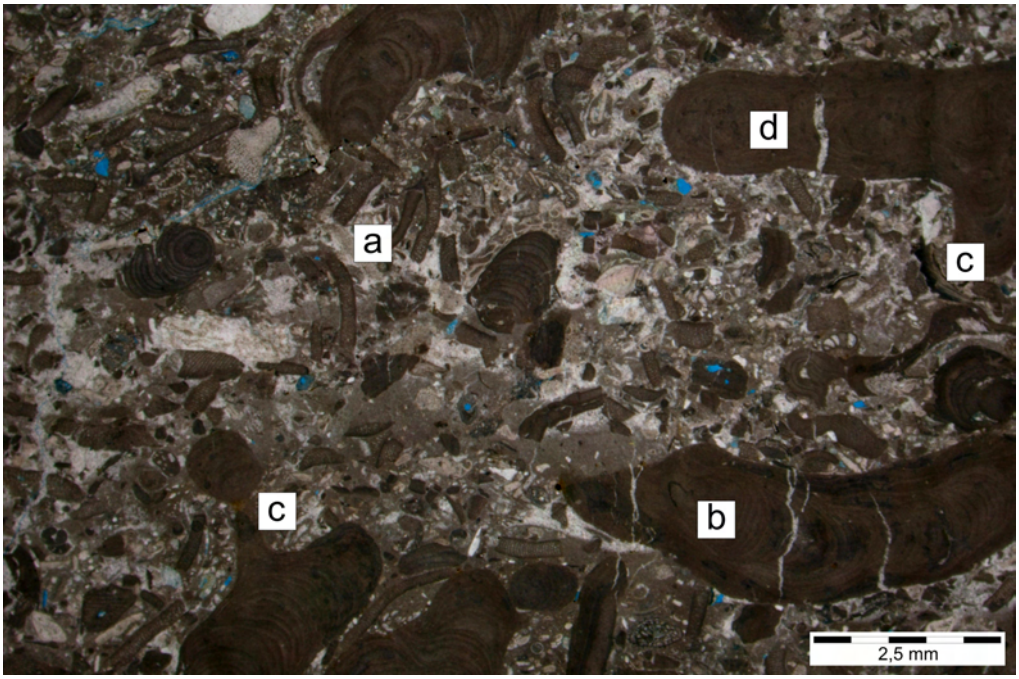

Fig. II.1.c. 6: Coralline algae in Facies 4. Note geniculate coralline algae (a), and fruticose and branched protuberances of non-geniculate coralline algae (b, c, d). Sample IDC2-2.0.

Facies 5: Cross-Bedded Coralline-Algal Debris Floatstones and Rudstones

Facies 5 is defined by large-scale, planar cross-bedding, forming bedsets up to 9m thick. Cross-bedded bodies have lateral extensions of several hundred meters (Fig. II.1.a.4). The main components are highly fragmented coralline-algal debris, small rhodoliths, echinid fragments, and bivalve fragments. Other components are *Amphistegina sp.*, barnacle fragments, coral fragments, and bryozoan fragments. Deposits are very well sorted (Fig. II.1.c.7). Directions of cross-bed dip are constant to the east, with subordinate directions to south-east and north-east. Dip angles are around 15°. This Facies crops out in Sequence 1 in the northern Ispilunca valley transect (sections S2, and S5) as well as in the village of Sedini behind the bank building (40°50´59.61´´N; 8°49´03.85´´S; no section). Large-scale cross-bedded deposits are interpreted to have formed by migrating, straight-crested submarine

dunes moved by strong currents. Varying dips towards easterly directions (ranging from east to north-east and south-east) indicate that these current were stable and unidirectional.

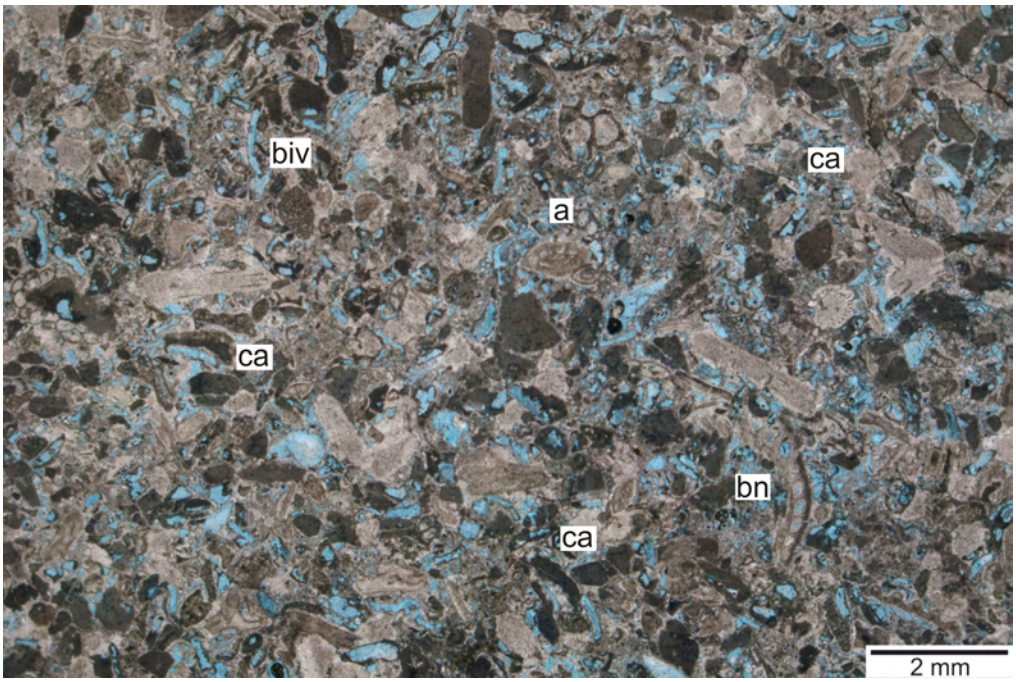

Fig. II.1.c. 7: Rudstone of Facies 5. Coralline-algal fragments (ca), echinid fragments, bivalve fragments (biv), *Amphistegina sp*. (a) and barnacles (bn) are the major constituents of this Facies. Sample S2-0.8.

Facies 6: Oyster Rudstones

Up to 3m thick, oyster-rich floatstones to rudstones occur at different levels in the succession of the Sedini carbonate platform. These packages laterally change into rudstones with coralline algae. Locally, the oyster-rich floatstones to rudstones contain large (up to 15cm), endobenthic bivalves, locally in living position. In thin sections, the oyster rudstones contain mainly well preserved oyster and other bivalve shells, of which some are preserved with both valves. Other components are rhodoliths, coralline-algal debris, *Amphistegina* sp., rare *Heterostegina* sp., barnacle fragments and bryozoans. Bivalves and other components are frequently encrusted by coralline algae (Fig. II.1.c.8). The oyster-rich deposits occur in the proximal part of the Grotta Su Coloru Transect (section TM1) and in the Sedini transect (section 7) as an up to 1m thick bed, at the limit between sequences 1a and 1b.

The oyster floatstones to rudstones are interpreted to reflect colonization of a hardground surface in a middle ramp setting. Encrustations of bivalves by coralline algae and borings in coralline algae point to reduced sedimentation rates. Thick-shelled bivalves record shallow water depths, and barnacle fragments indicate the

vicinity of hard substrates. It is proposed that the oyster colonization record flooding of a hardground formed during a prior relative sea-level fall.

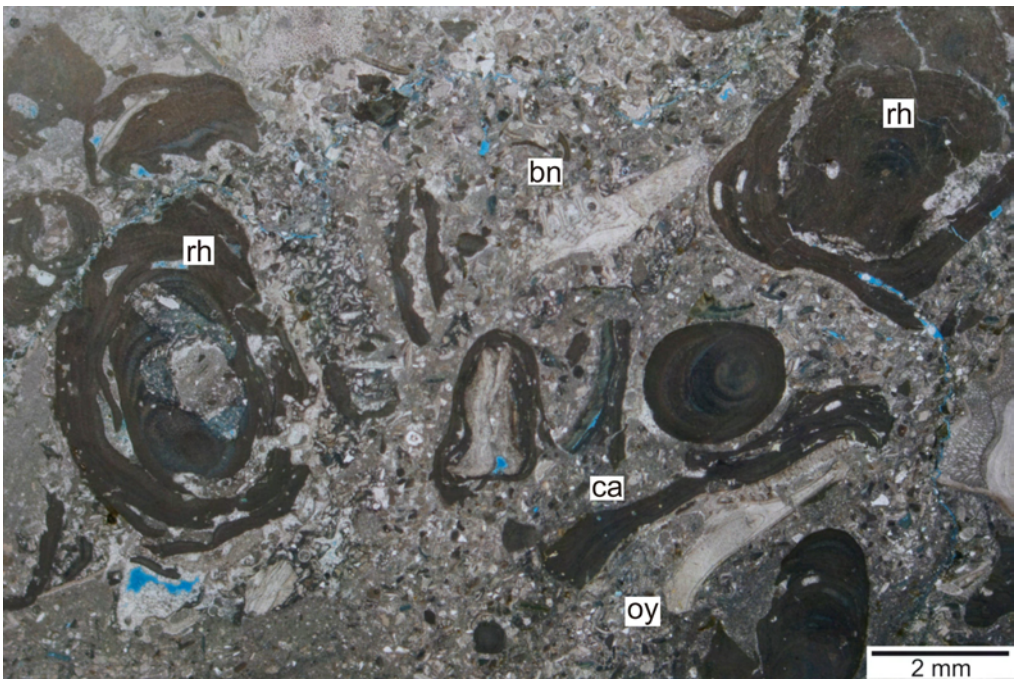

Fig. II.1.c. 8: Oyster rudstone of Facies 6. Oysters (oy), coralline algae (ca, rh) and barnacles (bn) are frequent contributors to this Facies. Note coralline algae encrusting shell fragments in the centre. Sample: S4A-10.4.

Facies 7: Coralline-Algal Debris and Echinid Packstones and Floatstones

This Facies occurs as an up to 6m thick, poorly bedded to massive package in the southernmost part of the Sedini Transect. It consists of fine-grained, well-sorted packstones to grainstones and coralline-algal debris and echinid fragments. Other components are *Heterostegina sp.*, *Amphistegina sp.*, and barnacle fragments (Fig. II.1.c.9). Although this Facies is rather monotonous, there is a systematic coarsening-upward trend in the sections 6 and 7, which is caused by an increase in the content of bivalves and small branched rhodoliths. Facies 7 is interpreted to have formed below wave base in an outer ramp setting. The coarsening-upward trend points to a progradation of shallower water facies.

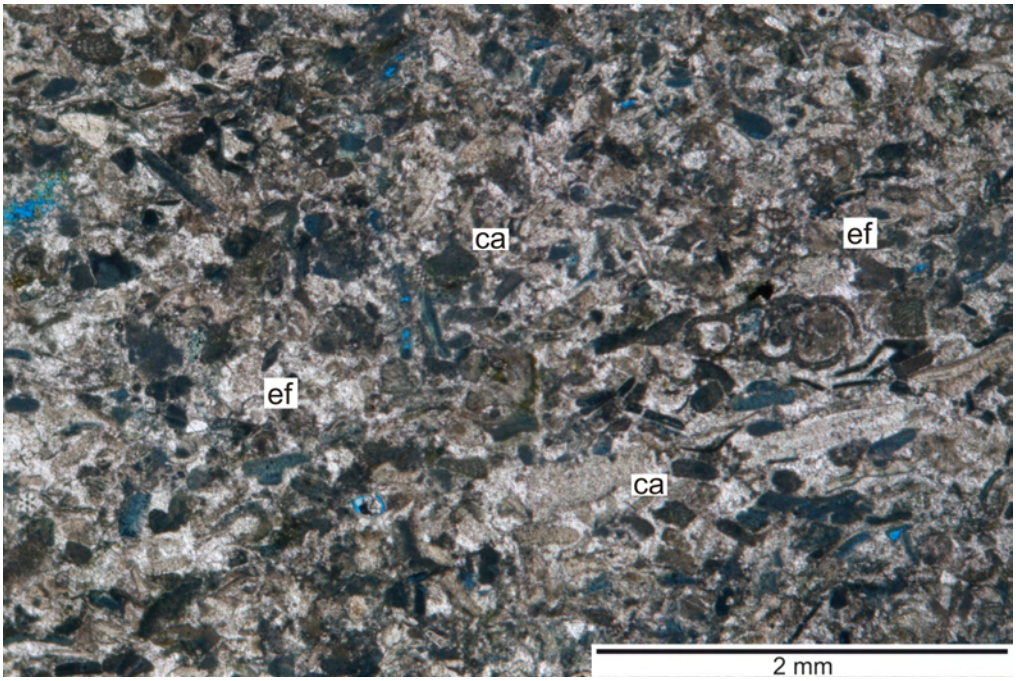

Fig. II.1.c. 9: Coralline-algal debris (ca), and echinid fragments (ef) as the main portion of Facies 7. Note the good sorting. Sample S4A-11.6.

Facies 8: Coralline-Algal Bindstones

Coralline-algal bindstones form irregular layers. Between the coralline-algal crusts there is trapped sediment with a yellowish to greenish colour. The coralline-algal bindstones contain a rich bivalve fauna, including *Ostrea sp.*, *Spondylus sp.*, *Pecten sp*. and *Isognomon sp.* (often in living position), echinids and their spines, barnacles, bryozoans, encrusting foraminifers, encrusting corals and fragments of solitary corals (figs. II.1.c.10, 11, 12, and 13). The bindstones contain a variety of coralline-algal genera, such as *Lithophyllum sp*., *Sporolithon sp.*, *Neogoniolithon sp*., *Mesophyllum sp.*, *Hydrolithon sp.* and others. Growth forms and growth patterns are encrusting to layered with minor warty or fruticose protuberances. Coralline crusts are often fused, resulting in robust frameworks (with minor delicate tendency) and frequently intergrown by encrusting foraminifers. This sometimes made the determination of coralline algae impossible. According to BRAGA (pers. comm., 2007), the overgrowth of encrusting foraminifers prevents the achievement of reproductive maturity in the coralline algae. As a result, they do not develop reproductive conceptacles, one of the major features for their taxonomic affiliation. Coralline-algal layers also alternate with bryozoan layers.

In most samples, crusts are locally broken, and fractures are filled with granular cements. The bound sediment consists of fine-grained material, which is locally micritic. Some dissolved components are preserved as micritic rims. Bioclasts are

highly fragmented coralline algae, *Amphistegina sp.*, echinid fragments, bivalve fragments, bryozoans, barnacle fragments, small benthic foraminifers, and rare *Borelis sp*. (Fig. II.1.c.14). Furthermore, fecal pellets and intraclasts occur in some samples. Red algae and bivalves are often bored. In the majority of the samples, acicular and bladed rims around components such as bivalves occur. More or less thick and isopachous syntaxial cements around echinid fragments are abundant. Samples of the coralline-algal bindstones are frequently dolomitized and show dedolomite porosity, which makes the determination of coralline algae difficult.

The coralline-algal bindstones are interpreted to have been formed in water depths of 40–60m, with low sedimentation rates. This depth assignment relies on BOSENCE (1991). Early diagenetic cements, together with the occurrence of fecal pellets reflect a high early diagenetic potential of this Facies. According to FLÜGEL (2004), the fossilization of fecal pellets needs bacterial decomposition of the organic mucus, and intragranular cementation. Lithification of these allochems takes place preferentially in calcium carbonate supersaturated waters, i.e. in warm and shallow waters. The coralline-algal bindstones occur at different positions in sequence 2 and locally form lenses in the large-scale trough cross-bedded packstones and grainstones (Facies 12). They are therefore interpreted to have acted as temporal stabilizers of these submarine dunes, forming the incipient platform margin at the mid- to late stage of platform formation (SCHLAGER, 2005).

Fig. II.1.c. 10: *Spondylus sp.* in living position in the coralline-algal bindstones.

Fig. II.1.c. 11: *Isognomon sp*. in the coralline-algal bindstones. Note partial dissolution of the aragonitic shell.

Fig. II.1.c. 12: Barnacle in the coralline-algal bindstones.

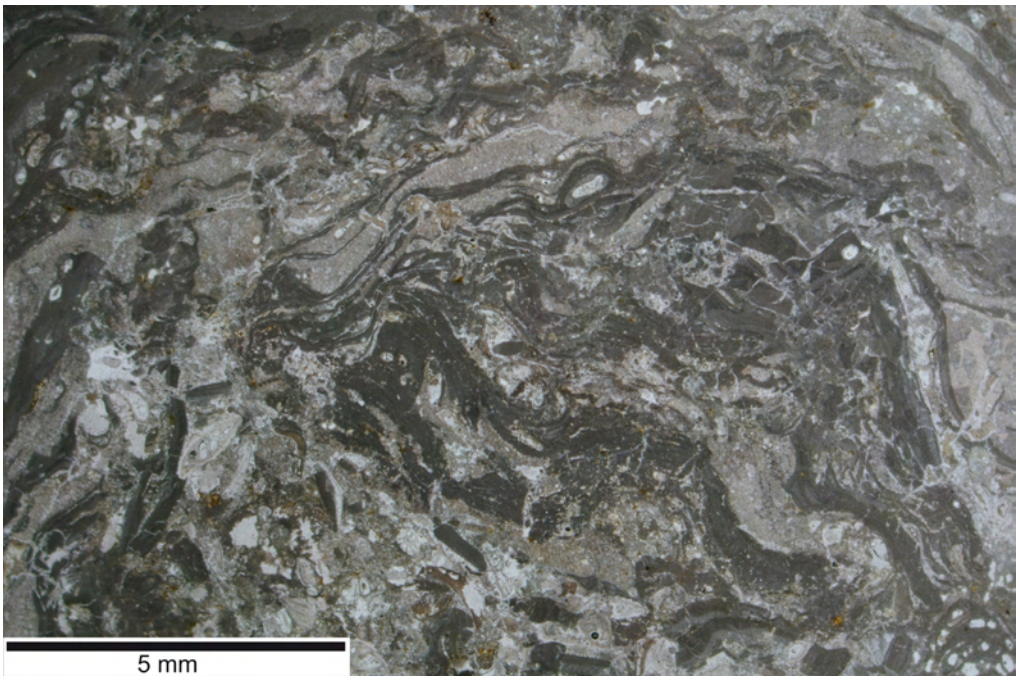

Fig. II.1.c. 13: Thin section of coralline-algal bindstones. Note frequent intergrowth of encrusting foraminifers and healing of broken crusts without major displacement. Sample VTTopN.

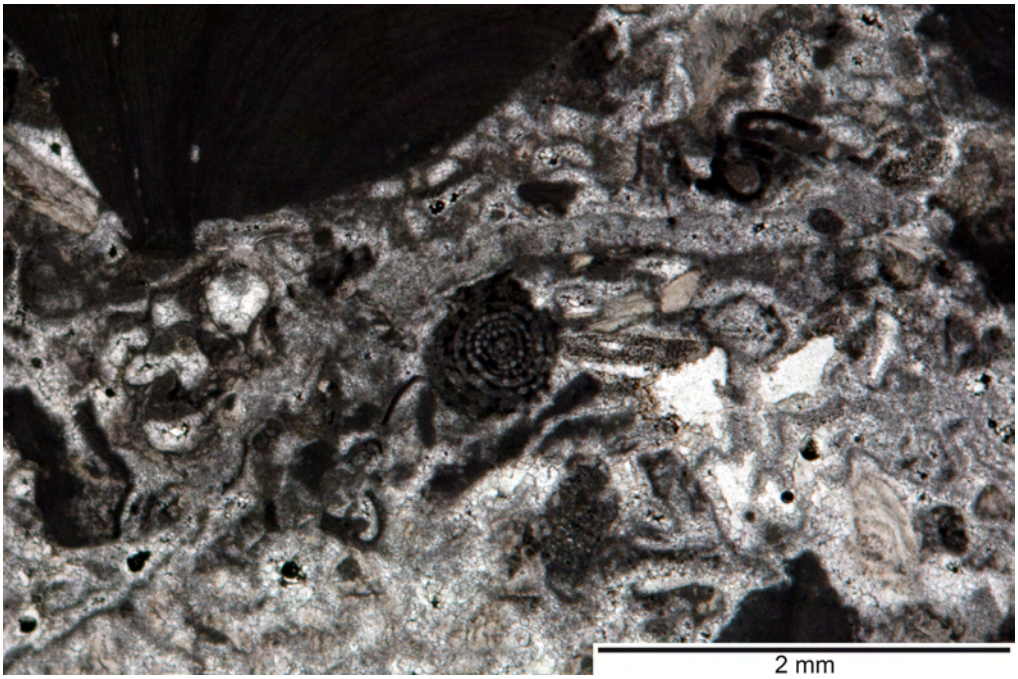

Fig. II.1.c. 14: The larger benthic foraminifer *Borelis sp*. in Facies 8. Sample VT Top.

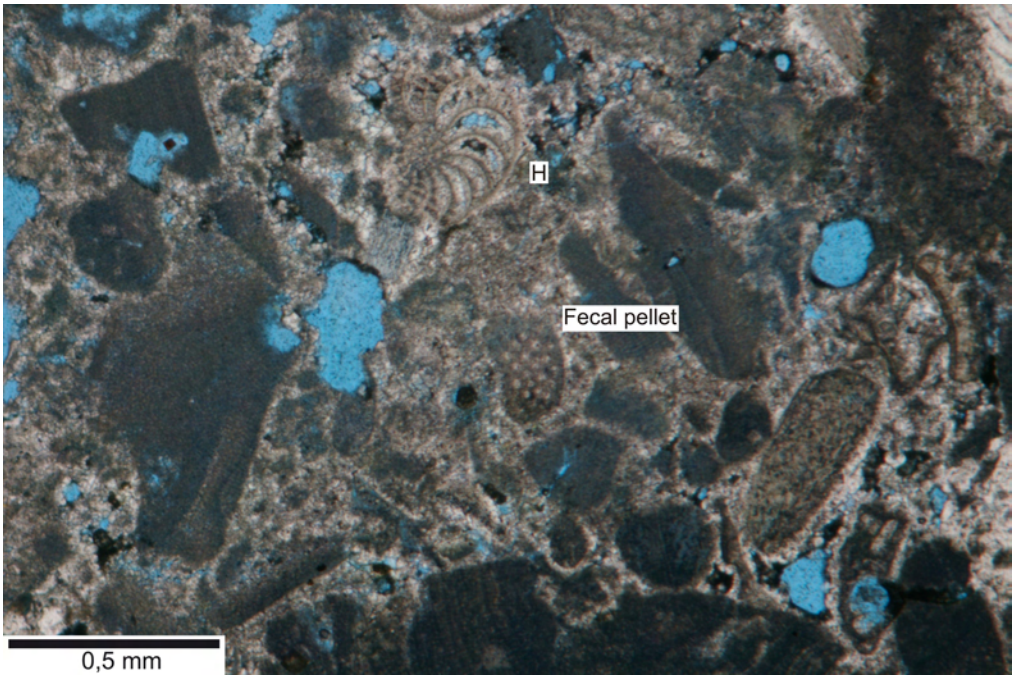

Fig. II.1.c. 15: Fecal pellet in the coralline-algal bindstones. H: *Heterostegina sp.* Sample VTC 32.

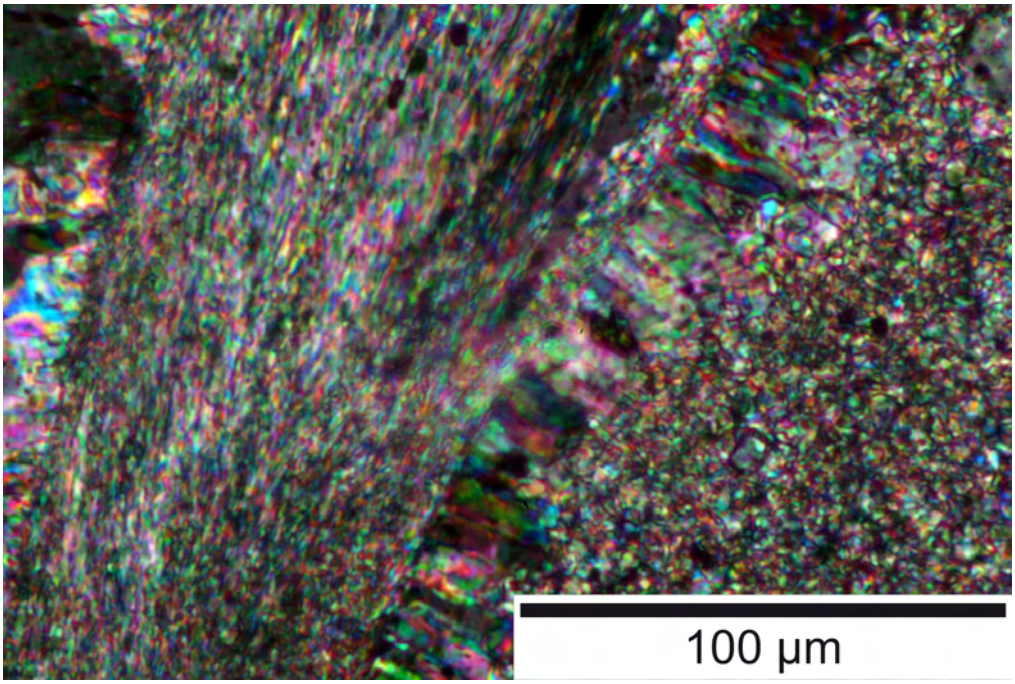

Fig. II.1.c. 16: Acicular cements around a bivalve bioclast in Facies 8. Nichols crossed. Sample VTC 32.

Facies 9: Coral Framestones

This Facies crops out on top of the plateau at the northern termination of the southern Ispilunca valley transect (Iscala Su Entu, "Entu reefs") and around the location of section BE1. Residual boulders of corals are found on the entire plateau. Coral framestones usually have coralline-algal bindstones (Facies 8) or oyster and coral framestones to rudstones (Facies 11) at their base. They are assigned to sequences 2 c-e.

Coral framestones form up to 6m thick bodies with domal corals. Tubiform (*Tarbellastrea*?) growth forms and crustose corals also occur (figs. II.1.a.8, II.1.b.1). Trapped sediment between corals and coralline algae is a very fine-grained, locally micritic (micropeloidal) packstone. Bioclasts are echinid fragments, bivalve fragments, miliolid foraminifers, other small benthic foraminifers, coralline-algal fragments and bryozoans. Most components are dissolved and recrystallized. Cement is granular to small blocky calcite.

This Facies only occurs in Sequence 2, and crops out on top of the plateau at the northern termination of the southern Ispilunca valley transect (Iscala Su Entu, "Entu reefs") as well as in the middle part of the Southern Ispilunca valley transect. Coral boulders occur on the entire plateau Bena Ecrabas. The coral framestones are interpreted to have formed biostromal complexes in an inner-platform setting in the late stage of platform development. Their occurrence indicates the existence of a tropical carbonate factory at that time. Although reefs are preserved at only two

localities in the Sedini carbonate platform, the occurrence of coral boulders over a large area indicates that reefs covered large areas of the inner platform. Due to the patchy occurrence of the coral framestone, a detailed assignment of water depth is not straightforward. Domal coral growth forms in Miocene reefs comparable to the example of the Sedini carbonate platform are generally interpreted to be characteristic of water depths of around 20m (ESTEBAN, 1996).

Facies 10: Rhodolith Floatstones

This Facies is composed of rhodoliths, coralline-algal debris, barnacles, echinid debris and coral fragments (Fig. II.1.c.17). Rhodoliths are sphaeroidal to ellipsoidal, morphologies are laminar concentric to moderately branched. The rhodolith floatstones contain *Amphistegina sp.*, *Heterostegina sp.*, coral fragments and encrusting foraminifers. Intraclasts occur. Components have micritic envelopes. The rhodolith floatstones occur in the northern Ispilunca valley transect (section S5) in sequence 1b and in section S7 in sequence 2c. They occur in lense-shaped bodies 30-50cm thick and up to 60m wide (Fig. II.1.a.3).

In the Sedini carbonate platform, the rhodolith floatstone Facies is interpreted to record flooding events due to relative sea-level rises (NALIN et al., 2007). The main process of rhodolith formations was sporadic reworking, indicating a depositional environment in the middle to outer ramp (sequence 1), and in the inner to middle platform (sequence 2). The occurrence of intraclasts records reworking of early lithified material.

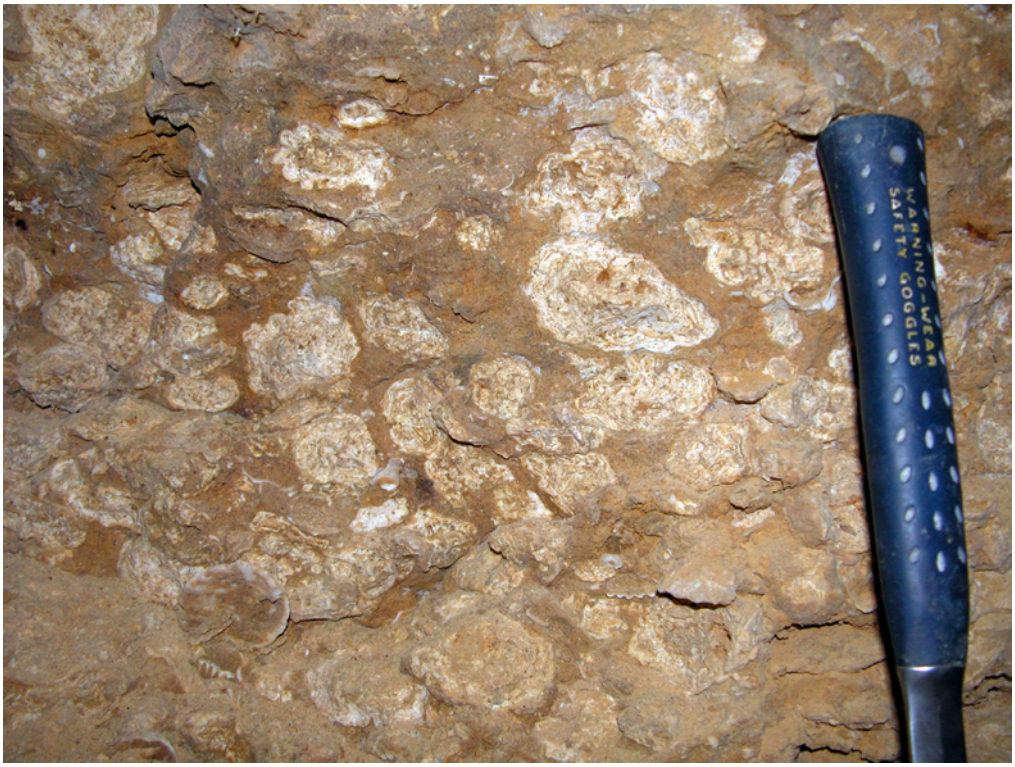

Fig. II.1.c. 17: Rhodolith floatstone (Facies 10).

Facies 11: Oyster and Coral Framestones to Rudstones

This Facies is characterized by the occurrence of up to 20cm big, thick-shelled oysters, which are encrusted by corals. In thin sections, Facies 11 contains bivalve fragments, bryozoans, small benthic foraminifers, echinid debris and some *Amphistegina sp*. The framestones to rudstones occur in a 1m thick layer (Fig. II.1.c.18) in Sequence 2 at one locality (section BE1) only. The base of this layer contains small, dome-shaped coral colonies up to 40cm in diameter, as well as solitary corals (Fig. II.1.c.19).

The oyster and coral framestones to rudstones are interpreted to have formed in an inner-platform to platform-margin environment. Thick shelled bivalves and the presence of hermatypic corals point to a shallow-marine setting. The oyster banks are thought to reflect the early colonization of hardgrounds during phases of relative sea-level rise.

Fig. II.1.c. 18: Oyster and coral framestones to rudstones. Note thick shells.

Fig. II.1.c. 19: Small coral bioherms at the base of the oyster and coral framestones. In this layer, also solitary corals occur.

Facies 12: Large-Scale, Trough Cross-Bedded Packstones and Grainstones

This Facies consists of large-scale, low-angle, trough cross-bedded packstones and grainstones (Fig. II.1.c.20), forming bodies 12m thick and 70–100m wide. Based on compositional variations, three subfacies of the packstones to grainstones can be differentiated (Facies 12a-c). Facies 12 occurs in both Ispilunca valley transects (section S7, S8) and the Sa Rocca Manna transect (section CL1, CHIN and VT7) and is assigned to sequences 2a-d.

Facies 12a: Heterostegina sp. Packstones to Grainstones

Facies 12a is a very well to moderately sorted packstone to grainstone with frequent *Heterostegina sp*., *Amphistegina sp*., coralline-algal debris, some miliolid foraminifers, and bivalve fragments (Fig. II.1.c.21). Echinid fragments have thick, but not continously isopachous rims. Some bivalve shells are dissolved at their margins; some are completely leached and preserved as molds. Micritic rims are rare, some samples (S7-1.0 and -4.5) contain phosphate or glauconite (S7-5.0 and -5.5). This Facies occurs in the lower part of Sequence 2 (2b, section S7).

Facies 12 b: Amphistegina sp. Packstones to Grainstones

This Facies is characterized by abundant *Amphistegina sp.* and echinid fragments with extensive syntaxial overgrowths, bivalve fragments, fragments of bryozoans, encrusting foraminifers, and coralline-algal debris (Fig. II.1.c.22). One sample (CHIN 6.6) contains coral fragments and remnants of a coralline-algal framework. Most of the components in sample CHIN-5.0 are preserved as micritic rims. The majority of thin sections contain acicular to bladed early cements. This Facies occurs in the upper part of section CL1 and in the complete section CHIN (Fig. II.1.c.24).

Facies 12c: Echinid Packstones to Grainstones

The Echinid packstones and grainstones are very well sorted and fine grained. In addition to echinids, this Facies contains some *Amphistegina sp*., small benthic foraminifers, bryozoans, coralline algae, coral- and barnacle fragments (Fig. II.1.c.23). Mostly all echinid fragments have thick, inclusion-rich, syntaxial cements, other cements are acicular rims around larger benthic foraminifers.

The large-scale, low-angle, trough cross-bedded packstones and grainstones are interpreted as deposits of submarine dunes, located at the platform margin. Several evidences indicate periodical stabilization and stagnancy of sediment relocation within the submarine dune belt by

1. the occurrence of coralline-algal bindstone lenses in between the large-scale trough cross-bedded deposits (Facies 8),
2. the existence of inclusion-rich, syntaxial cements indicating early cementation (FLÜGEL, 2004),
3. the occurrence of glauconite,
4. the occurrence of inhabitants of sea-grass meadows such as *Amphistegina sp.* point to the existence of sea-grass meadows, which may have stabilized parts of the dunes or interdunes area.

The differentiation of the trough cross-bedded Facies into three subfacies is interpreted to reflect ambiental variations (water depth and/or water temperature). In the lower sequence 2 (Facies 12a), the occurrence of *Heterostegina sp.* points either to a deeper depositional environment or warmer ambient water temperatures than during the formation of the sequences 2c and d (Facies 12b and c). The echinid packstones to grainstones (Facies 12c) are a more distal equivalent to the *Amphistegina sp*. packstones to grainstones (Facies 12b), which results from the correlation of the sections CL1, CHIN and VT7 (Fig. II.1.c.24).

Fig. II.1.c. 20: Low angle, large-scale trough cross-beds in Facies 12. Note general dipping of the unit to the southeast. Location: Sa Rocca Manna (sequence 2d), view direction is to the west.

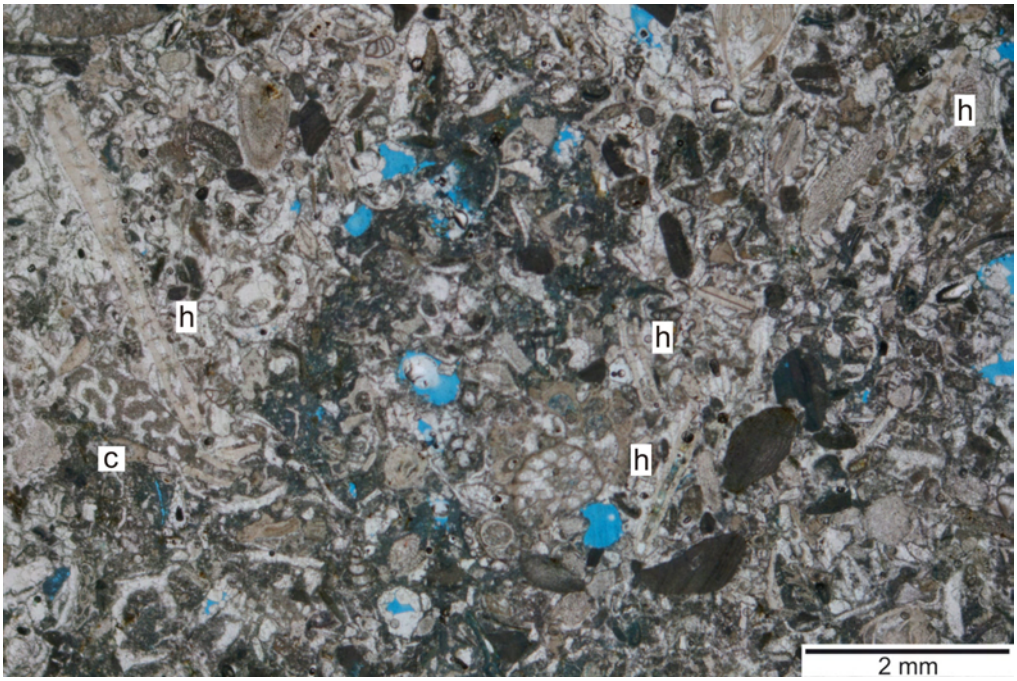

Fig. II.1.c. 21: Thin section of the *Heterostegina sp.* (h) packstones to grainstones. In some places, coral fragments (c) occur. Sample S7-5.

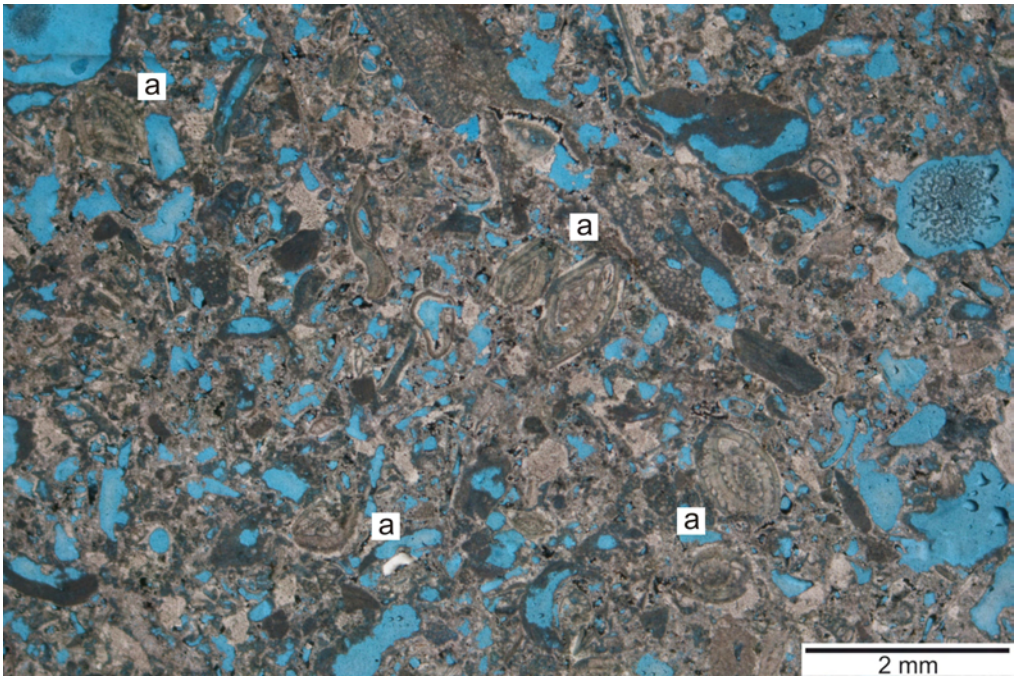

Fig. II.1.c. 22: Thin section of the *Amphistegina sp*. (a) packstones to grainstones. Sample CHIN-base.

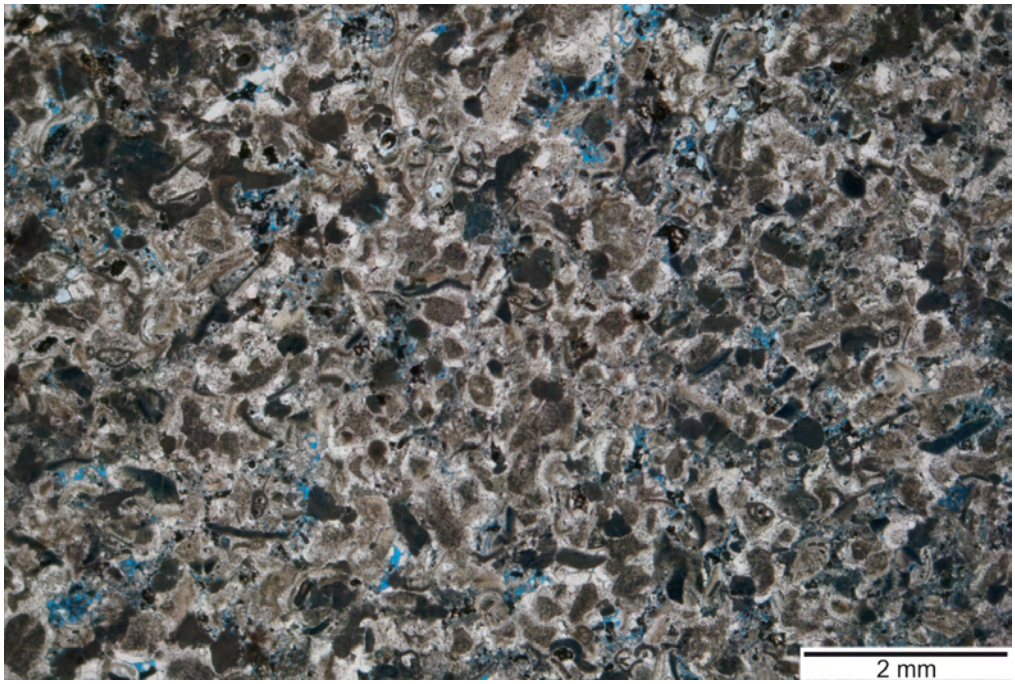

Fig. II.1.c. 23: Thin section of the Echinid packstones to grainstones. Note the abundant echinid fragments surrounded by a thick, light rim, which is syntaxial cement. Sample VT7-3.1.

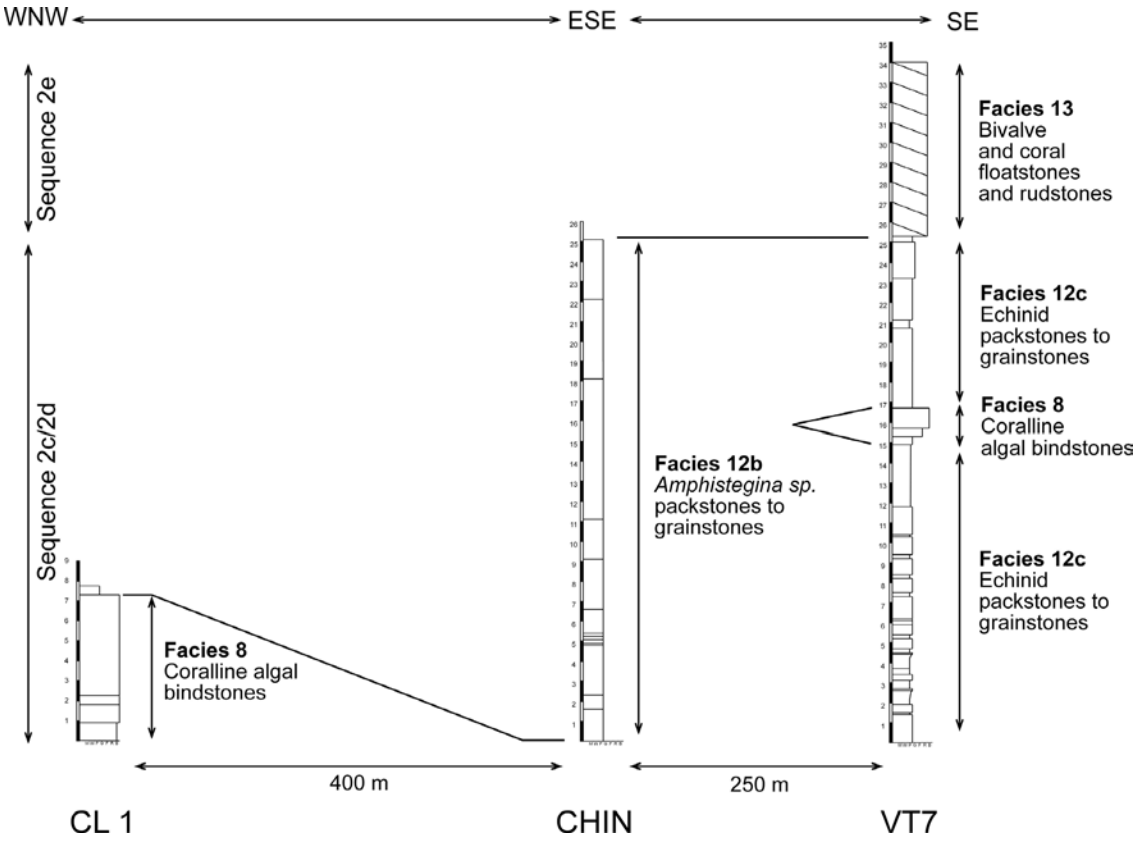

Fig. II.1.c. 24: Correlation of sections CL1, CHIN, and VT7 (for location see Fig. II.1.c.1). The echinid packstones to grainstones (Facies 12 c) are a distal equivalent of the *Amphistegina sp.* packstones to grainstones (Facies 12b). Note coralline-algal bindstone (Facies 8) embedded in the Echinid packstones to grainstones.

Facies 13: Bivalve and Coral Floatstones and Rudstones

This Facies occurs in large-scale, planar cross-beds dipping with up to 25° (Fig. II.1.c.25). The floatstones to rudstones contain bivalves (some preserved with both valves), abundant coral fragments and echinid fragments, as well as encrusting foraminifers, small benthic foraminifers and *Amphistegina sp*. (Fig. II.1.c.26). The amount of corals increases upsection, where up to 5cm large coral fragments occur. Coralline-algal branches are present. The Facies is characterized by very abundant micritic rims around all components. Bivalves and corals are mostly preserved as molds. Some intervals contain small intraclasts. In general, the floatstones and rudstones are cement-rich, cements are acicular to bladed. This Facies crops out in the Sa Rocca Manna transect (section VT7) in Sequence 2 e (Fig. II.1.c.24).

The Bivalve and coral floatstones and rudstones are interpreted as fore-reef deposits. Correlation of different outcrop shows that it formed distally to the coral framestone Facies (Facies 9).

Fig. II.1.c. 25: Large-scale, planar cross-bedded bivalve and coral floatstones to rudstones. Scale bar in the lower right is 4 m. Sa Rocca Manna, view direction is to the north-east.

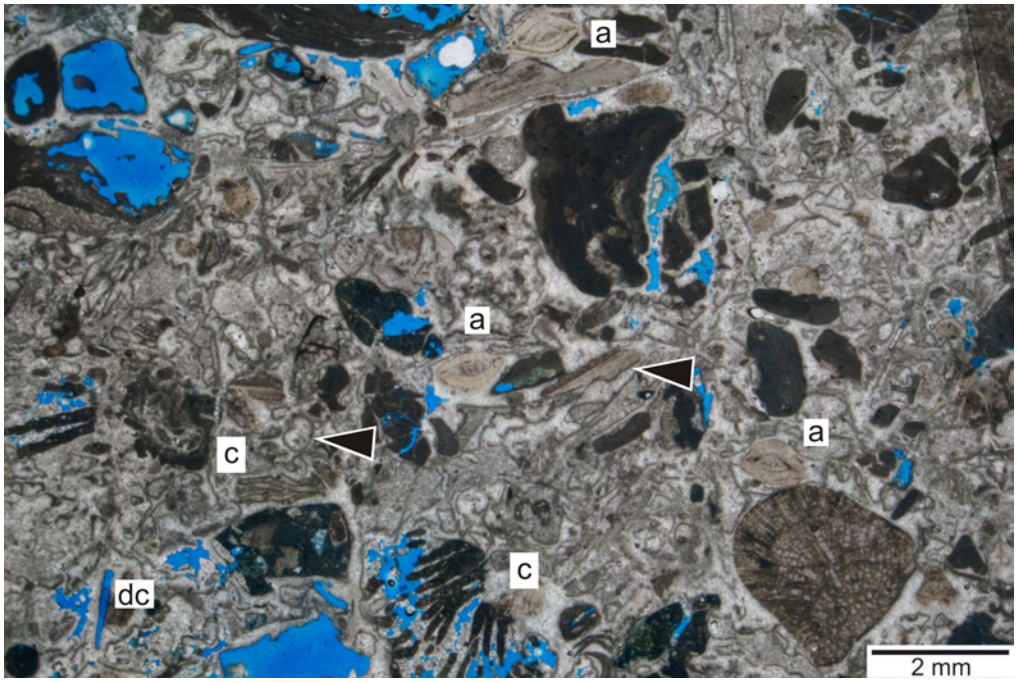

Fig. II.1.c. 26: Facies 13. Bivalves and coral fragments (c) are the main components of this Facies. Other contributors are *Amphistegina sp.* (a). Note dissolved component (dc) and micritic envelopes (arrows). Sample SRR-3.3.

Facies 14: Rhodolith Rudstones and Floatstones to Coralline-Algal bindstones

This Facies contains abundant discoidal to ellipsoidal rhodoliths, which are closely packed and often fused by subsequent coralline-algal encrustation. Rhodolith growth forms are laminar concentric with minor warty or fruticose protuberances. Coralline-algal crusts form a robust to delicate framework, and are often heavily broken in-situ, and afterwards healed. Other components are pectinid bivalves. Deposits appear layered, with wavy and irregular bedding surfaces. Bedding is gently inclined basinwards. Rhodoliths frequently contain encrusting foraminifers, as well as bryozoans. Small benthic foraminifers, *Amphistegina sp*. and echinid fragments occur in the matrix between the red algae. Acicular or bladed cement rims around components occur in the majority of the samples. This Facies crops out in the Sa Rocca Manna transect as the clinoform rollover to upper foreset part of the rhodolith clinoforms. Numerous outcrop and thin section photos are provided in chapter II.1.b.

This Facies is interpreted to form the platform margin in the late stage of platform formation (sequence 2e). The dominant processes were alternating slope-break stabilization by organic construction and episodical reworking.

Facies 15: Rhodolith Rudstone Clinoforms

The rhodolith rudstones are arranged in 20m high clinoform beds with up to 27° steep basinward dips. Rhodoliths are discoidal to sphaeroidal. Along the clinoform, rhodolith size decreases from 10-15cm to 5-10cm in diameter. The amount of matrix between rhodoliths increases downslope. In some of the clinoform bodies, rudimentary, subhorizontal stratification occurs. The stratification is mainly developed horizontally, but may also slightly dip towards the slope. Some clinoforms wedge out upslope. The rhodolith rudstone clinoforms make up the majority of the Sa Rocca Manna transect. Numerous outcrop and thin section photos are provided in chapter II.1.b.

This Facies is interpreted as forming at the slope of the carbonate platform during its latest growth stage. The dominant processes were in-situ rhodolith growth, minor platform shedding and episodical storm-reworking. Early cements reflect early diagenetic potential and a fluctuating hydrodynamic energy.

Facies 16: Bioturbated Wackestones and Packstones

A Facies of well-bedded, bioturbated wackestones and packstones occurs at several locations around the inner parts of the Sedini carbonate platform, namely in the Sedini transect (section S1, section 6), the northern Ispilunca valley transect (sections S6 and S8), the southern Ispilunca valley transect, the Sa Rocca Manna transect (section VT1 and VT2), Sa Rocca Rutta (section SRR), and the Grotta Su Coloru transect (section TM1). This Facies is well-bedded, producing terrace-shaped hillocks. The main components are complete and fragmented echinids, bivalves, serpulids and rare, small rhodoliths. Additional components are bryozoans and coral fragments. Horizontal and vertical bioturbation is a major feature of this Facies. Layers with abundant, complete echinids occur at the bases of fining-upwards cycles. In thin section, the wackestones and packstones contain planktic foraminifers (Fig. II.1.c.27). Phosphate and glauconite is frequent in most samples, some thin sections contain biotite. The wackestones and packstones are interpreted to represent outer-ramp and outer-platform deposits. The main processes were allochthonous accumulation and periodical storm reworking, as reflected by the occurrence of echinid layers, which are interpreted as tempestite beds.

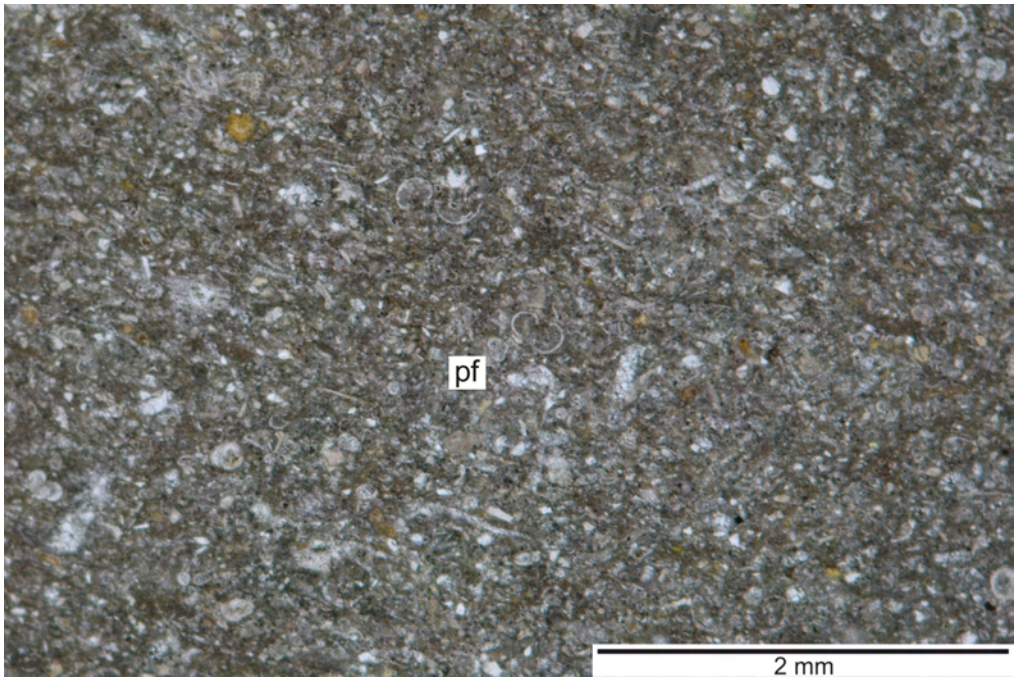

Fig. II.1.c. 27: Thin section of the bioturbated wackestones and packstones. Note well sorting and the occurrence of planktic foraminifers (pf). Sample S1-15.

Facies 17: Well-Bedded Marls and Marlstones

This Facies consists of an alternation of soft, marly intervals and 2–15cm thick marlstone beds. Some of the calcareous layers are partly silicified. In thin section, Facies 17 comprises a fine lamination. It contains frequent sponge spicules, planktic and small benthic foraminifers, as well as siliceous phytoplankton and frequent fish remains (figs. II.1.c.28, 29, 30). This Facies crops out in the village of Sedini (section SM), and due to the dense building development, there is only minor outcrop control. It forms the stratigraphically youngest unit in the area

The well bedded marls and marlstones are interpreted as basin deposits, formed in areas below the reach of wave-action. There are two explanations possible to explain the lack of neritic components: the source area for neritic input was located too far away at time of deposition of this Facies, or there was no active neritic carbonate production at all. Occurrence of sponge spicules and siliceous phytoplankton indicates that the deposits may have formed under influence of an elevated nutrient influx.

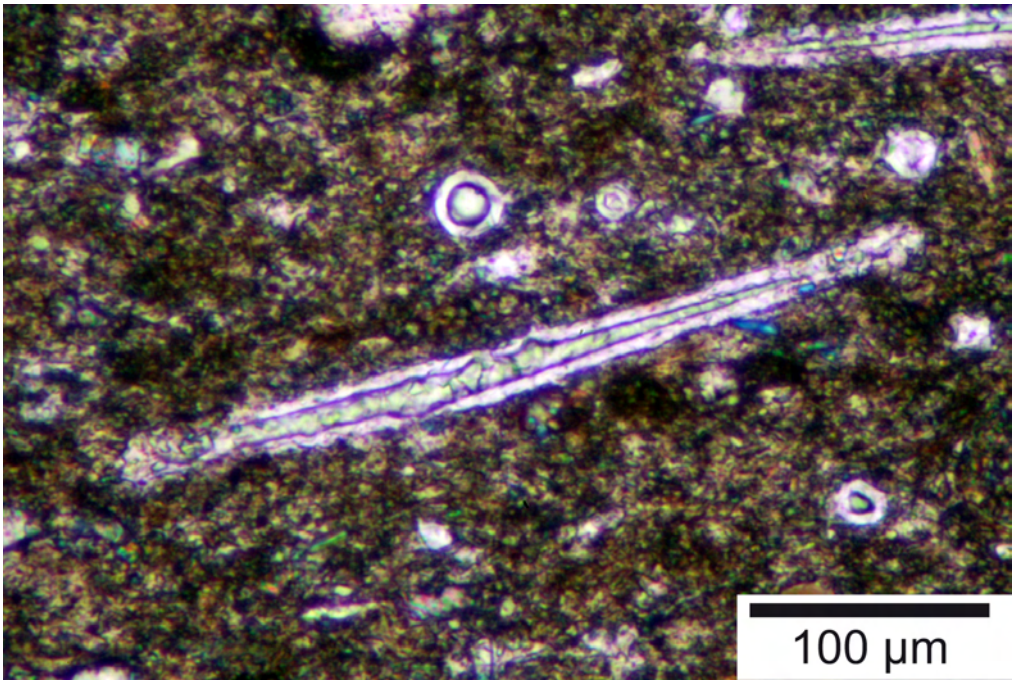

Fig. II.1.c. 28: Sponge spicule in the well bedded marls and marlstones. Sample ST.

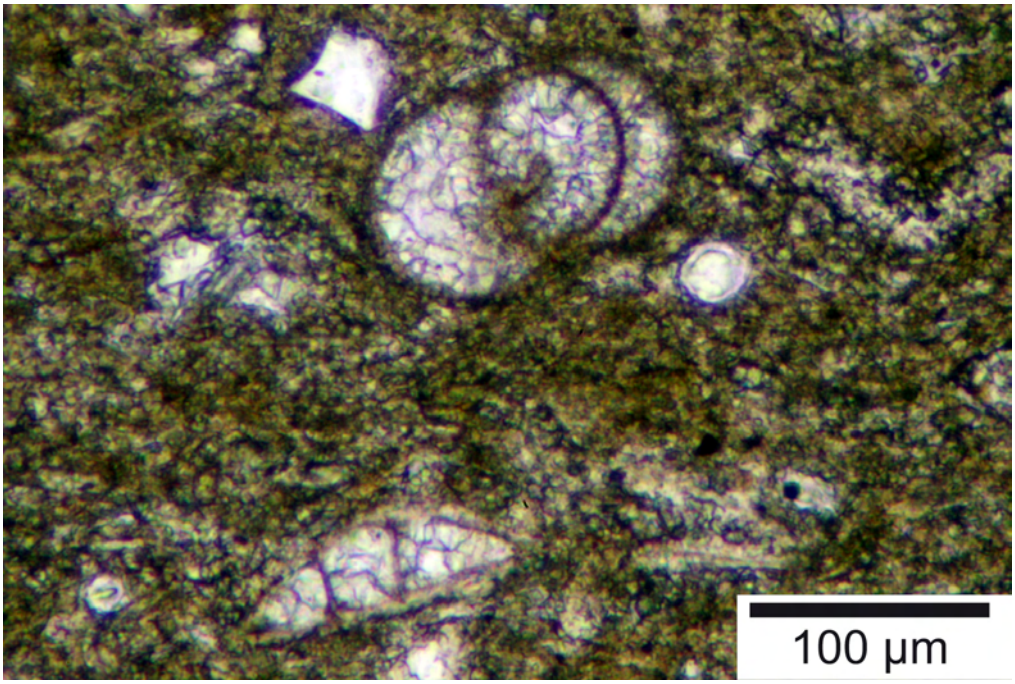

Fig. II.1.c. 29: Small benthic foraminifers in the well bedded marls and marlstones. Sample ST

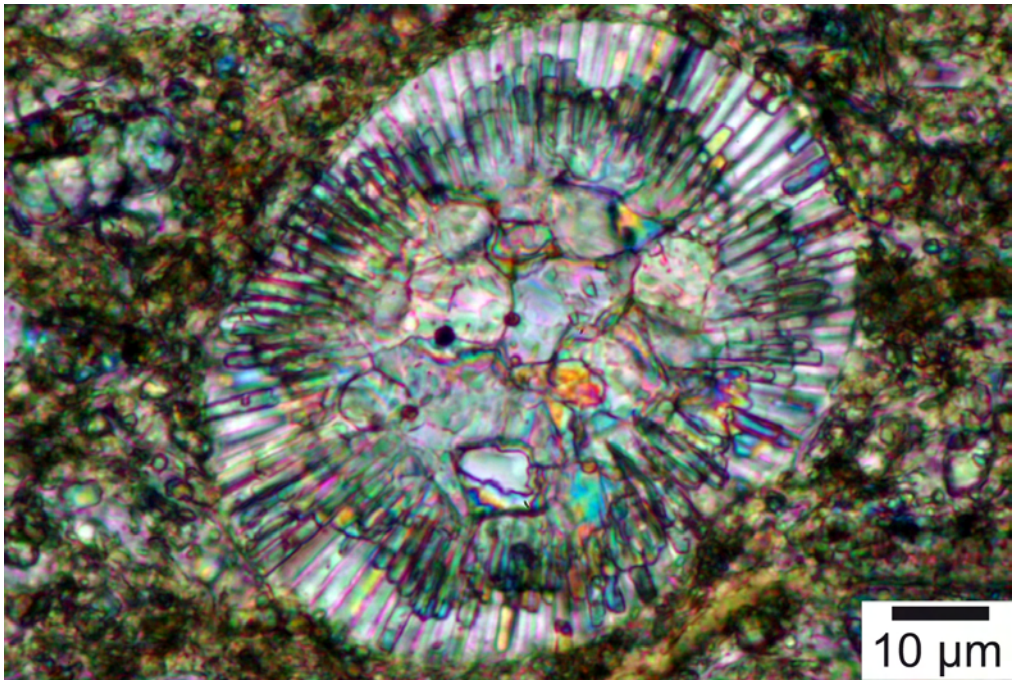

Fig. II.1.c. 30: Siliceous phytoplankton in the well bedded marls and marlstones. Sample ST

II.2. The Porto Torres Basin

The Porto Torres Basin is the second working area (Fig. I.2.4). It is situated to the north-west of Sassari, between the villages Sennori and Osilo, covering an area of approximately 100km^2.

II.2.a. Stratigraphy and Ages

The Porto Torres Basin is the northern segment of a halfgraben, which is exposed onshore around the province capital Sassari, covering an area of approximately 200km^2 (see Fig. I.2.4.). It has an offshore continuation of approximately 450 km^2 to the north in the Gulf of Asinara (Fig. I.2.5., THOMAS & GENNESSEAUX, 1986, FUNEDDA et al., 2000). To the south, a transfer zone marks the transition to the Logudoro Basin (FUNEDDA et al., 2000). The calcalkaline magmatic activity that accompanied halfgraben formation lasted between 33 and 11Ma b.p., with a peak activity around 21-19Ma b.p. (BECCALUVA et al., 1985). It included andesitic and basaltic flows, pyroclastic and ignimbritic events, as well as deposition of volcanic ashes. Two extensive, rhyodacitic, ignimbritic layers are spread in northern Sardinia. The upper one (τ2) was dated radiometrically and has been formed between 19.5 and 18.9Ma (BECCALUVA et al., 1985). Active extension and volcanic activity led to the formation of a very irregular topography, which was filled with volcanoclastic deposits, and later with alluvial conglomerates. Continuous subsidence led to marine conditions in the Burdigalian (THOMAS & GENNESSEAUX, 1986, FUNEDDA et al., 2000, SOWERBUTTS, 1997, 2000, CASULA et al., 2001).

The marine carbonates of northwestern Sardinia were described by a number of authors, amongst them POMESANO CHERCHI (1971), MAZZEI & OGGIANO (1990), MARTINI et al. (1992), FRANCOLINI (1994), FUNEDDA et al. (2000, 2003), SOWERBUTTS (2000) and VIGORITO et al. (2006). Most of these studies refer to the Logudoro Basin. The stratigraphy established by MAZZEI & OGGIANO (1990), which was expanded by MARTINI et al. (1992) and FUNEDDA et al. (2000, 2003), includes three sedimentary cycles ranging from the Oligocene to the Messinian.

VIGORITO et al. (2006), amending the stratigraphy of MAZZEI & OGGIANO (1990) and FUNEDDA et al. (2000, 2003), recognize two post-rift sedimentary sequences (PRS 1 and PRS 2, Fig. II.2.a.1), separated by a post-rift sedimentary unconformity (PRU 1, Fig. II.2.a.1). The lower sequence (PRS 1) is subdivided into units A and B. The upper sequence (PRS 2) comprises four units (C-F, Fig. II.2.a.1). Units D-F correlate with the "Calcari di Monte Santo" (POMESANO CHERCHI, 1971), which are analogous to the "Calcari superiori" of MAZZEI & OGGIANO (1990). The units D-F in VIGORITO et al. (2006) range from the Middle Langhian to the Upper Serravallian, whereas the third sedimentary cycle of MAZZEI & OGGIANO (1990) is Tortonian to Messinian in age. The datation of Vigorito et al (2006) shows a good fit to Sr-datations of

SOWERBUTTS (1997), who dates the top of the Scala di Giocca section with 11.32 Ma. (Fig. II.2.a.1), which is Upper Serravallian using the timescale of BERGGREN et al. (1995), or lowermost Tortonian according to the timescale of GRADSTEIN et al. (2004) (Fig. II.2.a.1.). The carbonate deposits studied pertain to the second and third sedimentary cycle of MAZZEI & OGGIANO (1990), reported to be Burdigalian to Messinian in age (Fig. II.2.a.1).

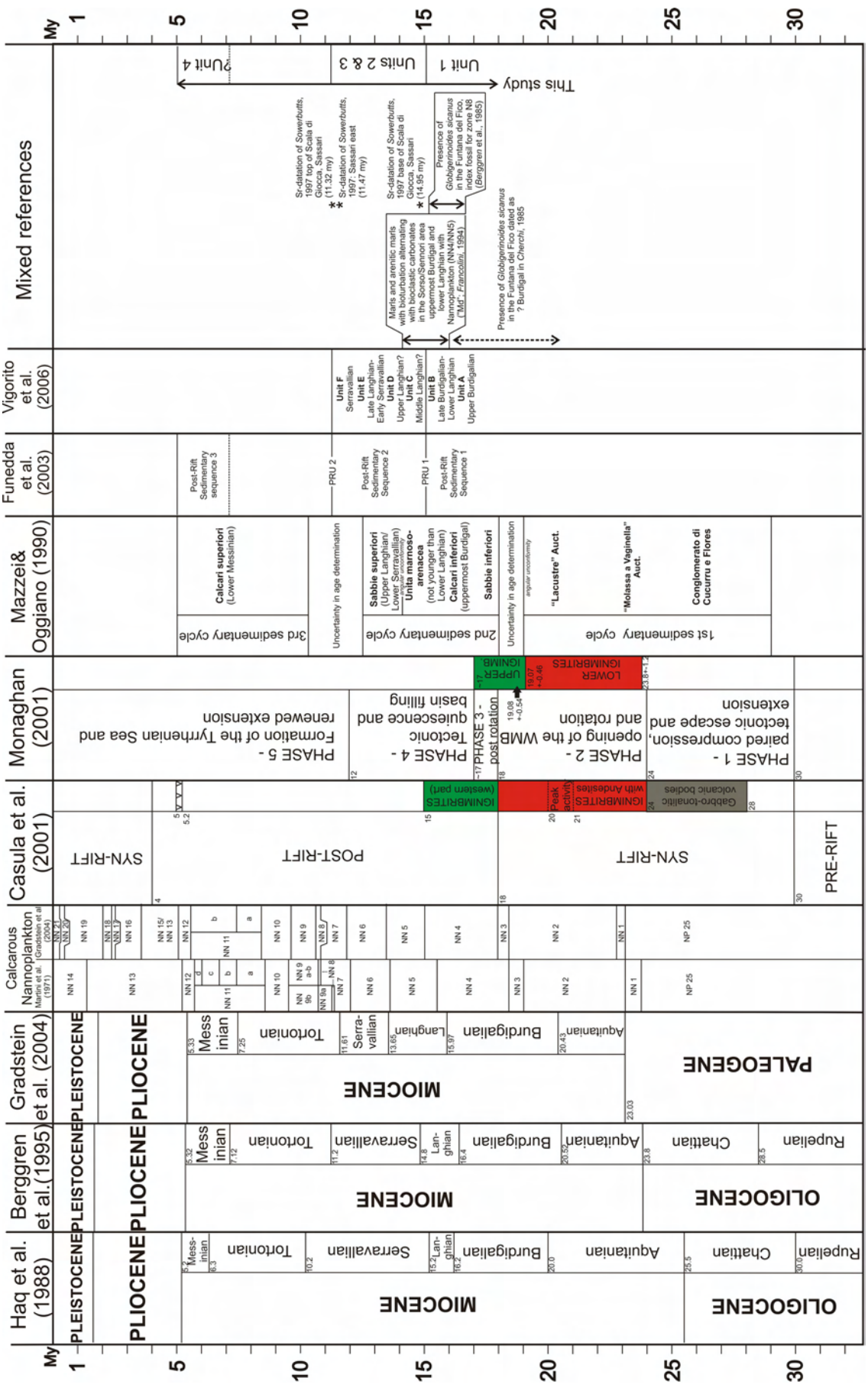

Fig. II.2.a. 1: Stratigraphic compilation after different authors for the deposits of the Porto Torres Basin with major structural events, tectonostratigraphic units, and ages.

II.2.b. Tectonostratigraphy

The following chapter describes the facies, geometries, and limits of the depositional Units. The marine carbonate sediments in the studied area of the Porto Torres basin are up to 120m thick, and are composed of calcisiltites, calcarenites, calcirudites, rhodolithic deposits and boundstones. Sands and conglomerates occur at various stratigraphic levels in the succession (VIGORITO et al., 2006). The whole succession dips gently to the northwest. Lateral variations of thickness, lithology, and facies are common. Three angular and erosional unconformities, delimiting four tectonostratigraphic Units, were mapped in the area between Sennori, Sassari and Osilo (Fig. II.2.b.1). The lithofacies definitions described here are based on the results of a mapping project of Hamburg University students in autumn 2006 (CÄSAR, 2008, JARAMILLO, 2007, JUST, 2007, KARDAS, in prep., MAYR, 2007, RÖBEN, in prep., RÖMER, 2007, WIGGERSHAUS, 2007).

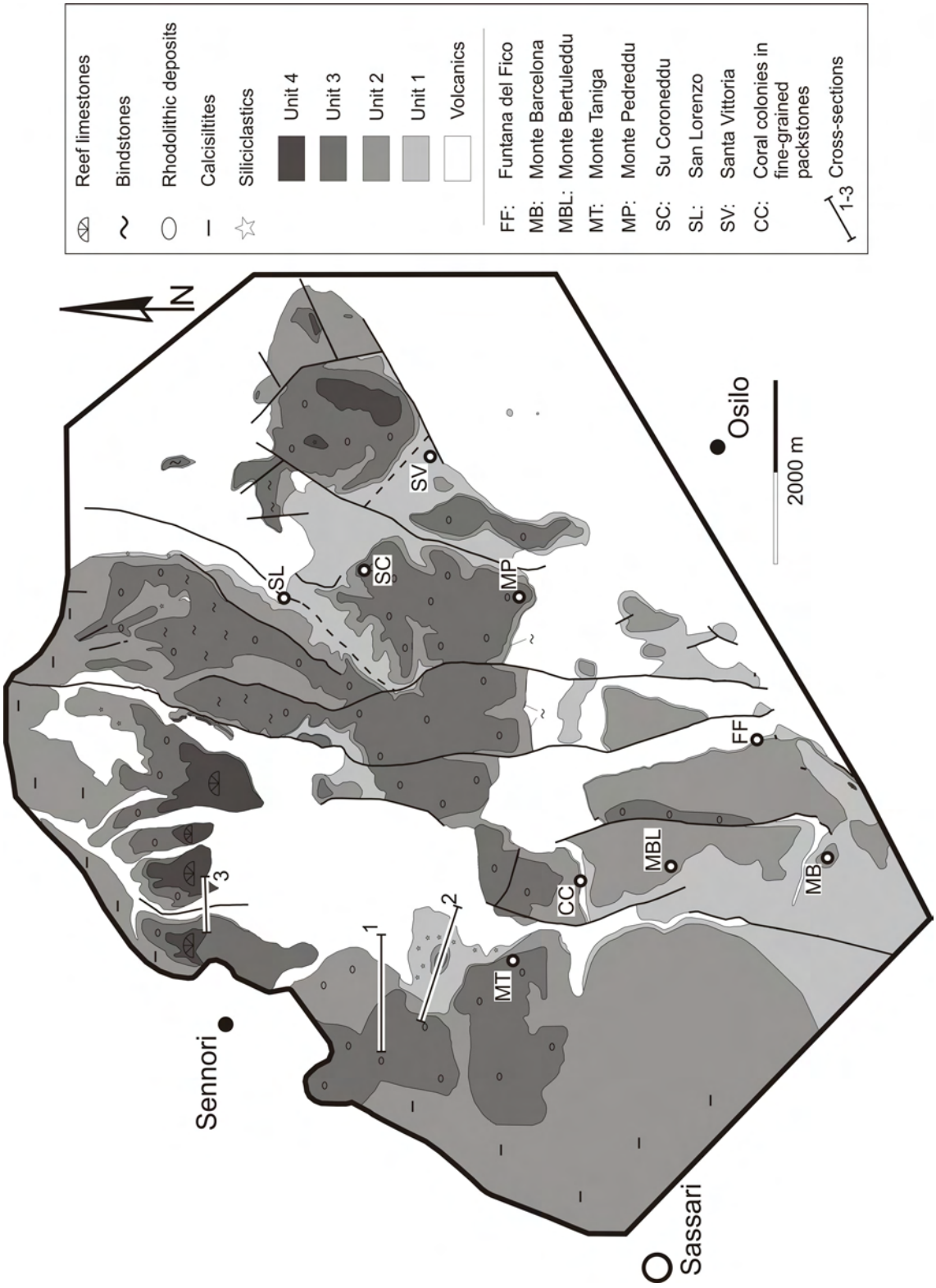

Fig. II.2.b. 1: Tectonostratigraphic map of the study area in the Porto Torres Basin. Four Units are subdivided based on mapping of angular and erosional unconformities. Lithologies are calcirudites and calcarenites, if not indicated otherwise. Abbreviations and numbers refer to localities and cross-sections discussed in the text. Based on CÄSAR (2008), JARAMILLO (2007), JUST (2007), KARDAS (in prep.), MAYR (2007), RÖBEN (in prep.), RÖMER (2007), WIGGERSHAUS (2007).

UNIT 1

The lowermost Unit 1 is between 6 and 50m thick, and consists of boundstones, calcirudites and calcarenites. The base of the Unit 1 is late Burdigalian in age, indicated by the presence of *Globigerinoides sicanus* (CHERCHI & SCHROEDER, 1985), which is the index fossil for the N8 zone (BERGGREN et al., 1985). *Heterostegina sp.* is abundant in the lower part of the carbonates throughout the entire working area. The "Funtana del Fico" locality in the southern part of the study area is the type-locality of *Heterostegina complanata* (CHERCHI & SCHRÖDER, 1985, Fig. II.2.b.1 "FF"). Unit 1 contains three facies: oyster floatstones to rudstones, bindstones, and calcirudites/calcarenites.

Oyster Floatstones and Rudstones

Oyster floatstones and rudstones, up to 30cm thick, occur at the base and in the middle part of the Unit 1. Oysters are up to 15cm large and thick shelled.

Bindstones

Coralline-algal bindstones occur as an up to 8m thick package in the central and eastern part of the working area (Fig. II.2.b.2). Bindstones mainly are composed of crusts of coralline algae and rhodoliths. Other components are bivalves, such as pectinids and ostreids, solitary corals and bryozoans. In the upper part of the bindstone interval, the amount and size of hermatypic coral colonies increases, and individual coral colonies are up to 1.5m high (Fig. II.2.b.2). In the uppermost interval of the bindstone package, there are abundant coralline-algal debris, branching bryozoans, larger benthic foraminifers (*Heterostegina sp.*) and articulated pectinids.

Calcirudites and Calcarenites

The major part of Unit 1 consists of an alternation of calcirudites and calcarenites with a minimum thickness of 10m. *Heterostegina sp*. is a major component in the lower parts of Unit 1. The calcirudites and calcarenites contain coralline-algal debris and small rhodoliths (0.5–2cm). Rhodolith morphology is laminar concentric to moderately branched. The amount of rhodoliths increases upsection. Other components are echinid fragments and bivalves, rare bryozoans and larger benthic foraminifers. In the southern part of the study area, a 20–50cm thick layer of volcanic ash documents volcanic activity during the early stages of carbonate deposition.

Up to 1.5m high, in-situ coral colonies occur embedded in the upper part of the fine-grained calcarenites to calcisiltites (Fig. II.2.b.3) at one locality (CC, Fig. II.2.b.1).

Fig. II.2.b. 2: Outcrop view of the upper, coral-rich part of the bindstone in Unit 1.

Fig. II.2.b. 3: Coral colonies in fine-grained calcisiltites in the south-western part of the working area. For location see Fig. II.2.b.1 (CC).

Depositional controls

Unit 1 is affected by synsedimentary, normal faults. Synsedimentary faults affect the lower parts of Unit 1. In the southwestern part of the study area, in direction of the center of the local graben structure, the dip of Unit 1 strata diminishes from base to top, attesting synsedimentary tilting. Unit 1 deposits are capped by an angular and an erosional surface, which defines the limit between Units 1 and 2. Figures II.2.b.4 and II.2.b.5 show line-drawings of this angular unconformity at Monte Bertuleddu (MBL, Fig. II.2.b.1) and Monte Barcelona (MB, Fig. II.2.b.1). Unit 1 deposits at Monte Bertuleddu dip to the north-west with an angle of approximately 25°, whereas Unit 2 dips with approximately 10° to the south-west.

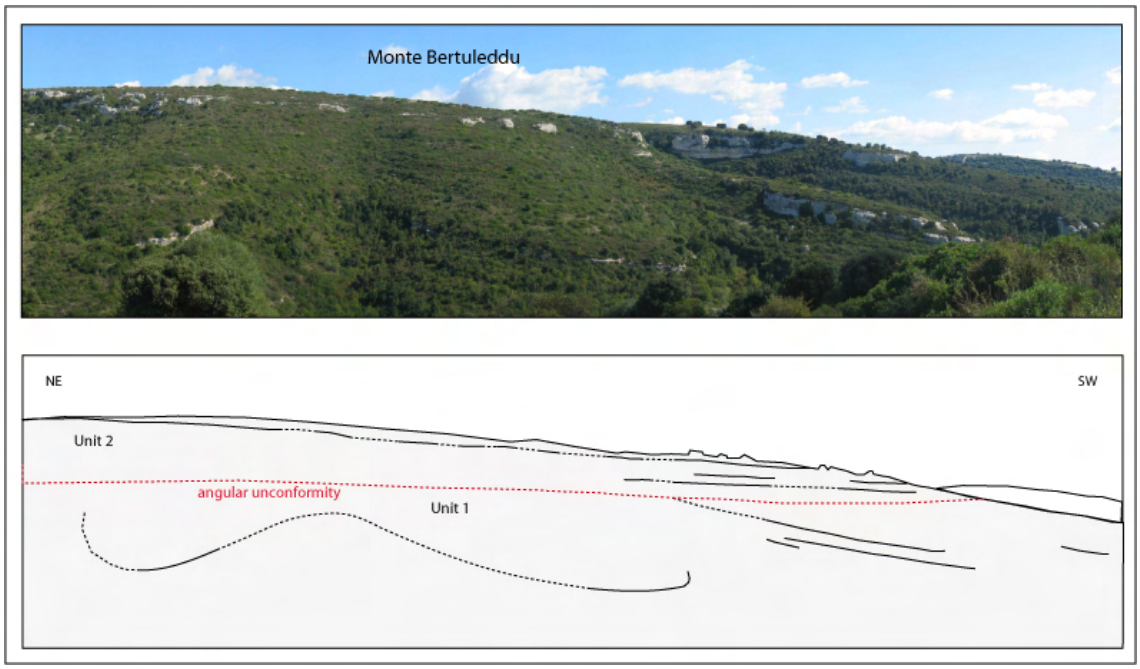

Fig. II.2.b. 4: Angular unconformity separating Unit1 from Unit 2 in the southern part of the study area. For location see Fig. II.2.b.1 (MBL). From JARAMILLO (2007).

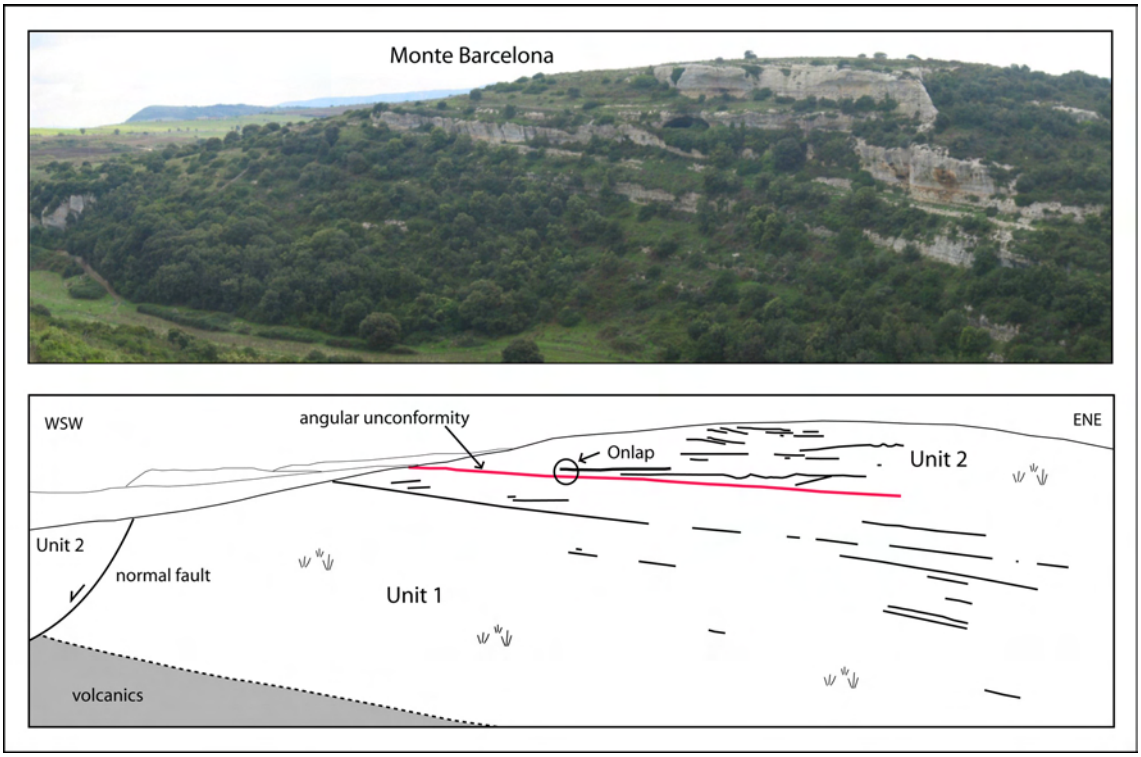

Fig. II.2.b. 5: Outcrop view of the angular unconformity separating Units 1 and 2 in the southern part of the study area. Unit 1 deposits dip to the east northeast, whereas Unit 2 deposits onlap the unconformity. For location see Fig. II.2.b.1 (MB). From JARAMILLO (2007)

Mapping of unconformities and physical tracing of Units does not unequivocally resolve whether Unit 1 occurs in the northern part of the study area or not. A patchy occurrence (patches up to 2m wide, and 1.5m thick) of autochthonous coral bioherms is recorded at the base of the succession, in the north-western part of the working area, which may be attributed to Unit 1.

UNIT 2

The deposits of the Unit 2 are between 14 and 120m thick and mainly consist of bioclastic calcarenites and calcirudites with lateral transitions to calcisiltites. Some rhodolithic intervals occur. The minimum thickness is found in the central part of the working area, whereas the thickness increases towards the marginal areas. The major features of Unit 2 are several sets of large-scale cross-beds. Measurements of cross-beds yield directions ranging from WNW to W and SW, with subordinate directions to the SW and SE (Fig. II.2.b.6).

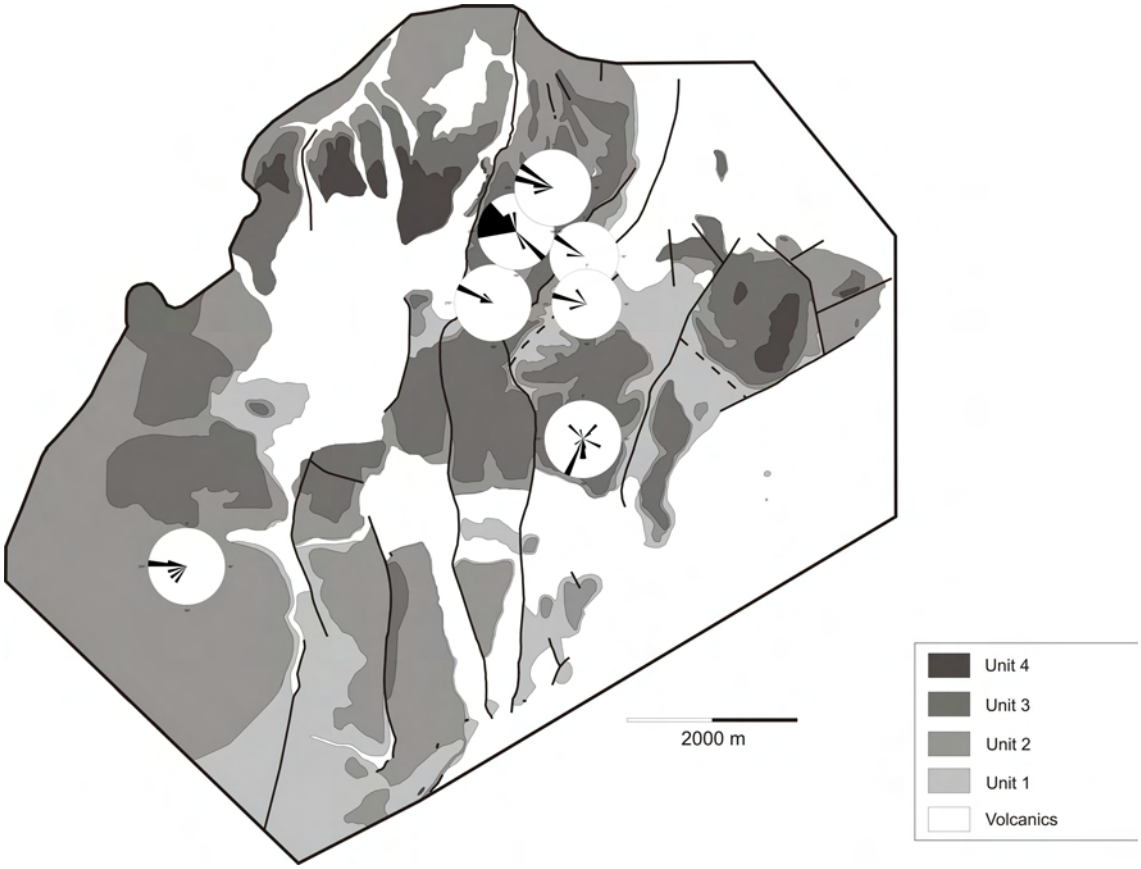

Fig. II.2.b. 6: Rose diagrams of Unit 2 large-scale cross-beds. The dominating directions are WNW to W and SW; subordinate directions are to the SE.

The type of cross-bedding changes within the succession: large-scale, planar cross-beds and trough cross-bedded sediment bodies dominate in the lower part of the Unit 2, whereas several meter-thick bundles of trough cross-beds with reactivation surfaces occur in the upper part.

An example of the large-scale cross-beds is shown in Fig II.2.b.7). The cliff of Monte Pedreddu (MP, Fig. II.2.b.1) is NW-SE oriented, approximately 15m high and approximately 600m long. The limestones are medium to fine-grained calcarenites arranged in several sets of cross-bedded deposits. Above the cliff, coralline-algal bindstones and rhodolith-rich deposits form a plateau. The coralline-algal bindstones and rhodolith-rich deposits rest horizontally upon the underlying deposits, separated from these by an erosional and angular unconformity. This unconformity is the limit between the Units 2 and 3. Cross-beds display variations in dipping direction (Fig. II.2.b.8). Directions are to the SW and S with subordinate values to the NW, NE, and SE. In the uppermost part, topsets are cut by the erosional surface separating Unit 2 and Unit 3. Within Unit 2, several higher-order Units, defined by erosional and angular unconformities, occur.

Another outcrop showing the large-scale, cross-bedded deposits occurs near San Lorenzo (Fig. II.2.b.9). Two sets of trough cross-bedded deposits, the lower one with a thickness of approximately 8m (base is not exposed), and the upper one approximately 4m thick, are exposed (Fig. II.2.b.9). The lower set is made of fine-grained calcarenites to calcisiltites with vertical and transverse burrows (Fig. II.2.b.10). The sediments contain bivalve fragments and echinids, which are preserved both fragmented and complete.

The upper set contains layers with abundant pectinids and echinids with barnacles, bryozoans and minor, small rhodoliths (Fig. II.2.b.11). At their bottomsets, the cross-bedded deposits get finer-grained and bioturbated. Dipping directions of cross-beds are West northwest to West with angles up to 30° (Fig. II.2.b.12).

Fig. II.2.b. 7 (next page): Line drawing of the Monte Pedreddu outcrop. For position see Fig. II.2.b.1 (MP).

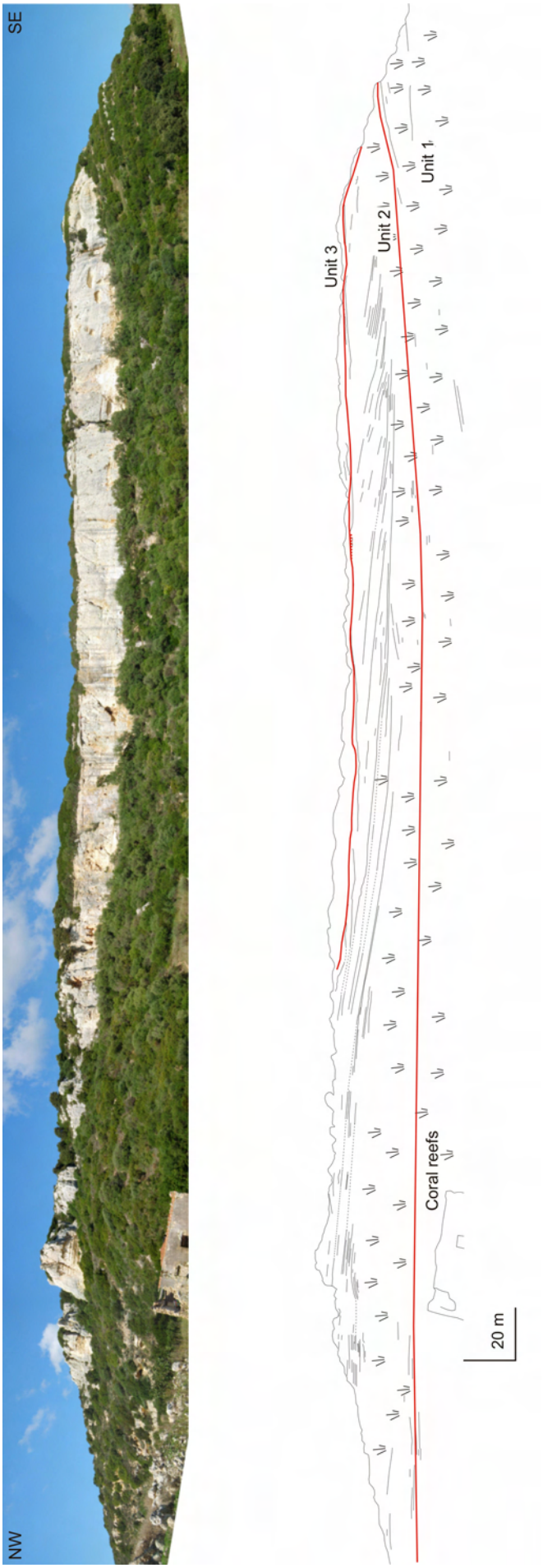
SE
NW
Unit 3
Unit 2
Unit 1
Coral reefs
20 m

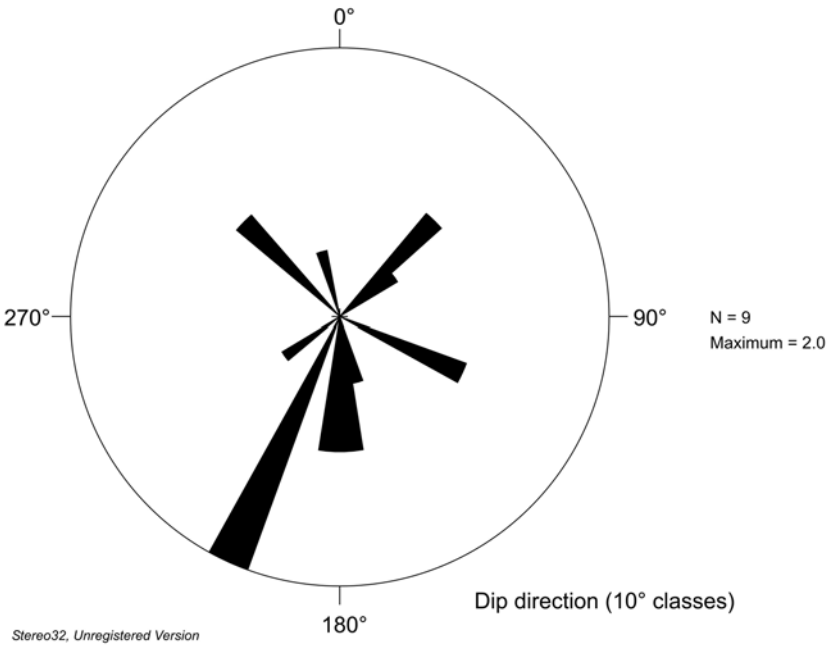

Fig. II.2.b. 8: Rose diagram of cross-bed dip directions in the Monte Pedreddu outcrop (see also Fig. II.2.a.2).

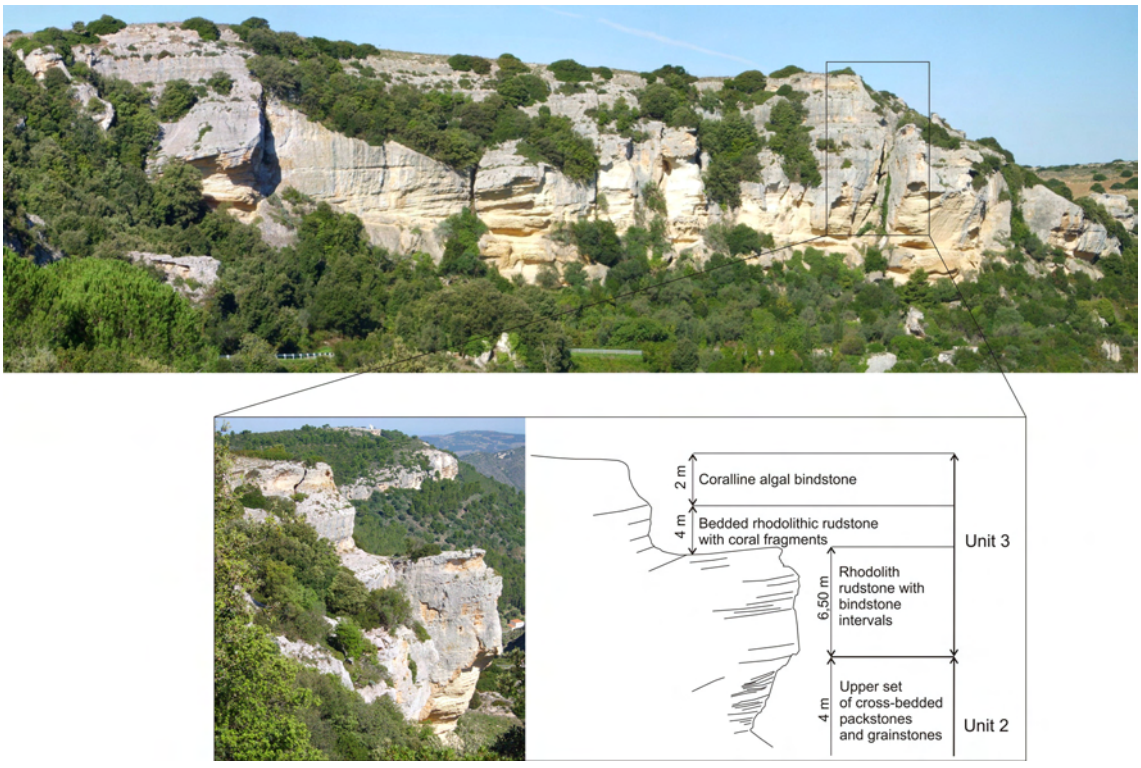

Fig. II.2.b. 9: Large-scale cross-bedded calcarenites of Unit 2 overlain by Unit 3 near San Lorenzo (SL, Fig. II.2.b.1).

Fig. II.2.b. 10: Bioturbated bottomsets of large-scale cross-bedded calcirudites and calcarenites.

Fig. II.2.b. 11: Bivalve dominated layer in the large-scale cross-bedded calcirudites and calcarenites. Note complete pectinid bivalve above pencil.

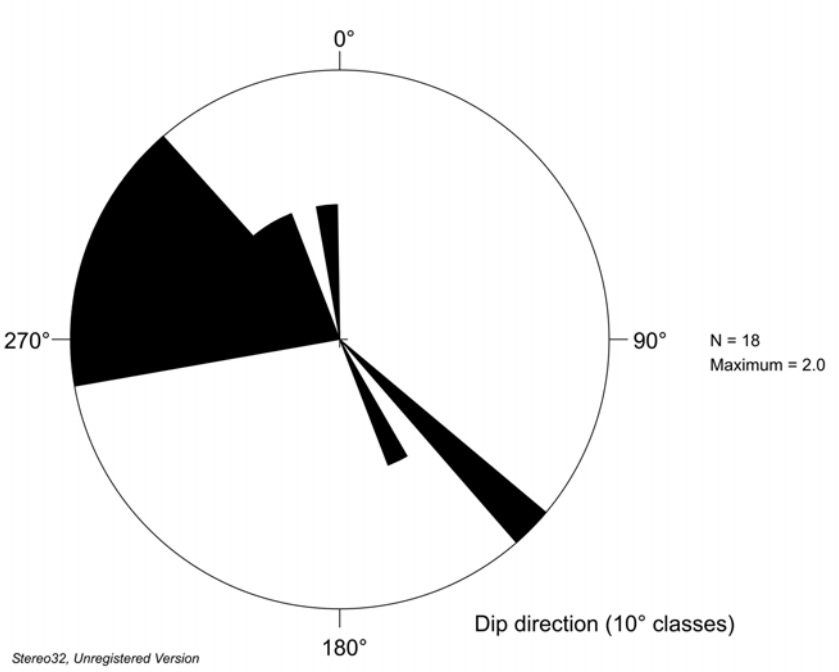

Fig. II.2.b. 12: Rose diagram of cross-bed dip directions in the San Lorenzo outcrop. For location see Fig. II.2.b.1 (SL).

The calcarenites of Unit 2 have basinal equivalents represented by calcisiltites in the western and northern part of the working area (Fig. II.2.b.1). These calcisiltites were dated as late Burdigalian to early Langhian in age by FRANCOLINI (1994), using calcareous Nannoplankton.

In the northern outcrops of the study area, up to 1m thick sand intervals occur within Unit 2 (Fig. II.2.b.1). Sands are interbedded with calcarenites and calcirudites and have sheet-like geometries, sheets have extensions of up to 100m.

UNIT 3

Deposits of Unit 3 are between 2 and 60m thick. They overlie the cross-bedded deposits of Unit 2 with an angular unconformity or an erosional surface. Figure II.2.b.13 shows a cross-section cutting this angular unconformity in the north-western part of the study area (for location of cross-section see Fig. II.2.b.1). Unit 2 deposits dip to the west with an angle of 30°, whereas Unit 3 strata dip to the north-west with an angle of approximately 20°.

Deposits are dominated by coralline algae, which occur as bindstones or rhodoliths (figs. II.2.b.14, 15). Small patchy coral colonies also occur in the bindstones, as well as fragmented corals in the rhodolithic deposits. Coralline-algal bindstones laterally interfinger with rhodolithic deposits in the central part of the working area (Fig.

II.2.b.1). At one locality (Su Coroneddu; figs. II.b.16, 17), rhodolithic beds are arranged as clinoforms, indicating the occurrence of small, red-algal shoals.

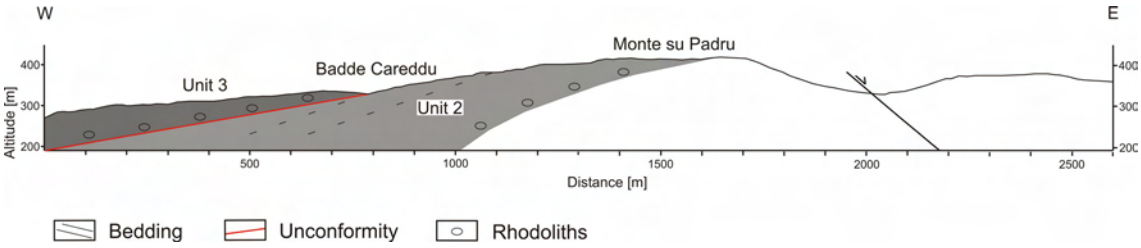

Fig. II.2.b. 13: Angular unconformity between Unit 2 and Unit 3. Unit 2 deposits dip to the west with approximately 30°, and Unit 3 deposits dip to the north west with approximately 20°. For position of section see Fig. II.2.b.1 (cross-section 1). Modified from RÖBEN (in prep).

Fig. II.2.b. 14: Coralline-algal bindstones of the Unit 3.

Fig. II.2.b. 15: Rhodolith-dominated deposits of Unit 3 underlying and interfingering with the coralline-algal bindstones (Fig. II.2.b.14).

Fig. II.2.b. 16: Rhodolithic clinoforms in Unit 3 deposits. The cliff is approximately 15m high.

Fig. II.2.b. 17: Detail of rhodolith clinoforms shown in Fig. II.2.b.16.

UNIT 4

Unit 4 consists of coral reefs and sands. Coral reefs occur in the north-western part of the study area and are up to 10m thick. Coral reefs are separated from the underlying coralline-algal-dominated deposits of Unit 3 by an angular unconformity. In one locality, Unit 4 overlies the volcanic basement above a conglomerate layer. The basal part of Unit 4 contains coralline-algal debris. Overlying coral bioherms can be up to several meters large. Extensive *Lithophaga* borings occur in the reef deposits. Aragonitic material is almost completely replaced by chert. In the eastern part of the study area, Unit 4 is represented by sands.

Growth-form variations in the coral reefs, from massive colonies to branching growth-forms, occur from east to west (Fig. II.2.b.18). These different facies are separated by an east-dipping normal fault with a present-day offset of approximately 40m. Based on the growth-form variation as a result of depth-adapted variation (JAMES, 1984; TUCKER & WRIGHT, 1990), deepening took place from east to west. Unstripping the present day offset, plus adding a minimum depth difference of 10m between the massive and the branching corals (TUCKER & WRIGHT, 1990), leads to a minimum offset of 50m postdating the deposition of Unit 4. This is in agreement with FUNEDDA et al. (2000), who propose a N-S trending Pliocene

faulting episode. This finding enhances the necessity of unravelling the timing and sequence of faulting events with more accuracy.

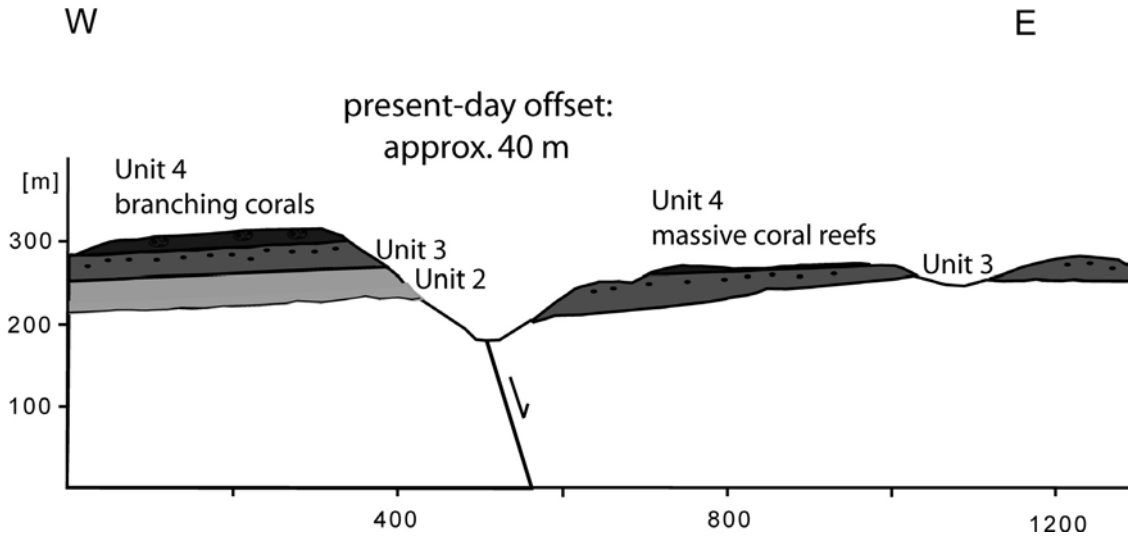

Fig. II.2.b. 18: Present-day offset between massive coral reefs and branching corals in Unit 4. For location of cross-section see Fig. II.2.b.1 (cross-section 3). Modified from JUST (2007).

The deposition of the marine carbonate succession of the Porto Torres Basin was strongly controlled by synsedimentary tectonic activity and a pre-existing palaeotopography. Formation of unconformities was mainly triggered by movements along east-dipping normal faults resulting in block rotation. As a result, the mapped unconformities have different expressions throughout the working area, depending on their relative position to the rotational pole of the faulted blocks. Thickness is greatest in the vicinity of faults, whereas thickness decreases with decreasing distance to the rotational pole (Fig. II.2.b.19). This is a result of varying sedimentation rates along the hangingwall dip slope. Erosion occurs beyond the fulcrum, where rotation leads to uplift, to a high rate in the hangingwall depocenter (LEEDER & GAWTHORPE, 1987). Fault movement may therefore be recorded as an erosional surface or an angular unconformity towards footwall highs. Whereas in the hangingwall depocenter, syndepositional movement is recorded stepwise, with wedge-shaped strata arranged in a fan geometry opening towards the fault (BOSENCE, 1998, BOSENCE et al., 1998, CROSS et al., 1998, BOSENCE, 2005).

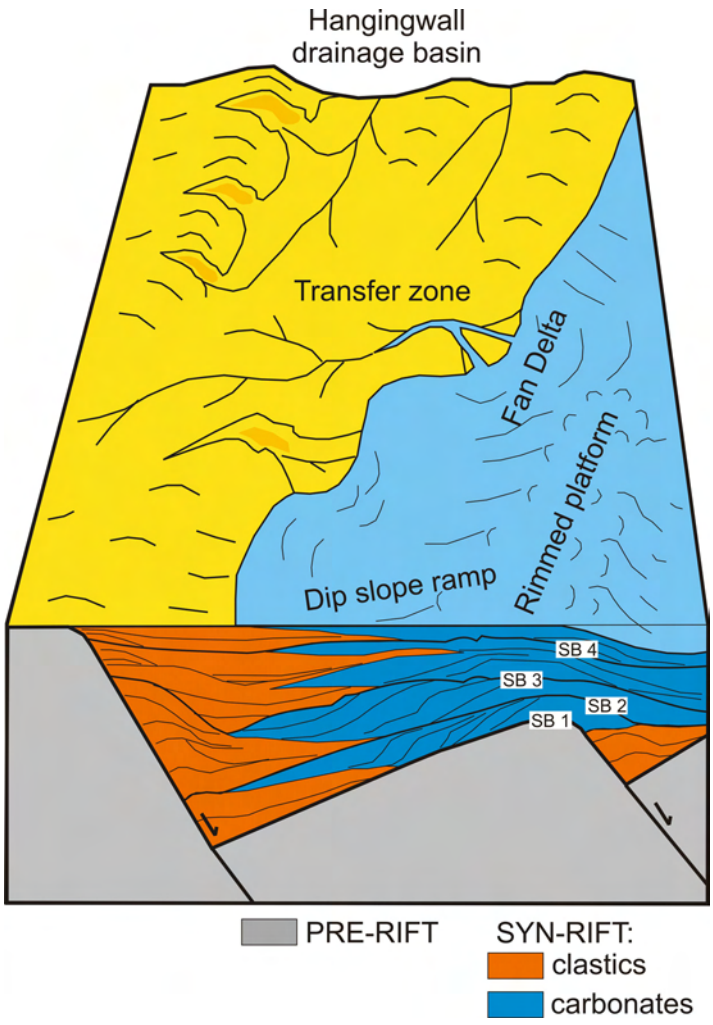

Fig. II.2.b. 19: Model of fault-block carbonate platform geometry and stratigraphy, after BOSENCE (2005).

In addition to syndepositional tectonics, the palaeotopography has a strong impact on thickness variations in the different Units. In Unit 1, deposits onlap onto a N-S trending volcanic palaeohigh. This palaeohigh strongly controlled the deposition in the western part of the working area. Figure II.2.b.20 shows this situation in the southern part of the study area.

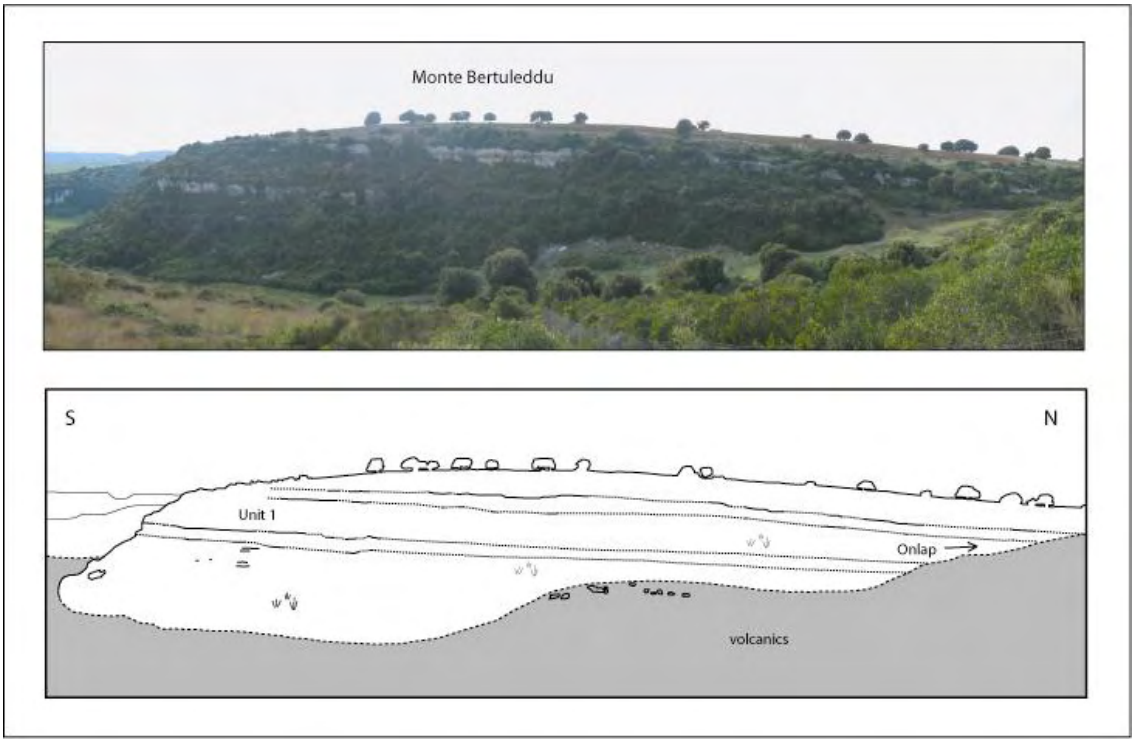

Fig. II.2.b. 20: Onlap of Unit 1 deposits on a volcanic palaeohigh. For location see Fig. II.2.b.1 (MBL). Modified from JARAMILLO (2007).

Further north, the strata of Unit 1 laterally interfinger with conglomerates. In Fig. II.2.b.21, the lateral variation from conglomerates to carbonate deposits is shown by correlation of three sections using *Heterostegina sp.* marker beds. Volcanic basement rocks form a northward ascending high. Two conglomeratic horizons attached to this high are traceable several hundred meters to the south, where they interfinger with Unit 1 calcarenites and calcirudites.

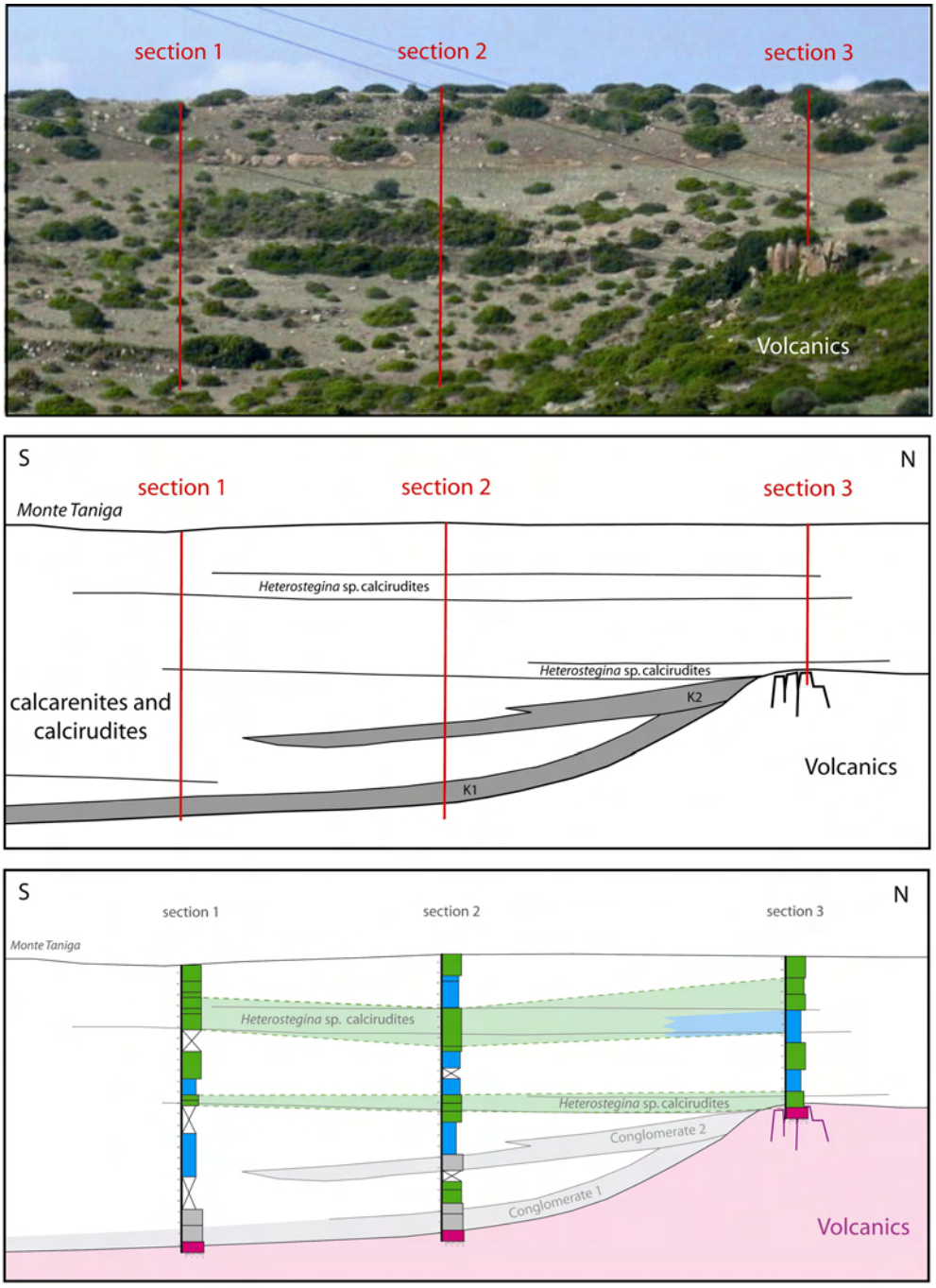

Fig. II.2.b. 21: Unit 1 conglomerates attached to the volcanic palaeohigh interfingering with marine carbonates. Green=Calcirudites, Blue=Calcarenites, Grey=Conglomerates, Purple=Volcanics. For location see Fig. II.2.b.1 (MT). Modified from WIGGERSHAUS (2007).

Further north (Fig. II.2.b.22), Unit 1 is almost completely represented by four cycles of conglomerates alternating and interfingering with marine carbonates. The conglomerates were deposited on and shedded from the volcanic high. The

palaeoslope is oriented to the north-west, indicating that Unit 1 was deposited in circular formation around the palaeohigh.

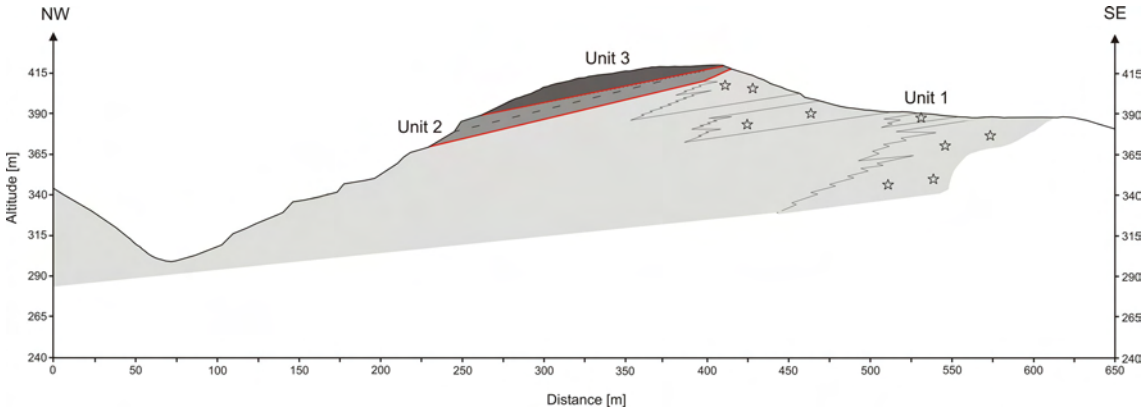

Fig. II.2.b. 22: Conglomerates (stars) interfingering with marine carbonates in Unit 1. For location see Fig. II.2.b.1 (cross section 2). Modified from RÖBEN (in prep).

II.2.c. Depositional Model

Unit 1 deposits were formed on a carbonate ramp (sensu BURCHETTE & WRIGHT, 1992) under conditions of a rising relative sea level. On the inner ramp, small coralline-algal and coral build-ups, surrounded by coralline-algal gravel, formed. Large benthic foraminifers, such as *Heterostegina* sp., inhabited inner and middle-ramp environments. Terrigenous input occurred in areas close to a nearby coastline in the north and around a palaeotopographic high. Synchronous volcanic activity is recorded by tuffs in the southern part of the ramp. Syndepositional tectonic movements on east-dipping, normal faults induced a successive differentiation of the ramp into areas with high subsidence, and thus high sediment accumulation. In contrast, the inner ramp was uplifted to base-level and was reworked.

During relatively stable structural conditions, and a relative sea-level high stand, a system of submarine dunes developed above an erosional unconformity. Patchy occurrences of sands embedded in the Unit 2 in proximal areas indicate terrigenous input by a river delta. Large submarine dunes were moved by west-directed strong currents. Carbonate production is recorded by bivalve factories or rhodolithic intervals, which are interbedded between the bar deposits. The bar deposits merge into basinal deposits to the west and north-west. The origin of the bottom currents is thought to be the result of wind-congested waters flowing back after storms, associated with undertow currents. Tidal currents may have occurred during the formation of the upper Unit 2 deposits. At this time relative sea-level was dropping, and accommodation space was filled until intertidal conditions were prevalent. This resulted in tidal bundling and reactivation surfaces in sediments of the south-western part of the study area. Faulting and block-rotation, in possible coherence with a relative sea-level drop, resulted in major erosion of large parts of the Unit 2, leading to the formation of a further angular and erosional unconformity.

Unit 3 records the subsequent flooding of the carbonate platform. Lateral facies variations from coralline-algal bindstones to rhodolithic deposits point to differential depositional processes. The bindstones were formed in shallower, higher-energy areas, whereas the rhodolithic deposits reflect deeper-water environments. The most probable analogy would be a carbonate ramp.

Unit 4 is represented by coral reefs. No associated sediments are encountered in the working area, except for sands, indicating a nearby coastline to the east. It is most

probable that the unit 4 represents a lowstand, during which shallow-marine coral reefs were attached to the underlying deposits. Lateral variations in coral growth form point to a deepening from west to east, which is presently inversed due to Pliocene faulting.

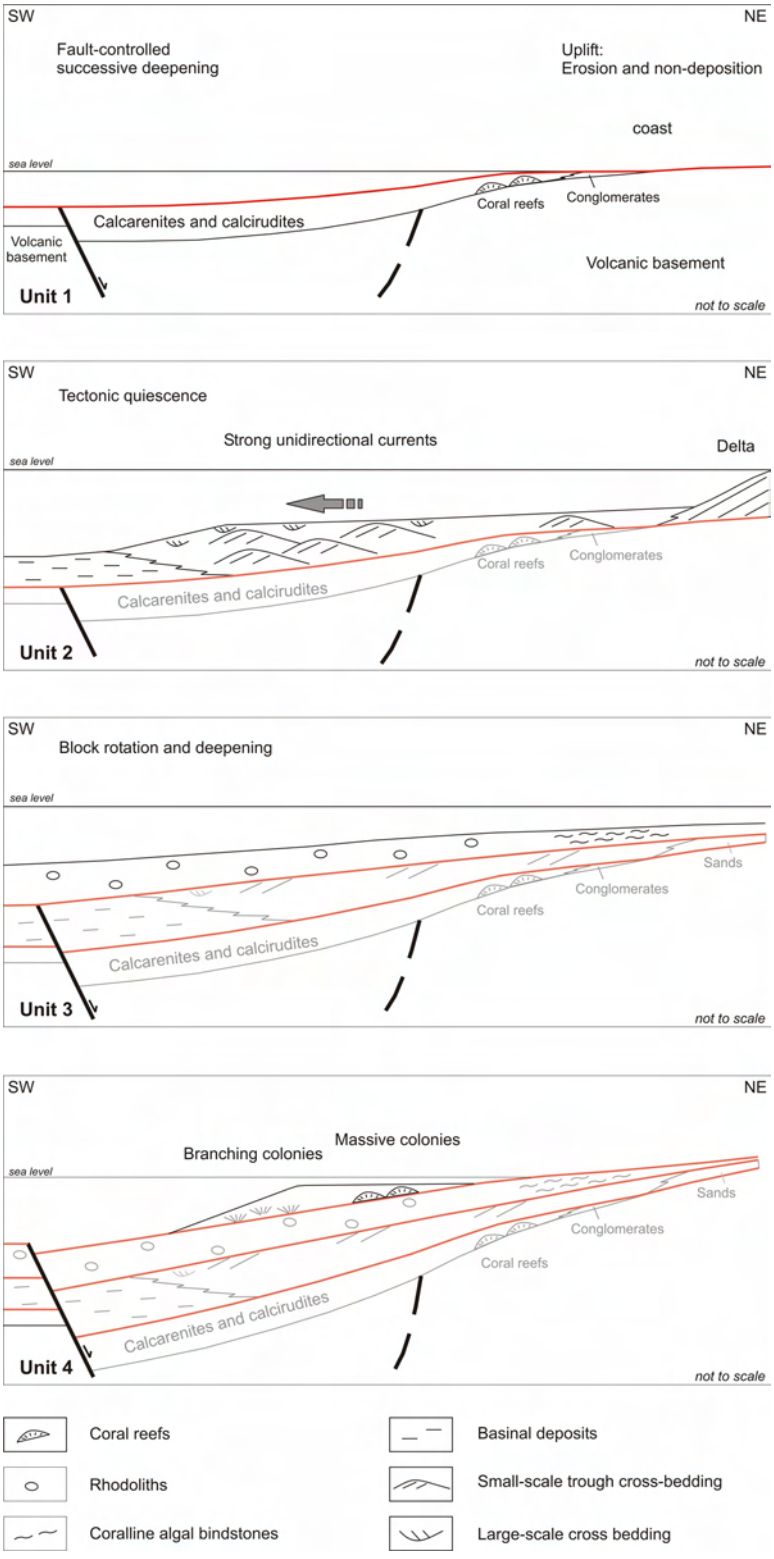

Fig. II.2.c. 1: Depositional model for the marine carbonates of the Porto Torres Basin. Depositional environment for individual units 1-4 is shown from top to base. Not to scale.

II.2.d. Outlook

To completely understand the stratigraphy of the studied deposits and to develop a final depositional model, more data need to be collected. In particular, there is still uncertainty about the occurrence of the Unit 1 in the northern parts of the working area. Here, no final conclusion has been drawn yet. More precise tracing of unconformities and a thorough biofacies analysis could help solving this matter, though the original context of the deposits is strongly disrupted due to the strong tectonic overprint of the study area. Moreover, Pliocene fault-reactivation (e.g. FUNEDDA et al., 2000) obscured original offsets and therefore complicates the recognition of the full extent of syndepositional tectonics, which could be unravelled with a full understanding of facies relations. The nature and geometries of the unit 3 and unit 4 need to be figured out more precisely. With the existing data, a good basis for further examination exists.

III. GENERAL DISCUSSION

III.1. The Relation Between the Carbonate Factory and Depositional Geometries

The relation between the carbonate factory and depositional geometries is uttermost important for the understanding of carbonate systems in the geological record. A historical perspective of evolving knowledge is given in POMAR (2001). According to TUCKER & WRIGHT (1990), the general description of shallow water carbonate accumulations is unified under the collective term `carbonate platform´. Five types of carbonate platforms are differentiated: rimmed shelf (subdivided in accretionary, bypass, and erosional shelf margins), carbonate ramp (subdivided in homoclinal ramp and distally steepened ramp), epeiric platform, isolated platform, and drowned platform.
The existing categories are assigned to certain carbonate factories. A photozoan factory (*sensu* JAMES, 1997) builds reef-rimmed shelfs (such as the Great Barrier Reef, Australia), and isolated platforms (such as the Bahama Banks, Atlantic ocean). A heterozoan factory (sensu JAMES, 1997) forms ramps. Epeiric platforms are not known nowadays, for the eustatic sea-level is comparatively low due to glaciation. They did exist in the geological record, e.g. during the Cretaceous in western Europe (TUCKER & WRIGHT, 1990).

However, due to increased insight into shallow water carbonate systems being important hydrocarbon reservoirs, and the sequence stratigraphical approach to predict their reservoir capacity on a seismic scale, transitions were recognized, which are no longer explicable with specific carbonate factories forming certain geometries (e.g. south-western Australian shelf, JAMES et al., 1999, COLLINS et al., 1997). This study is a further example contributing to the stratigraphical architecture of such transitional carbonate depositional systems.

The terms rimmed shelf and carbonate ramp are valuable to describe the actual state of a platform at a certain time, but they are less successful in categorizing the entire morphology and stratigraphy of carbonate platforms through time (BOSENCE,

2005). BOSENCE (2005) therefore suggests an approach to classify Cenozoic carbonate platforms based on their basinal and tectonic setting and proposes eight types of carbonate platforms (Fault-Block, Salt Diapir, Subsiding Margin, Offshore Bank, Volcanic Pedestal, Thrust-Top, Delta-Top and Foreland Margin carbonate platforms). However, individual factors such as climate, sea-level fluctuations and ocean chemistry are still important parameters to specify internal characteristics.

The studied Neogene shallow water carbonates of north western Sardinia (the Sedini Limestone unit and the marine carbonates of the Porto Torres Basin) represent Fault-Block carbonate platforms sensu Bosence (2005). They were formed in an active to post-active intra-arc setting (SOWERBUTTS, 1997, 1998, 2000, MONAGHAN, 2001) due to rifting processes related to the Alpine and Apennine orogeny (CHERCHI & MONTADERT, 1982, THOMAS & GENNESSEAUX, 1986, FUNEDDA et al., 2000, CASULA, 2001, MONAGHAN, 2001, MURRU et al., 2001, FACCENNA et al., 2002, SPERANZA et al., 2002). Block-rotations along normal faults and rapid subsidence resulting in relative-sea-level oscillations were the dominating structural processes.

SEDINI CARBONATE PLATFORM

Carbonate factories

The carbonate factories involved in the Sedini Limestone Unit are heterozoan (*sensu* JAMES, 1997) with photozoan (*sensu* JAMES, 1997) elements (Sequence 1) to photozoan with heterozoan components (sequence 2d/2e). The transitional stage (sequences 2a-2d) is dominated by a heterozoan factory with an increasing photozoan portion. According to CARANNANTE et al. (1988), the deposits are a molechfor (*sensu* LEES & BULLER, 1972) to rhodalgal factory in sequence 1 and a rhodalgal to chlorozoan factory in sequence 2.

Depositional geometries

The geometries in the sequence 1 of the Sedini Limestone unit are typical for a homoclinal ramp *sensu* BURCHETTE & WRIGHT (1992). The sequences 2a-2d are a transitional stage between a ramp and a steep-flanked carbonate platform. Because the relief angle increases from sequence 1 to sequence 2 (up to 27°), the deposits are interpreted as a steep-flanked platform with an incipient margin represented by large-scale cross-bedded submarine dunes (TUCKER & WRIGHT, 1990, SCHLAGER, 2005) locally stabilized by coralline algal bindstones. The late stage of carbonate accumulation (sequence 2e) represents a rimmed carbonate platform with a reef flat

and a steep (up to 27°) coralline algal dominated platform margin situated below wave-base. The best-fit analogy to existing facies models would be a rimmed shelf (*sensu* TUCKER & WRIGHT, 1990) or a distally steepened ramp (*sensu* BURCHETTE & WRIGHT, 1992). However, the term distally steepened ramp (*sensu* BURCHETTE & WRIGHT, 1992) is not adequate enough to express the transitional nature of sequence 2e, because the slope is much steeper than expected from a distally steepened ramp. Moreover, the definition of BURCHETTE & WRIGHT (1992) requires fine-grained, ramp-shedded material in the slope, whereas the slope of the Sedini Limestone Unit is made by coarse-grained, in situ coralline algal deposits.
However, either the term rimmed shelf *sensu* TUCKER and WRIGHT (1990), or rimmed platform *sensu* SCHLAGER (2005) fails to describe the geometry of this platform. The term "steep-flanked platform" is therefore proposed to firstly clarify the geometry consisting of a reef flat with a steep slope, and secondly to emphasize the absence of an authentic rim in the sense reefs or shoals achieving sea-level.

Relations between carbonate factories and depositional geometries

The coralline algal platform margin and slope formed in water depths of approximately 40-60m, and associated inner platform coral reefs established in depths of approximately 20m. The unravelling of this setup can provide useful information for future studies: the edge of a transitional carbonate depositional system may not necessarily build up to sea level.

The Perfugas Basin (which contains the Sedini Limestone unit) is thought to be a marginal basin with an access to open marine conditions only to the west. Hence, fluctuations of the open marine conditions are thought to have attained with a certain delay or at least diluted. However, the occurrence of relative sea-level fluctuations is indicated by the occurrence of high-frequency sequences within two depositional sequences. Syndepositional tectonic activity was minor. The carbonate factory evolved from an "immature" heterozoan/photozoan carbonate ramp to a transitional, photozoan/heterozoan, steep-flanked platform. It is most probable that sea-level fluctuations triggered this evolution of the depositional system. HOMEWOOD (1996) stated that "pioneer communities" develop under increasing accommodation, i.e. a base-level rise. "Climax communities" develop under decreasing accommodation, i.e. a base-level fall. Climatic change is not thought to be the major driver of this evolution. The occurrence of the coralline algal genus *Sporolithon sp.* indicates the predominance of subtropical to tropical conditions (BRAGA & BASSI, 2007) throughout the entire Sedini Limestone Unit.

THE PORTO TORRES BASIN

The carbonates in the Porto Torres Basin are different from the Sedini Limestone Unit. Block rotation along normal faults was the dominant structural process along with carbonate platform formation. Terrigenous input was more important than in the Sedini carbonate platform.

Carbonate factories

Unit 1 contains a heterozoan (*sensu* JAMES, 1997) factory with a photozoan (*sensu* JAMES, 1997) imprint. Unit 2 consists of a heterozoan assemblage. In Unit 3, a heterozoan factory with a strong photozoan imprint occurs. Unit 4 is a pure photozoan factory. According to CARANNANTE et al. (1988), the Unit 1 is a foramol (*sensu* LEES & BULLER, 1972) to rhodalgal factory with chlorozoan elements. Unit 2 is a molechfor to rhodalgal factory. Unit 3 is dominated by rhodalgal deposits with considerable chlorozoan aspects. Unit 4 is purely chlorozoan.

Depositional geometries

The geometries of the Porto Torres Basin are strongly controlled by syndepositional tectonics. An irregular palaeotopography contributed to occurrence of differential depositional environments.

Thus, the carbonate ramp of Unit 1 predominantly records the successive differentiation into areas of high subsidence in the hangingwall depocentres, and areas subjected to uplift towards footwall highs. Along hangingwall dip slopes, wedge-shaped strata with great thickness and decreasing dipping angles from base to top occur, whereas at footwall highs, reworking and erosion were the dominant processes. This is typical for Fault-Block carbonate platforms (BOSENCE, 1998, BOSENCE et al., 1998, CROSS et al., 1998, BOSENCE, 2005).

The depositional system in Unit 2 is represented by a system of submarine dunes, which occupied the entire working area and most probably expanded beyond it. A connection with the Perfugas Basin at that time is probable. During formation of Unit 2, a relative tectonic quiescence is proposed. Renewed tectonic tilting led to erosion of large parts of the Unit 2. Thus, geometries are obscured.

Unit 3 represents a carbonate ramp depositional system, which locally consisted of coralline algal shoals and rhodolithic clinoforms. Unit 4 consists of coral reefs, which were attached to the underlying deposits during a sea-level lowstand. They represent the youngest marine carbonates of the study area. Limited outcrop

conditions and absence of associated sediments do not allow a detailed interpretation.

Relations between the carbonate factories and depositional geometries

In the Porto Torres Basin, the depositional system did not evolve as continuously as in the Perfugas Basin, for it was repeatedly restructured by tectonic activity. These findings enhance the impact of the tectonic and basinal setting on carbonate platform geometries (BOSENCE, 2005), but they also show that different types of platform geometries can develop in the same structural and climatic setting with similar carbonate factories involved.

III.2. The Role of Coralline Algae in the Carbonate Successions of the Early/Mid Miocene

Carbonate factories dominated or characterized by a significant amount of coralline algae existed in the entire circum-Mediterranean area and the world during the Miocene (HALFAR & MUTTI, 2005). It is still a matter of debate what could have triggered the enormous productivity of coralline algae at that time of the geological record, as well as the fact that coralline algae displaced corals as the major reef-building organisms at that time. My question regarding this point is:

"Were the general conditions (such as ocean chemistry, sea-level fluctuations or climatic variations) favouring coralline-algal productivity at a certain time-slice (i.e. the Middle Miocene) or just inhibiting coral growth so coralline algae achieved the potential to displace corals in their ecological niche?"

A key paper regarding this question is certainly the work of HALLOCK & SCHLAGER (1986), in which they propose a direct correlation of nutrient excess to negative reef growth rates. Relating the nutrient-hypothesis to the Miocene, HALFAR & MUTTI (2005) propose enhanced nutrient levels in the world oceans as being the reason for the global decline of coral reefs and the subsequent coralline-algal heyday.
A point of further interest is a fact HALFAR & MUTTI (2005) allude to: "… A number of studies analyzed describe reef complexes, whereas the biofacies clearly indicates a low percentage of corals and a predominance of rhodalgal facies."
This finding confirms the necessity for a better knowledge of coralline-algal communities and a better understanding of them being reef-builders of similar importance as corals. To achieve this goal, more descriptions of coralline-algal assemblages are required.
However, in the past two decades, selected Miocene successions containing a significant amount of coralline algae have been in the focus of several authors. The carbonate successions of southern Spain (e.g. BRACHERT et al., 1996, BRAGA et al., 1996, MARTIN et al., 1996, BETZLER et al., 1997, BRAGA & AGUIRRE, 2001), Menorca (OBRADOR et al., 1992, POMAR et al., 2002, 2004, BRANDANO et al., 2005), Malta (e.g. BOSENCE & PEDLEY, 1982, BOSENCE, 1983), the Apennines (e.g. BRANDANO, 2003, CIVITELLI & BRANDANO, 2005), or southern Turkey (BASSANT, 1999, BASSANT et al., 2004) are just a few examples of well-described, coralline algae-bearing Mediterranean carbonates outside Sardinia. Furthermore, the recent and sub-recent ecology of coralline algae is investigated by a series of researchers, amongst them

LUND et al. (2000), BRAGA & AGUIRRE (2004), HALFAR et al. (2004, 2006). WOELKERLING, who provides an online-bibliography has done long-time research on coralline algae (e.g. WOELKERLING et al., 1993).

Parts of this thesis are an attempt to contribute to the complex subject of coralline algae in the Miocene by delivering a detailed description of a rhodalgal platform slope in northern Sardinia, where coralline algae have not been described yet (see chapter II.1.b). Thorough descriptions of the coralline-algal assemblages exist from the Isili area in Central Sardinia (VIGORITO et al., 2005, BASSI et al., 2006), where a complex temperate-type carbonate depositional system with a carbonate factory and an associated channel system has been described.

The deposits rich in coralline-algal debris in sequence 1 of the Sedini Limestone unit are similar to the maërl-deposits of the Recent Mediterranean (PÉRÈS & PICARD, 1964, BETZLER et al, 1997). The carbonate factory of sequence 1 is represented by coral patch reefs embedded in coralline-algal- and additional bioclastic debris. This situation can be found on the modern Abrolhos shelf in SW Australia (COLLINS et al., 1993, 1997, JAMES et al., 1999).
Coralline algae occur in a variety of appearances from bindstones to rhodoliths in the sequence 2 of the Sedini Limestone unit (see chapters facies description, Carbonate platform and coralline-algal manuscript).
At one locality (Sa Rocca Manna), rhodoliths are arranged in steep clinoforms, with upper foreset and topset rhodoliths stabilized by subsequent coralline-algal encrustation. The clinoforms resemble deposits in the Lower Bar Unit of the Tortonian distally steepened ramp on Menorca (OBRADOR et al., 1992, POMAR et al., 2002, 2004, BRANDANO et al., 2005). However, the clinoforms of Sa Rocca Manna are associated with coral reefs in the proximal part of the carbonate platform, a feature, which is missing in the Tortonian distally steepened ramp.

Lower Miocene carbonate platforms have been described from the Apennines (e.g. MUTTI et al., 1997, BRANDANO et al., 2001, BRANDANO & CORDA, 2002, BRANDANO, 2003). The Latium-Abruzzi carbonate ramp (BRANDANO, 2001, 2003) is interpreted as a rhodalgal carbonate ramp formed under topical to subtropical conditions with a Rhodolithic unit (RU), a Bryozoan–Echinoid unit (BEU), a Benthonic Foraminifer–Echinoid unit (BFEU), and a Planktonic Foraminifer–Echinoid unit (PFEU). The proximal Rhodolithic unit contains scattered coral boundstones. These are interpreted as coral carpets.

The general belief regarding the rhodalgal carbonate platforms in the Apennines and the entire Mediterranean is that they have been formed under subtropical to tropical conditions. The scarcity or absence of coral reefs is thought to be the result of enhanced nutrient concentration (e.g. MUTTI et al., 1997, 1999, MUTTI & HALLOCK, 2003, HALFAR & MUTTI, 2005) and not a climatic change.

The question whether the studied carbonates developed under the influence of enhanced nutrient levels or not cannot be solved here. There is some evidence for the occurrence of nutrient-rich waters in terms of occurrence of phosphates. The youngest deposits in the Sedini Limestone Unit contain sponge spicules and siliceous Phytoplankton. However, the studied carbonates show a development from "Heterozoan" dominated deposits to "Photozoan"-rich deposits. This might be the result of an establishing ("maturing") carbonate factory adapting to relative sea-level oscillations. The late stage of the Sedini Limestone Unit is rich in zooxanthellate corals. These are generally not attributed to fertile surface waters (HALLOCK & SCHLAGER, 1986).

IV. SYNTHESIS

SEDINI CARBONATE PLATFORM

Sedimentological and stratigraphical models for two fault-block-carbonate platforms in North Sardinia are presented. The Sedini Limestone Unit contains a transitional carbonate factory with rhodalgal and chlorozoan elements, and its depositional geometries evolve from a ramp to a steep-flanked platform. Steepening of the depositional relief is gradual and linked to the inception of coralline-algal bindstones, which stabilize an incipient margin formed by submarine dunes. In its late stage, the Sedini carbonate platform consists of a reef flat formed in water depths of approximately 20m. Basinwards, a transition from coralline-algal bindstones indicating a water depth of around 40m to steep, rhodolithic clinoforms with the lower foresets formed in water depths around 60m is evident.

The usage of the term "steep flanked platform" intends to emphasize the geometry of the transitional carbonate system in contrast to conventionally rimmed depositional systems. The margin of the Sedini carbonate platform is not represented by reefs or shoals building up to sea level. The platform interior coral reefs do not indicate sea level either. This may be characteristic for transitional carbonate platforms.

The unravelling of this setup might be useful for future work, either based on outcrop or seismic studies: if outcrop conditions do not allow a clear-cut view of platform geometries, the clinoform-rollover area may be misinterpreted, because the edge of the platform does not necessarily indicate sea-level position. Although the Sedini carbonate platform is small, and thus details are below conventional seismic resolution, it shows that a mere geometrical reconstruction of platform geometries in seismic data without knowledge of lateral facies relations may lead to misinterpretations.

I do not believe that the turnover in geometries is the result of a climatic change. Tropical to subtropical conditions are indicated throughout the entire Sedini Limestone Unit. I would rather consider it as resulting from a progressive establishment ("maturation") of the depositional system, adapting to relative sea-level fluctuations (cf. HOMEWOOD, 1996)

PORTO TORRES BASIN

The mixed carbonate-siliciclastic succession of the Porto Torres Basin shows similarities with the Sedini Limestone Unit in the carbonate factories involved. However, differences occur with regard to formation of depositional geometries, which were primarily controlled by syndepositional tectonics.

I conclude two outcomes from the comparison with the Sedini Limestone Unit:
1. The basinal and tectonic setting, as well as sea-level fluctuations have a considerable impact on the formation of depositional geometries in transitional carbonates (cf. HOMEWOOD, 1996; BOSENCE, 2005).
2. Transitional carbonates can develop different platform geometries within closely related structural and climatic environments. Generalization of facies models has to be considered with regard to that.

References

ALBERTSEN, J.C. (2005) Kartierung des Miozäns bei Sedini und Fazies miozäner Karbonate bei Sedini/Nordsardinien. Diplomarbeit, Universität Hamburg, 86 pp.

ANASTAS, A.S., DALRYMPLE, R.W., JAMES, N.P. and NELSON, C.S. (1997) Cross-stratified calcarenites from New Zealand: subaqueous dunes in a cool-water, Oligo-Miocene seaway. *Sedimentology*, **44**, 869-891.

ARNAUD, M., MAGNÉ, J., MONLEAU, C., NEGRETTI, B. and OGGIANO, G. (1992) Nouvelle données sur le Miocéne du Nord-Ouest de la Sardaigne (Italie). *Comptes Rendues Acadademie Science Paris* **315** II no. 8, 965-970

ASSORGIA, A., BALOGH, K., LECCA, L., IBBA, A., PORCU, A., SECCHI, F. and TILOCCA, G. (1995) Volcanological characters and structural context of Oligo-Miocene volcanic successions from Central Sardinia (Italy). In: *Rapporti tra Alpi e Apennino, Perverago* (eds. R. Polino and R- Sacchi), Accademia Nazionale delle Scienze, 14, 397-424.

BASSANT, P. (1999) The high-resolution stratigraphic architecture and evolution of the Burdigalian carbonate-siliciclastic sedimentary systems of the Mut Basin, Turkey. PhD thesis No. 1256, Fribourg.

BASSANT, P., VAN BUCHEM, F., STRASSER, A. and LOMANDO A. (2004) A comparison of two Early Miocene carbonate margins: the Zhujiang Carbonate platform (subsurface, South China Sea) and the Pirinc Platform (outcrop, southern Turkey). In: *Intergration of outcrop and modern analogs in reservoir modelling.* AAPG Memoir, 80, 153-170.

BASSI, D., CARANNANTE, G., MONLEAU, C., MURRU, M., SIMONE, L. and TOSCANO, F. (2006) Rhodalgal / Bryomol assemblages in temperate type carbonate, channelized depositional systems: the Early Miocene of the Sarcidano area (Sardinia, Italy). In: *Cool-Water Carbonates. Depositional Systems and Palaeoenvironmental controls*, (Ed. H.M. Pedley and G. Carannante) Geological Society Special Publication, **255**, 35-52.

BECCALUVA, L., CIVETTA, L., MACCIOTTA, G., OTELLI, L., and RICCI, C.A. (1985) Geochronology in Sardinia: Results and problems. *Rend. Soc. Ital. Min. Petr.* **40**, 57-72.

BERGGREN W.A., KENT, D.V., FLYNN, J.J., and VAN COUVERING, J.A. (1985) Cenozoic Geochronology. *Geological Society of America Bulletin*, **96, no. 11**, 1407-1418.

BERGGREN, W.A., KENT, D.V., SWISHER, C.C. III and AUBRY, M.-P. (1995) A revise Cenozoic geochronology chronostratigraphy. In: *Geochronology, time scales and global stratigraphic correlation* (eds. W.A. Berggren, D.V. Kent, M.P. Aubry and J. Hardenbol). SEPM Special Publication, 54, 129-212.

BETZLER, C., BRACHERT, T.C., and KROON, D. (1995) Role of climate in partial drowning of the Queensland Plateau carbonate platform (northeastern Australia). *Marine Geology*, **123**, 11-32.

BETZLER, C., BRACHERT, T.C., and NEBELSICK, J. (1997) The warm-temperate carbonate province. A review in the facies, zonations and deliminations. *Courier Forschungsinstitut Senckenberg*, **201**, 83-99.

BETZLER, C., REIJMER, J.J.G, BERNET, K., EBERLI, G.P. and ANSELMETTI, F.S. (1999) Sedimentary patterns and geometries of the Bahamian outer carbonate ramp (Miocene and Lower Pliocene, Great Bahama Bank). *Sedimentology*, **46**, 1127-1146.

BOSELLINI, F.R. and PERRIN, C. (2008) Estimating Mediterranean Oligocene-Miocene sea-surface temperatures: An approach based on coral taxonomic richness. *Palaeogeography, Palaeoclimatology, Palaeoecology*, **258**, 71-88.

BOSENCE, D. (1983a) Description and classification of Rhodoliths (Rhodoids, Rhodolithes). In: *Coated Grains* (Ed T.M. Peryt), pp. 217-224. Springer, Berlin, Heidelberg.

BOSENCE, D. (1983b) The occurrence and ecology of Rhodoliths (Rhodoids, Rhodolithes). In: *Coated Grains* (Ed T.M. Peryt), pp. 225-242. Springer, Berlin, Heidelberg.

BOSENCE, D.W.J. (1983c) Coralline algal reef frameworks. *Journal of the Geological Society, London*, **140**, 365-376.

BOSENCE, D. (1991) Coralline Algae: Mineralization, Taxonomy, and Palaeoecology. In: *Calcarous Algae and Stromatolites* (Ed. R. Riding), pp. 98-113. Springer.

BOSENCE, D.W.J. (1998) Stratigraphic and sedimentological models of rift basins. In: *Sedimentation and tectonics of rift-basins: Red Sea-Gulf of Aden* (Eds B.H. Purser, D.W.J. Bosence), Chapman & Hall, London.

BOSENCE, D. (2005) A genetic classification of carbonate platforms based on their basinal and tectonic settings in the Cenozoic. *Sedimentary Geology*, **175**, 49-72.

BOSENCE, D.W.J. and PEDLEY, H.M. (1982) Sedimentology and Palaeoecology of a Miocene Coralline Algal Biostrome from the Maltese Islands. *Palaeogeography, Palaeoclimatology, Palaeoecology*, **38,** 9-43.

BOSENCE, D., CROSS, N. and HARDY, S. (1998) Architecture and depositional sequences of Tertiary fault-block carbonate platforms; an analysis from outcrop (Miocene, Gulf of Suez) and computer modelling. *Marine and Petroleum Geology*, **15**, 203-221.

BRACHERT, T.C., BETZLER, C., BRAGA, J.C. and MARTIN, J.M. (1996) Record of climatic change in neritic carbonates: turnover in biogenic associations and depositional models (Late Miocene, southern Spain). *Geologische Rundschau*, **85**, 327-337.

BRAGA, J.C. and AGUIRRE, J. (2001) Coralline algal assemblages in upper Neogene reef and temperate carbonates in Southern Spain. *Palaeogeography, Palaeoclimatology, Palaeoecology*, **175**, 27-41.

BRAGA, J.C. and AGUIRRE, J. (2004) Coralline algae indicate Pleistocene evolution from deep, open platform to outer barrier reef environments in the northern Great Barrier Reef margin. *Coral Reefs*, **23**, 547-558.

BRAGA, J.C. and MARTIN, J.M. (1988) Neogene coralline algal growth-forms and their palaeoenvironments in the Almanzora river valley (Almeria, S.E. Spain). *Palaeogeography, Palaeoclimatology, Palaeoecology*, **67**, 285-303.

BRAGA, J.C., BOSENCE, D.W. and STENECK, R.S. (1993) New anatomical characters in fossil coralline algae and their taxonomic implications. *Palaeontology*, **36**, 535-547.

BRAGA, J.C. and MARTIN, J.M. (1996) Geometries of reef advance in response to relative sea-level changes in a Messinian (uppermost Miocene) fringing reef (Cariatiz Reef, Sorbas Basin, SE Spain). *Sedimentary Geology*, **107**, 61-81.

BRAGA, J.C. and BASSI, D. (2007) Neogene history of *Sporolithon Heydrich* (Corallinales, Rhodophyta) in the Mediterranean region. *Palaeogeography, Palaeoclimatology, Palaeoecology*, **243**, 189-203.

BRANDANO, M. (2003) Tropical/subtropical inner ramp facies in Lower Miocene "Calcari a Briozi e Litotamni" of the Monte Lungo area (Cassino Plain, Central Appenines, Italy). *Bollettino della Società Geologica Italiana*, **122**, 85-98.

BRANDANO, M., CIVITELLI, L.C. and MARIOTTI, G. (2001) A foramol-type carbonate ramp in tropical-subtropical setting, the link between tectonics and nutrients. AAPG Annual meeting, Denver.

BRANDANO, M. and CORDA, L. (2002) Nutrients, sea-level and tectonics: constratints for the facies architecture of a Miocene carbonate ramp in Central Italy. *Terra Nova*, **14**, 257-262.

BRANDANO, M., VANNUCCI, G., POMAR, L. and OBRADOR, A. (2005) Rhodolith assemblages from the lower Tortonian carbonate ramp of Menorca (Spain): Environmental and palaeoclimatic implications. *Palaeogeography, Palaeoclimatology, Palaeoecology*, **226**, 307-323.

BURCHETTE, T.P. and WRIGHT, V.P. (1992) Carbonate ramp depositional systems. *Sedimentary Geology*, **79**, 3-57.

BURGESS, C.J. and ANDERSON, J.M. (1983) Rhodoids in Temperate Carbonates from the Cenozoic of New Zealand. In: *Coated Grains* (Ed T.M. Peryt), pp. 243-258.

CAESAR , S. 2008 Kartierung miozäner Karbonate im Gebiet Santa Vittoria bei Sassari, NW-Sardinien. Diplomarbeit, Universtät Hamburg, 88 pp.

CARANNANTE, G., ESTEBAN, M., MILLIMAN, J.D. and SIMONE, L. (1988) Carbonate lithofacies as palaeolatitude indicators: problems and limitations. *Sedimentary Geology*, **60**, 333-346.

CARANNANTE, G. and SIMONE, L. (1996) Rhodolith Facies in the central-Southern Apennines Mountains, Italy. In: *Models for carbonate Stratigraphy from Miocene reef complexes of Mediterranean regions*, (Ed. E.K. Franseen, M. Esteban, W.C. Ward, J.M. Rouchy) SEPM Concepts in Sedimentology and Palaeontology 5, 261-275.

CARMIGNANI, L., CHERCHI, A. AND RICCI, C.A. (1989) Basement structure and Mesozoic –Cenozoic evolution of Sardinia. *Atti Academia Nazionale Linzei*, **80**, 63-92.

CARMIGNANI L., CAROSI, R., DISPERATI, L., FUNEDDA, A., MUSUMECI, G., PASCI, S. and PERTUSATI, P.C. (1992) Tertiary transpressional tectonics in NE Sardinia (Italy). In: *Contributions to the Geology of Sardinia with special regards to the Palaeozoic basements.* (eds. L. Carmignani and F.P. Sassi) IGPC, 276, 83-96.

CARMIGNANI, L. (Coordinamento scientifico), BARCA, S., OGGIANO, G., PERTUSATI, P.C., SALVADORI, I. (Comitato scientifico), CONTI, P., ELTRUDIS, A., FUNEDDA, A. and PASCI, S. (Coordinamento editoriale), Presidenza del Consiglio dei Ministri, Dipartimento per i Servizi Tecnici Nazionali, Servizio Geologico Nazionale (2001). Geologia della Sardegna, Note illustrativa della Carta Geologica della Sardegna in scala 1:200 000. *Memorie descrittive della Carta Geologica d´Italia*, 60. 283 pp, two maps.

CAROSI, R., DI PISA, A., MONTOMOLI, C. and OGGIANO, G. (2004) The structural evolution of the Asinara Island (NW Sardinia, Italy). *Geodinamica Acta,* **17**, 309-329.

CASULA, A., CHERCHI, A., MONTADERT, L., MURRU, M. and SARRIA, E. (2001) The Cenozoic Graben System of Sardinia (Italy): geodynamic evolution from new seismic and field data. *Marine and Petroleum Geology*, **18**, 863-888.

CHAPRONIERE, G.C.H. (1975) Palaeoecology of Oligo-Miocene larger benthic foraminiferida, Australia. *Alcheringa*, **1**, 37-58.

CHERCHI, A. (1985) Micropalaeontological researches in Sardinia. In: *19th European Micropalaeontological Colloquium* (Ed. A. Cherchi), Sardinia.

CHERCHI, A. and MONTADERT, L. (1982) Oligo-Miocene rift of Sardinia and the early history of the Western Mediterranean Basin. *Nature*, **298**, 736-739.

CHERCHI, A. and TRÉMOLIÈRES, P. (1984) Nouvelles données sur l´evolution structurale au Mésozoique et au Cenozoique de la Sardaigne et leur implications géodynamiques dans le cadre Méditerranéenne. *Comptes Rendues Academie Sciences Paris*, **298, II, no. 20**, 889-894.

CHERCHI, A. and SCHRÖDER, R. (1985) Neritic Miocene of Funtana del Fico (Osilo). Type-locality of Heterostegina complanata (Meneghini 1857). In: *Guidebook of the 19th European Micropalaeontological Colloquium, Sardinia* (Ed. A. Cherchi), AGIP.

CHERCHI, A., MURRU, M. and SIMONE, L. (2000) Miocene Carbonate Factories in the Syn-rift Sardinia Graben Subbasins (Italy). *Facies*, **43**, 223-240.

CIVITELLI, G. and BRANDANO, M. (2005) Atlante delle litofacies e modello deposizionale dei Calcari a Briozoi e Litotamni nella Piattaforma carbonatica laziale-abruzzese. *Bollettino della Società Geologica Italiana*, **124**, 611-643.

COHEN, C.R. (1980) Plate tectonic Model for the Oligo-Miocene Evolution of the Western Mediterranean. *Tectonophysics*, **68**, 283-311.

COLLINS, L.B., ZHU, Z.R., WYRWOLL, K.-H., HATCHER, B.G., PLAYFORD, P.E., EISENHAUER, A., CHEN, J.H. and BONANI, G. (1993) Holocene growth history of a reef complex on a cool-water carbonate margin: Easter Group of the Houtman Abrolhos, eastern Indian Ocean. *Marine Geology*, **115**, 29-46.

COLLINS , L.B., FRANCE R.E., ZHU, Z.R, and WYRWOLL, K.-H. (1997) Warm-water platform and cool-water shelf carbonates ot the Abrolhos schelf, Southwest Australia. In: *Cool-water carbonates* (Ed N.P. James, Clarke, J. A. D.), *SEPM Special Publications*, 56, 23-36.

COCOZZA, T. and JACOBACCI, A. (1975) Geological outline of Sardinia. In: *The Geology of Italy* (Ed. C. Squyres), Earth Sciences of the Lybian Arabic Republic, Tripoli, 49-81.

CONTI, P., CARMIGNANI, L., OGGIANO, G., FUNEDDA, A. and ELTRUDIS, A. (1999) From thickening to extension in the Variscan belt – Kinematic evidence from Sardinia (Italy). *Terra Nova*, **11**, 93-99.

CROSS, N.E., PURSER, B.H. and BOSENCE, D.W.J. (1998) The tectono-sedimentary evolution of a rift margin carbonate platform: Abu Shaar, Gulf of Suez, Egypt. In: *Sedimentary and tectonic evolution of rift basins: The Red Sea-Gulf of Aden* (eds. B.H. Purser, D.W.J. Bosence) pp. 271-295, Chapman Hall-Kluwers, London.

DEINO, A., GATTACCECA, J., RIZZO, R. and MONTANARI, A. (2001) $^{40}Ar/^{39}Ar$ Dating and Paleomagnetism of the Miocene Volcanic Succession of Monte Furru (Western Sardinia): Implications for the Rotation History of the Corsica-Sardinia Microplate, *Geophysical Research Letters*, **28 (17)**, 3373–3376.

EBERLI, G.P. and GINSBURG, R.N. (1987) Segmentation and coalescence of Cenozoic carbonate platforms, northwestern Great Bahama Bank. *Geology*, **15**, 75-79.

EBERLI, G.P. and GINSBURG, R.N. (1989) Cenozoic progradation of northwestern Great Bahama Bank, a record of lateral platform growth and sea-level fluctuations. *SEPM Special Publication*, **44**, 339-351

EDEL, J.B. (1980) Etude paléomagnétique en Sardaigne. Conséquences pour la géodynaique de la Méditterranée occidentale. *PhD thesis*, Strasbourg, 310 pp.

ESTEBAN, M. (1996) An overview of Miocene reefs from Mediterranean areas: General trends and facies models. In: Models for carbonate Stratigraphy from Miocene reef complexes of Mediterranean regions (Ed. E.K. Franseen, Esteban, M., Ward, W.C., Rouchy, J.M.)*SEPM Concepts in Sedimentology and Palaeontology*, 5, 3-53.

FACCENNA, C., SPERANZA, F., D´AJELLO CARACCIOLO, F., MATTEI, M. and OGGIANO, G. (2002) Extensional tectonics on Sardinia (Italy): insights into the arc-back-arc transitional regime. *Tectonophysics*, **356**, 213-232.

FAULDS, J.E. and VARGA, R.J. (1998) The role of accomodation zones and transfer zones in the regional segmentation of extended terranes. In: *Accomodation zones and transfer zones: The regional segmentation of the Basin and Range Province* (Eds J.E. Faulds, Steward, J.H.), Geological Society of America Special Paper, **323**, pp. 1-45.

FRANCOLINI, C. (1994) Sull´ età di un ciclo miocenico dell´ area di Sorso e Sennori, a Nord di Sassari (Sardegna Settrentionale). *Atti Soc. Tosc. Sci. Nat. Mem. Serie A*, **101**, 137-144.

FUNEDDA, A., OGGIANO, G., and PASCI, S. (2000) The Logudoro Basin: A key area for the tertiary tectono-sedimentary evolution of North Sardinia. Bolletino della Societa Geologica Italiana, **119**, 31-38.

FUNEDDA, A., OGGIANO, G. , and PASCUCCI, V. (2003) I depositi Miocenici della Sardegna settrentionale: il bacino Logudoro. In: *Atti del Convegno GEOSED 2003* (Ed. V. Pascucci), pp.381-414. Editoria e Stampa, Sassari, Italy.

GALLONI, F., CORNEE, J.J., REBELLE, M., and FERRANDINI, M. (2001) Sedimentary anatomies of early Miocene coral reefs in South Corsica (France) and South Sardinia (Italy). *Géologie Mediterranéenne*, **28, no.1-2**, 73-77.

GATTACCECA, J. and DEINO, A. (1999) Rotation Miocéne du bloc corso-sarde: nouvelles constraintes paleomagnetiques e chronologiques. *B.R.G.M.*, **291**, 15-16.

GIENAPP, H.P. (2005) Die miozänen Karbonate im Gebiet Nulvi, Region Anglona (N-Sardinien), Diplomarbeit, Universität Hamburg, 78 pp.

GRADSTEIN, F.M., OGG, J.G., and SMITH, A.G. (2004) A Geologic Time Scale 2004. (Eds. F. M. Gradstein, James G. Ogg and Alan G. Smith) Cambridge University Press, 610 pp.

GUEGUEN, E., DOGLIONI, C. and FERNANDEZ, M. (1998) On the post 25 Ma geodynamic evolution of the western Mediterranean. *Tectonophysics*, **298**, 259-269.

HAGEN, M.F., MARCANO, G., BETZLER, C. and MUTTI, M**.** (2005) "A Neogene transitional Carbonate System in the Central Mediterranean, Sardinia (Italy)(II): Rhodalgal bank margin geometries. *Abstracts of 24th IAS Meeting of Sedimentology, Muscat, Oman*, p. 76.

HALFAR, J., GODINEZ-ORTA, L., MUTTI, M., VALDEZ-HOLGUIN, J. and BORGES, J. (2004) Nutrient- and temperature controls on modern carbonate production: an example from the Gulf of California, Mexico. *Geology*, **32**, 213-216.

HALFAR, J. and MUTTI, M. (2005) Global dominance of coralline red algal facies: A response to Miocene oceanographic events. *Geology*, **33**, 481-484.

HALFAR, J., GODINEZ-ORTA, L., MUTTI, M., VALDEZ-HOLGUIN, J. and BORGES, J. (2006) Carbonates calibrated against oceanographic parameters along a latitudinal transect in the Gulf of California, Mexico. *Sedimentology*, **53**, 297-320.

HALLOCK, P. and SCHLAGER, W. (1986) Nutrient excess and the demise of coral reefs and platforms. *Palaios*, **1**, 389-398.

HAQ, B.U., HARDENBOL, J. and VAIL, P.R. (1988) Mesozoic and Cenozoic Chronostratigraphy and cycles of sea-level change. In: *Sea-Level Changes: An integrated approach*. (Ed. B. Lidz), *SEPM Special Publications*, 42, 71-108

HOMEWOOD, P. (1996) The carbonate feedback system: interaction between stratigraphic accomodation, ecological succession and the carbonate factory. *Bulletin de la Société Géologique de France*, **167**, 701-715.

JAMES, N.P. (1997) The cool-water depositional realm. In: *Cool-water carbonates* (Ed N.P. James, Clarke, J. A. D.), *SEPM Special Publications*, 56, 1-20.

JAMES, N.P, COLLINS, L.B and BONE, Y. (1999) Subtropical carbonates in a temperate realm: Modern sediments on the southwest Australian Shelf. *Journal of Sedimentary Research* **69**, 1297-1321.

JARAMILLO, D. (2007) Kartierung der neogenen Schichtenfolge östlich von Sassari, Porto Torres Becken, NW-Sardinien. Diplomkartierung, Univerität Hamburg, 47 pp.

JONES, B. and DESROCHERS, A. (1992) Shallow platform carbonates. In: *Facies Models. Response to sea level changes* (Ed R.G. Walker, James, N.P.), pp. 277-301. Geological Association Canada.

JUST, J. (2007) Diplomkartierung im Porto Torres Becken, NW-Sardinien. Diplomkartierung, Universität Hamburg, 67 pp.

KARDAS, P. (in prep.) Diplomkartierung im Porto Torres Becken, NW-Sardinien. Diplomarbeit, Universität Hamburg.

KROEGER, K.F., REUTER, M., and BRACHERT, T.C. (2006) Palaeoenvironmental reconstruction based on non-geniculate coralline algal assemblages in Miocene limestone of central Crete. *Facies*, **52**, 381-409.

LECCA, L., LONIS, R., LUXORO, S., MELIS, E., SECCHI, E. and BROTZU, P. (1997) Oligo-Miocene volcanic sequences and rifting stages in Sardinia: a review. *Periodico Mineralogico*, **66**, 7-61.

LEEDER, M.R. and GAWTHORPE, R.L. (1987) Sedimentary models for extensional tilt-block/half-graben basins. In: *Continental Extensional Tectonics* (eds. M.P. Coward, J.F. Dewey, and P.L. Hancock), Geological Society Special Publication, 28, 139-152.

LEES, A. (1975) Possible influence of salinity and temperature on modern shelf carbonate sedimentation. *Marine Geology*, **19**, 159-198.

LEES, A. and BULLER, A.T. (1972) Modern temperate-water and warm-water shelf carbonate sediments contrasted. *Marine Geology*, **13**, 67-73

LONGMAN, M.W. (1993) Future Bright for Tertiary Carbonate Reservoirs in Southeast Asia. *Oil & Gas Journal*, **91, no. 51** 107-112.

LOWRIE, W. and ALVAREZ, W. (1981) One hundred million years of ego magnetic polary history. *Geology*, **9**, 392-397.

LUND, M., DAVIES, P. and BRAGA, J.C. (2000) Coralline Algal Nodules off Fraser Island, Eastern Australia. *Facies*, **42**, 25-34.

MARCANO, G. (in prep.) Sedimentological and early diagenetic characterization of a Heterozoan-Photozoan transition (Miocene, Sardinia): controls over facies stabilization and depositional geometries. PhD thesis, Universität Potsdam.

MARRACK, E.C. (1999) The Relationship between Water Motion and Living Rhodolith Beds in the Southwestern Gulf of California, Mexico. *Palaios*, **14**, 159-171.

MARTIN, J.M.M. and BRAGA, J.C. (1994) Messian events in the Sorbas Basin and their implications in the recent history of the Mediterranean. *Sedimentary Geology*, **90**, 257-268.

MARTIN, J.M., BRAGA, J.C., BETZLER, C. and BRACHERT, T. (1996) Sedimentary model and high-frequency cyclicity in a Mediterranean, shallow shelf, temperate carbonate environment (uppermost Miocene, Agua Amarga Basin, Southern Spain) *Sedimentology*, **43**, 263-277.

MARTINI, I.P., OGGIANO, G. and MAZZEI, R. (1992) Siliciclastic-carbonate sequences of Miocene grabens of Northern Sardinia, western Mediterranean Sea. *Sedimentary Geology*, **76**: 63-78.

MAYR, C. (2007) Diplomkartierung im Porto Torres Becken, NW-Sardinien. Diplomkartierung, Universität Hamburg.

MAZZEI, R. and OGGIANO, G. (1990) Messa in evidenza di due cicli sedimentari nel Miocene dell´area di Florinas (Sardegna Settrentionale). *Atti Soc. Tosc. Sci. Nat. Mem.* **Serie A, 97** , 119-147.

MONAGHAN, A. (2001) Coeval extension, sedimentation and volcanism along the Cainozoic rift system of Sardinia. In: *Peri-Tethys Memoir 6: Peri-Tethyan rift/wrench basins and passive margins.* (Ed P.A. Ziegler and A.H.F. Cavazza), 186, pp. 707-734. Mem. Mus. natn. Hist. nat., Paris.

MONTIGNY, R., EDEL, J.B. and THUZIAT, R. (1981) Oligo-Miocene rotation of Sardinia: K-Ar ages and palaeomagnetic data of Tertiary volcanics. *Earth and Planetary Science Letters*, **54**, 261-271.

MURRU, M., SIMONE, L. and VIGORITO, M. (2001) Carbonate channel network in the Miocene syn-rift Sardinia basins. *Géologie Mediterranéenne*, **28, no. 1-2**, 133-137.

MUTTI, M., BERNOULLI, D. and STILLE, P. (1997) Temperate carbonate platform drowning linked to Miocene oceanographic events; Maiella platform margin, Italy. *Terra Nova*, **9**, 122.125.

MUTTI, M., BERNOULLI, D., SPEZZAFERRI, S. and STILLE, P. (1999) Lower and middle Miocene carbonate facies in the central Mediterranean: the impact of palaeoceanography on sequence stratigraphy. In: *Advances in carbonate sequence stratigraphy; application to reservoirs, outcrops and models* (eds. P.M. Harris, A.H. Saller, and J.A. Simo) Society for Sedimentary Geology Special Publication, 63, 371-384.

MUTTI, M. and HALLOCK, P. (2003) Carbonate systems along nutrient and temperature gradients. Some sedimentological constraints. *International Journal of Earth Sciences (Geologische Rundschau)*, **92**, 465-475.

NAGEL, B. (2005) Kartierung der neogenen Schichtenfolge zwischen Sedini und Laerru, NW-Sardinien, Diplomkartierung, Universität Hamburg, 54 pp.

NALIN, R., NELSON, C.S., BASSO, D. and MASSARI, F. (2007) Rhodolith bearing limestones as transgressive marker beds: fossil and modern examples from North Island, New Zealand. *Sedimentology*, **55**, 249-274.

NELSON, C.S. (1988) An introductory perspective on non-tropical shelf carbonates. *Sedimentary Geology*, **60**, 3-12.

OBRADOR, A., POMAR, L. and TABERNER, C. (1992) Late Miocene breccia of Menorca (Balearic Islands): a basis from the interpretation of a Neogene ramp deposit. *Sedimentary Geology*, 79: 203-223.

PEDLEY, M. (1996) Miocene reef distributions and their associations in the Central Mediterranean region: an overview. In: *Models for Carbonate Stratigraphy from Miocene reef complexes of Mediterranean regions* (Ed E.K. Franseen, M. Esteban, W.C. Ward, J.M. Rouchy), SEPM Concepts in Sedimentology and Palaeontology, 5, 73-88.

PÉRÈS, J.M. and PICARD, J. (1964) Nouveau manuel de bionomie benthique de la Mer Mediterranée *Recueil de Traveaux de la Station Marine d´Endoume-Marseille Bulletin*, **31**, 1-137.

POMAR, L. (2001) Ecological control of sedimentary accomodation: evolution from a carbonate ramp to rimmed shelf, Upper Miocene, Balearic Islands. *Palaeogeography, Palaeoclimatology, Palaeoecology*, **175,** 249-272.

POMAR, L., BRANDANO, M. and WESTPHAL, H. (2004) Environmental factors influencing skeletal-grain sediment associations: a critical review of Miocene examples from the Western Mediterranean. *Sedimentology*, **51**, 627-651.

POMAR, L., OBRADOR, A. and WESTPHAL, H. (2002) Sub-wavebase cross-bedded grainstones on a distally steepened carbonate ramp, Upper Miocene, Menorca, Spain. *Sedimentology*, **49**, 139-169.

POMAR, L. and HALLOCK, P. (2007) Changes in coral-reef structure through the Miocene in the Mediterranean province: Adaptive versus environmental influence. *Geology*, **35**, 899-902.

POMESANO CHERCHI, A. (1971) Microfaune planctoniche di alcune serie mioceniche del Logudoro (Sardegna). In: *Proceedings of the II planktonic conference* (Ed A. Farinacci, Matteucci, R.), 1003-1016, Roma.

PRAGER, R.J. and GINSBURG, R.N. (1989) Carbonate nodule growth on Florida´s outer shelf and its implications for fossil interpretations. *Palaios,* **4**, 310-317.

QUESNEY-FOREST, C. and QUESNEY-FOREST, F. (1984) Etude sedimentologique et structurale de la bordure orientale du fosse Oligo-Miocene sarde. *Ecole Nationale Superior Petrole Moteurs Institut Francais Petrole*, 120 pp.

READ, J.F. (1985) Carbonate Platform Models. *AAPG Bulletin*, **69**, 1-21.

RÖBEN, H. (in prep.) Diplomkartierung im Porto Torres Becken, NW-Sardinien. Diplomkartierung, Universität Hamburg.

RÖMER, M. (2007) Kartierung der sedimentären Abfolge bei San Lorenzo im Porto Torres Becken, Nord-Sardinien. Diplomkartierung, Universität Hamburg, 53 pp.

ROSEN, B.R. (1999) Palaeoclimatic implications of the energy hypothesis from Neogene corals of the Mediterranean. In: *Hominid evolution and climatic change in Europe* (Ed. C.U. Press), pp 309-327.

SCHLAGER, W. (2005) *Carbonate Sedimentology and Sequence Stratigraphy*, SEPM Concepts in Sedimentology and Paleontology: **8**, 200 pp.

SIMONE, L. and CARANNANTE, G. (1988) The fate of foramol ("temperate type") carbonate platforms. *Sedimentary Geology*, **60**, 347-354.

SIMONE, L., MURRU, M. and VIGORITO, M. (2001) A syn-rift temperate-type carbonate margin: morphology and depositional geometries. In: *Abstracts of 21st IAS-Meeting of Sedimentology, Davos.*

SOWERBUTTS, A. (1997). Coeval sedimentation, extension and arc-volcanism along the Oligo-Miocene Sardinian Rift. *PhD thesis, University of Edinburgh*, 521 pp.

SOWERBUTTS, A. (2000) Sedimentation and volcanism linked to multiphase rifting in an Oligo-Miocene intra-arc basin, Anglona, Sardinia. *Geological Magazine*, **137**, 395-418.

SPERANZA, F., VILLA, I.M., SAGNOTTI, L., FLORINDO, F., COSENTINO, D., CIPOLLARI, P. and MATTEI, M. (2002) Age of the Corsica-Sardinia rotation and Liguro-Provencal Basin spreading: new palaeomagnetic and Ar/Ar evidence. *Tectonophysics*, **347**, 231-251.

THOMAS, B. and GENNESSEAUX, M. (1986) A two-stage rifting in the basins of the Corsica-Sardinian straits. *Marine Geology*, **72**, 225-239.

TUCKER, M.E. and WRIGHT, V.P. (1990) Carbonate Sedimentology. Blackwell Science.

VIGLIOTTI, L. and LANGENHEIM, V.E. (1995) When did Sardinia stop rotating? *Terra Nova*, **7**, 424-435.

VIGORITO, M., MURRU, M. and SIMONE, L. (2005) Anatomy of a submarine channel system and related fan in a foramol/rhodalgal carbonate sedimentary setting: a case history from the Miocene syn-rift Sardinia Basin. *Sedimentary Geology*, **174**, 1-30.

VIGORITO, M., MURRU, M. and SIMONE, L. (2006) Architectural patterns in a multistorey mixed carbonate-siliciclastic submarine channel, Porto Torres Basin, Miocene, Sardinia, Italy. *Sedimentary Geology*, **186**, 213-236.

WIGGERSHAUS, S. (2007) Diplomkatierung der neogenen Schichtenfolge im Porto-Torres Becken (Nordsardinien). Diplomkartierung, Universität Hamburg, 55 pp.

WILSON, J.L. (1975) *Carbonate Facies in Geologic History*. Springer, Berlin, 471 pp.

WILSON, M.E.J. and BOSENCE, D.W.J. (1997) Platform-top and ramp deposits of the Tonasa Carbonate Platform, Sulawesi, Indonesia. In: *Petroleum Geology of Southeast Asia* (eds. A.J. Fraser, S.J. Matthews and R.W. Murphy) Geological Society Special Publication, 126, 247-279.

WOELKERLING, W., IRVINE, L.M. and HARVEY, A.S. (1993) Growth-forms in non-geniculate coralline red algae (Corallinales, Rhodophyta). *Aust. Syst. Bot.*, **6**, 277-293.

Table 1. Description of samples along one clinoform bed at the Sa Rocca Manna outcrop. See chapter II.2.b. for discussion.

Sample	Growth Pattern	Growth Forms	Coralline-Algal Genera	Other Biota	Matrix	Specials
12	Rhodolith Densely branched to laminar concentric	Foliose/layered with warty and fruticose protuberances	Melobesoids, *Lithoporella sp.*	Encrusting foraminifers	Bivalve fragments, bryozoans, echinid fragments, small benthic foraminifers, Amphistegina	Syntaxial cements around echinid fragments, partly dedolomitization, glaukonite
11	Rhodolith Densely branched to laminar concentric	Warty, fruticose, locally foliose	*Sporolithon sp., Lithophyllum sp.*	High amount of encrusting foraminifers	Echinid fragments, bryozoan fragments, coralline algal debris, barnacles, Amphistegina	Syntaxial cements
10	Rhodolith Densely branched to laminar concentric	Layered, foliose, warty, encrusting bioclasts	*Mesophyllum sp., Spongites sp., Lithophyllum sp.*	More than 50% encrusting foraminifers	Amphistegina, echinid debris, bryozoans	
9	Rhodolith Laminar concentric to densely branched	Layered, foliose				
8	Rhodolith Densely to moderately branched, laminar concentric, discoidal, 2 rhodoliths fused by ongoing encrustation	Warty, fruticose, layered	*Sporolithon sp.*, Melobesioids	Encrusting foraminifers, bryozoans		Heavily broken

Sample	Growth Pattern	Growth Forms	Involved Coralline-Algal Genera	Involved Biota	Matrix	Specials
7	Rhodolith moderately branched	Layered, warty	*Sporolithon sp.*	Encrusting foraminifers, bryozoans	Echinid fragments, bivalve fragments, coralline algal debris, Amphistegina	Bored
6	Rhodolith Moderately branched to laminar concentric	Foliose/layered with minor warty fruticose protuberances	*Hydrolithon sp., Neogoniolithon sp.*, Melobesioids	Encrusting foraminifers, bryozoans	Echinid fragments, Amphistegina, small benthic forams, bryozoans	Extensive syntaxial cements, matrix well cemented
5	Rhodolith Laminar concentric to moderately branched	Foliose/layered with minor warty protuberances		Encrusting foraminifers		Bored with Lithophaga remnant
4	Rhodolith Branched	fruticose	*Sporolithon sp.*, Melobesioids	bryozoans	Echinid fragments, coralline algal debris, Amphistegina, bivalve fragments	
3	Rhodolith Laminar concentric to branched	Densely layered, warty, fruticose, locally encrusting bioclasts	*Sporolithon sp.*	Encrusting foraminifers, bryozoans	Bryozoan fragments, barnacle fragments, bivalve fragments, fragments of encrusting foraminifers, small benthic forams, coralline algal debris, Amphistegina	bored
2	Three small rhodoliths Moderately branched	Layered to foliose with some warty protuberances		Encrusting foraminifers		bored
1	Two small rhodoliths Branched/laminar concentric	Central part: warty/fruticose, layered,foliose		Encrusting forams		

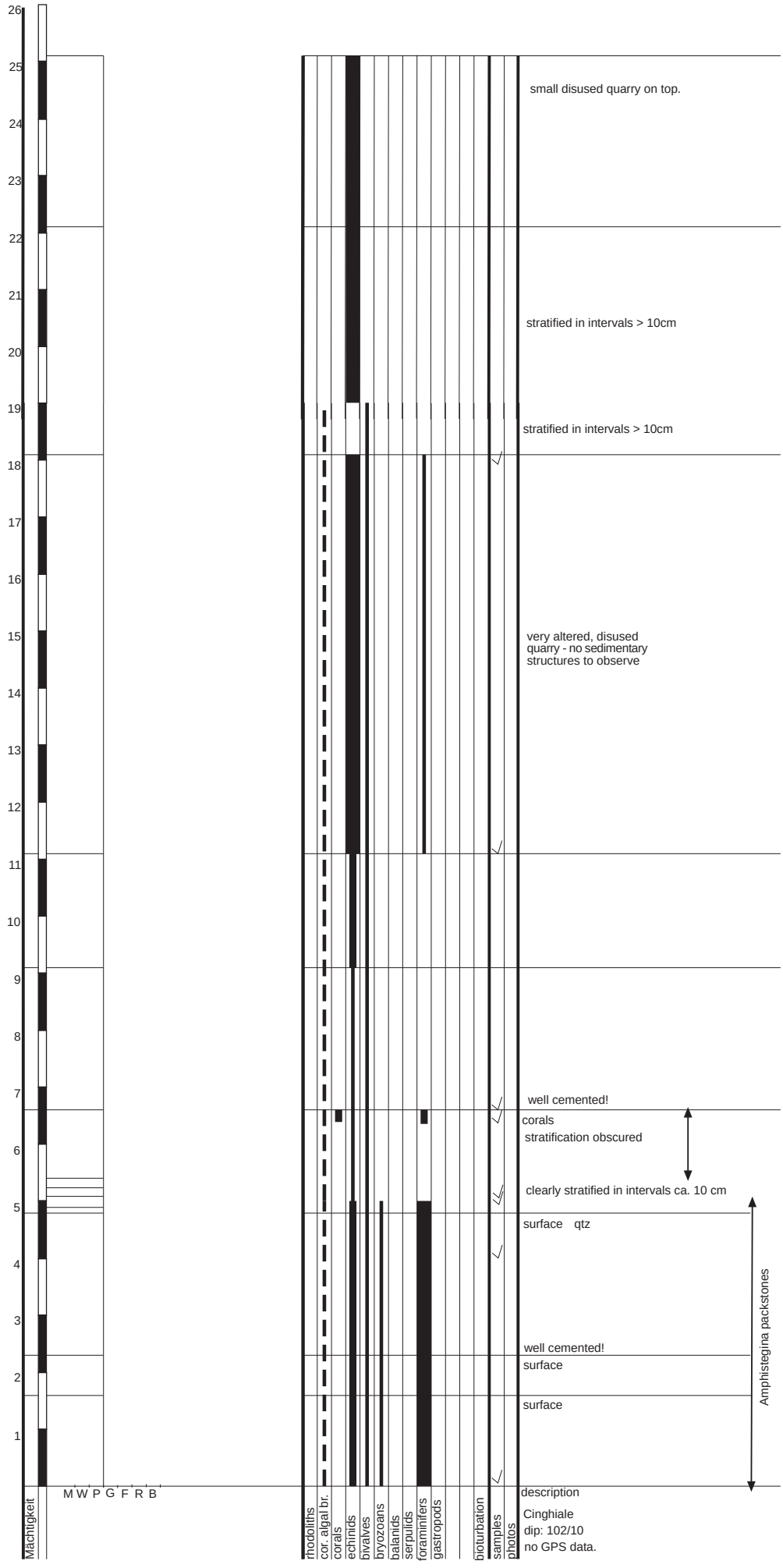
26
25
24
23
22
21
20
19
18
17
16
15
14
13
12
11
10
9
8
7
6
5
4
3
2
1
small disused quarry on top.
stratified in intervals > 10cm
stratified in intervals > 10cm
very altered, disused
quarry - no sedimentary
structures to observe
well cemented!
corals
stratification obscured
clearly stratified in intervals ca. 10 cm
surface qtz
well cemented!
surface
surface
Amphistegina packstones
description
Cinghiale
dip: 102/10
no GPS data.
Mächtigkeit
M W P G F R B
rhodoliths
cor. algal br.
corals
echinids
bivalves
bryozoans
balanids
serpulids
foraminifers
gastropods
bioturbation
samples
photos

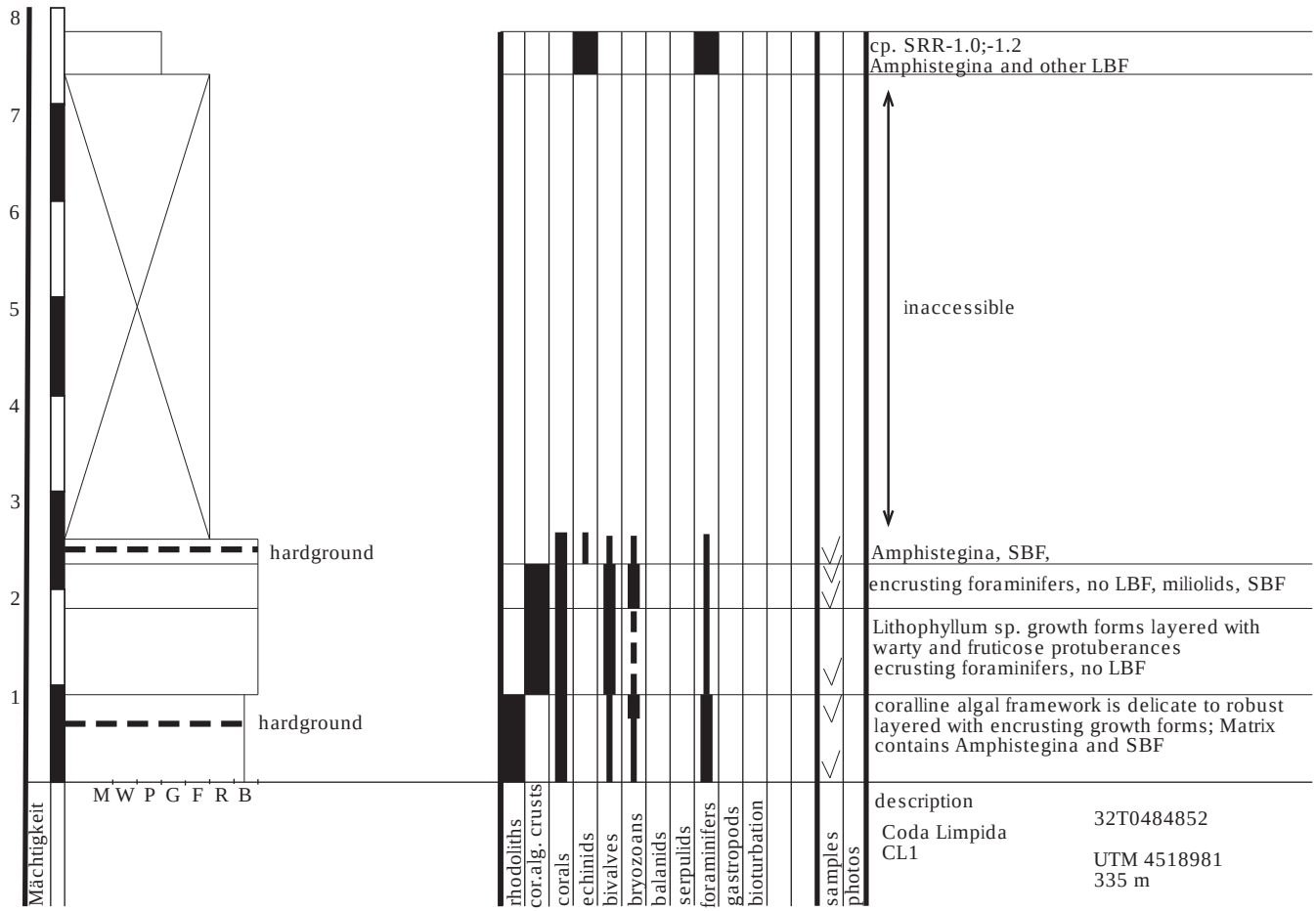
8
7
6
5
4
3
2
1
hardground
hardground
M W P G F R B
Mächtigkeit
rhodoliths
cor.alg. crusts
corals
echinids
bivalves
bryozoans
balanids
serpulids
foraminifers
gastropods
bioturbation
samples
photos
cp. SRR-1.0;-1.2
Amphistegina and other LBF
inaccessible
Amphistegina, SBF,
encrusting foraminifers, no LBF, miliolids, SBF
Lithophyllum sp. growth forms layered with warty and fruticose protuberances
ecrusting foraminifers, no LBF
coralline algal framework is delicate to robust layered with encrusting growth forms; Matrix contains Amphistegina and SBF
description
Coda Limpida
CL1
32T0484852
UTM 4518981
335 m

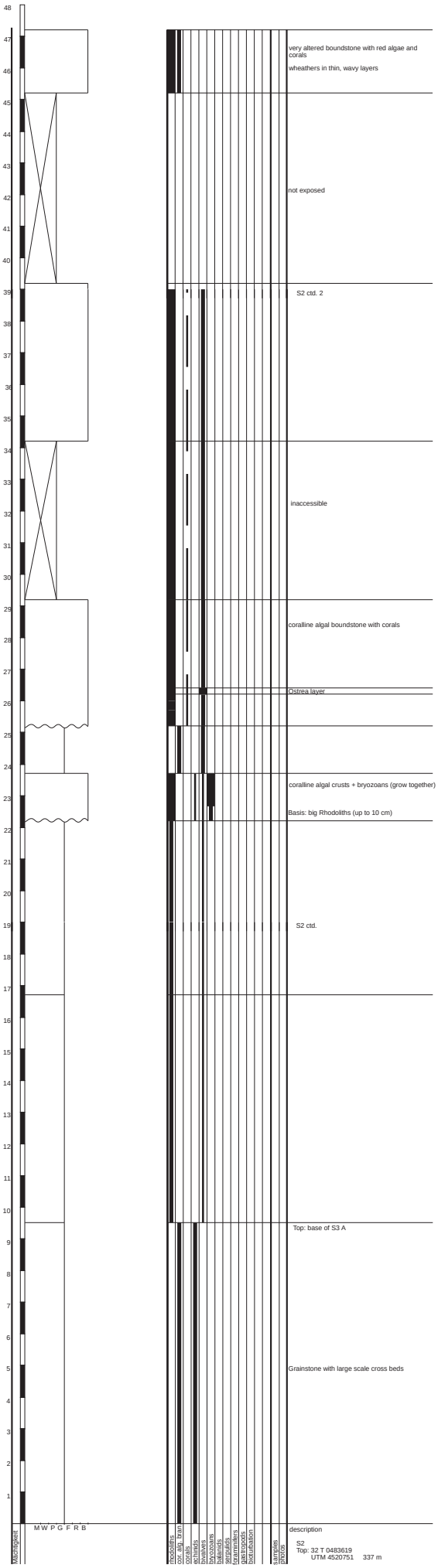
very altered boundstone with red algae and corals
wheathers in thin, wavy layers
not exposed
S2 ctd. 2
inaccessible
coralline algal boundstone with corals
Ostrea layer
coralline algal crusts + bryozoans (grow together)
Basis: big Rhodoliths (up to 10 cm)
S2 ctd.
Top: base of S3 A
Grainstone with large scale cross beds
Mächtigkeit
M W P G F R B
Rhodolithe
cor. alg. brain
corals
echinoids
bivalves
bryozoans
foraminifera
serpulids
foraminifers
gastropods
bioturbation
samples
photos
description
S2
Top: 32 T 0483619
UTM 4520751 337 m

14
13
12
11
10
9
8
7
6
5
4
3
2
1
sequence 1b
sequence 1a
M W P G F R B
Mächtigkeit
rhodoliths
cor. alg. bran.
corals
echinids
bivalves
bryozoans
balanids
serpulids
foraminifers
gastropods
bioturbation
samples
photos
description
S5
fine grained calcarenite with larger benthic forams
foreset
foreset
foreset
foreset
floatstone (bivalve fragments)
sharp contact
bivalve fragments
sharp contact
planar cross bedding (114/15)
fragments of bivalves & echinids

5
4
3
2
1
Mächtigkeit
M W P G F R B
sequence 2a
sequence 1b
rhodoliths
cor. alg. bran.
corals
echinids
bivalves
bryozoans
balanids
serpulids
foraminifers
gastropods
bioturbation
samples
photos
base dolomitized/contact with carstification
laterally grades into wackestone
laminated
description
S 6

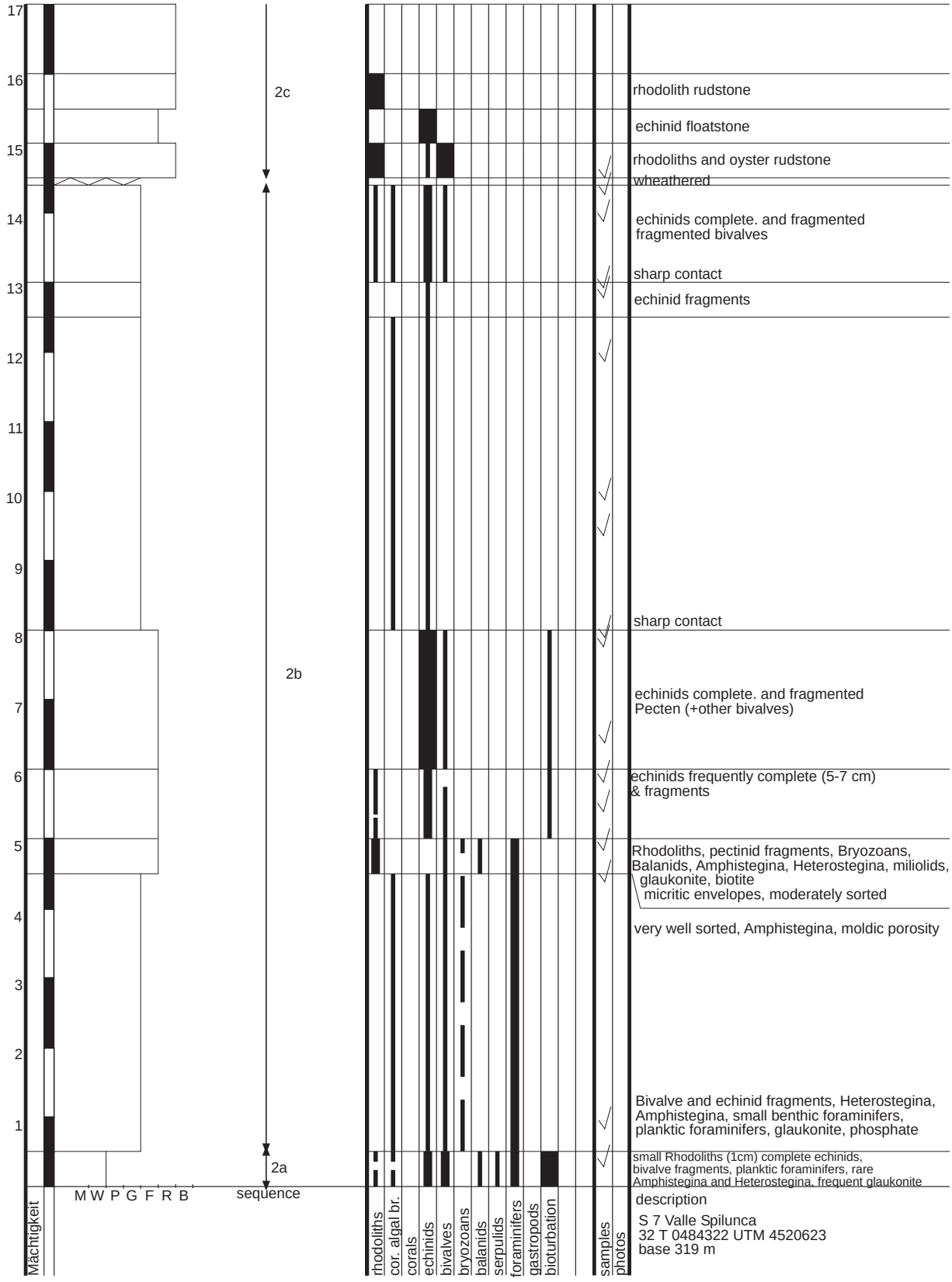
17
16
15
14
13
12
11
10
9
8
7
6
5
4
3
2
1
2c
2b
2a
M W P G F R B
sequence
Mächtigkeit
rhodoliths
cor. algal br.
corals
echinids
bivalves
bryozoans
balanids
serpulids
foraminifers
gastropods
bioturbation
samples
photos
description
rhodolith rudstone
echinid floatstone
rhodoliths and oyster rudstone
wheathered
echinids complete. and fragmented
fragmented bivalves
sharp contact
echinid fragments
sharp contact
echinids complete. and fragmented
Pecten (+other bivalves)
echinids frequently complete (5-7 cm)
& fragments
Rhodoliths, pectinid fragments, Bryozoans,
Balanids, Amphistegina, Heterostegina, miliolids,
glaukonite, biotite
micritic envelopes, moderately sorted
very well sorted, Amphistegina, moldic porosity
Bivalve and echinid fragments, Heterostegina,
Amphistegina, small benthic foraminifers,
planktic foraminifers, glaukonite, phosphate
small Rhodoliths (1cm) complete echinids,
bivalve fragments, planktic foraminifers, rare
Amphistegina and Heterostegina, frequent glaukonite
S 7 Valle Spilunca
32 T 0484322 UTM 4520623
base 319 m

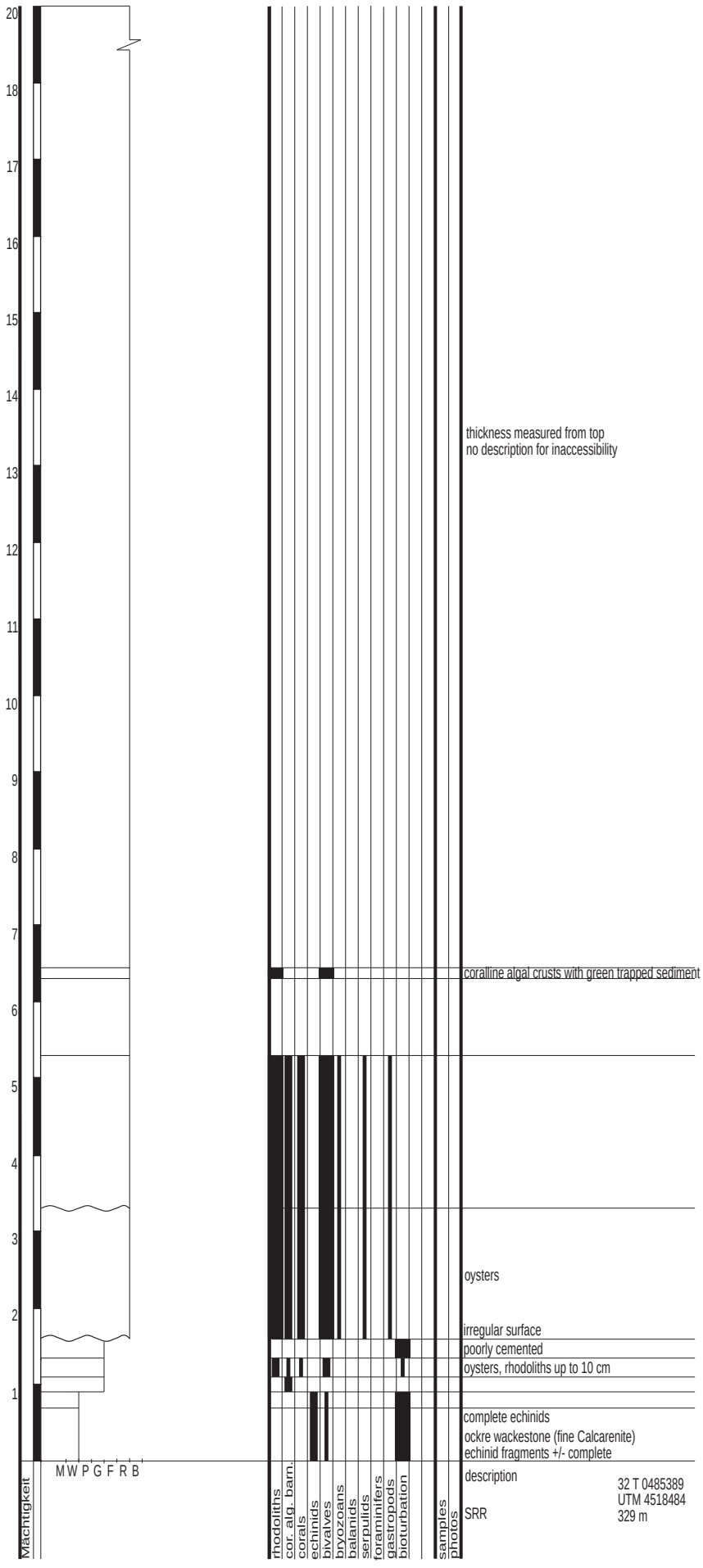
20
18
17
16
15
14
13
12
11
10
9
8
7
6
5
4
3
2
1
Mächtigkeit
M W P G F R B
rhodoliths
cor. alg. barn.
corals
echinids
bivalves
bryozoans
balanids
serpulids
foraminifers
gastropods
bioturbation
samples
photos
thickness measured from top
no description for inaccessibility
coralline algal crusts with green trapped sediment
oysters
irregular surface
poorly cemented
oysters, rhodoliths up to 10 cm
complete echinids
ockre wackestone (fine Calcarenite)
echinid fragments +/- complete
description
SRR
32 T 0485389
UTM 4518484
329 m

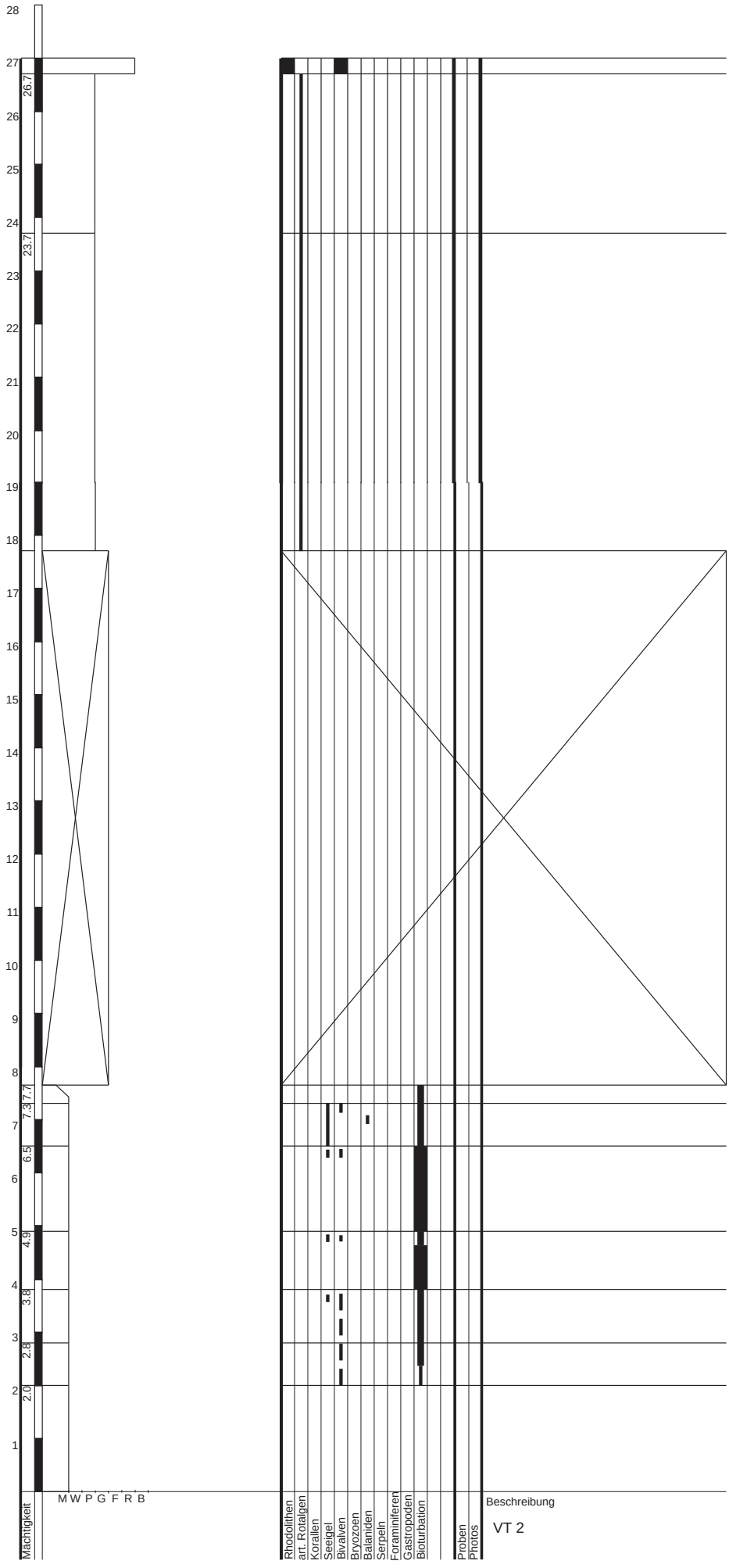
28
27
26
25
24
23
22
21
20
19
18
17
16
15
14
13
12
11
10
9
8
7
6
5
4
3
2
1
26.7
23.7
7.7
7.3
6.5
4.9
3.8
2.8
2.0
Mächtigkeit
M W P G F R B
Rhodolithen
art. Rotalgen
Korallen
Seeigel
Bivalven
Bryozoen
Balaniden
Serpeln
Foraminiferen
Gastropoden
Bioturbation
Proben
Photos
Beschreibung
VT 2

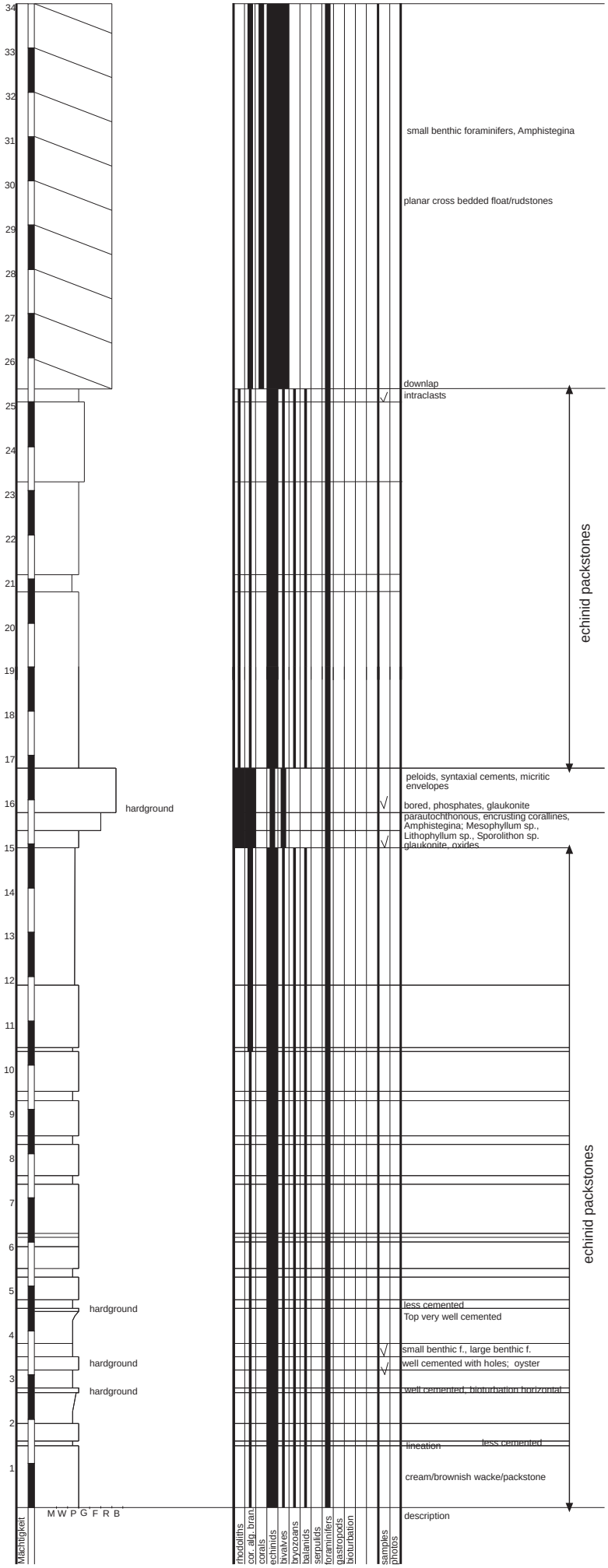
small benthic foraminifers, Amphistegina
planar cross bedded float/rudstones
downlap
intraclasts
echinid packstones
peloids, syntaxial cements, micritic envelopes
bored, phosphates, glaukonite
parautochthonous, encrusting corallines, Amphistegina; Mesophyllum sp., Lithophyllum sp., Sporolithon sp.
glaukonite, oxides
hardground
hardground
hardground
hardground
less cemented
Top very well cemented
small benthic f., large benthic f.
well cemented with holes; oyster
well cemented, bioturbation horizontal
lineation
less cemented
cream/brownish wacke/packstone
echinid packstones
description
Mächtigkeit
M W P G F R B
rhodoliths
cor. alg. bran.
corals
echinids
bivalves
bryozoans
balanids
serpulids
foraminifers
gastropods
bioturbation
samples
photos